

HU ISSN 1785-6892

DESIGN OF MACHINES AND STRUCTURES

A Publication of the University of Miskolc

Volume 2, Number 2 (2012)



**Miskolc University Press
2012**

HU ISSN 1785-6892

DESIGN OF MACHINES AND STRUCTURES

A Publication of the University of Miskolc

Volume 2, Number 2 (2012)



Miskolc University Press
2012

EDITORIAL BORD

Á. DÖBRÖCZÖNI Editor in Chief	Department of Machine- and Product Design University of Miskolc H-3515 Miskolc-Egyetemváros, Hungary machda@uni-miskolc.hu
Á. TAKÁCS Assistant Editor	Department of Machine- and Product Design University of Miskolc H-3515 Miskolc-Egyetemváros, Hungary takacs.agnes@uni-miskolc.hu
R. CERMAK	Department of Machine Design University of West Bohemia Univerzitní 8, 30614 Plzen Czech Republic rcermak@kks.zcu.cz
B.M. SHCHOKIN	Consultant at Magna International Toronto borys.shchokin@sympatico.ca
W. EICHLSEDER	Institut für Allgemeinen Maschinenbau Montanuniversität Leoben, Franz-Josef Str. 18, 8700 Leoben, Österreich wilfrid.eichlseder@notes.unileoben.ac.at
S. VAJNA	Institut für Maschinenkonstruktion, Otto-von-Guericke-Universität Magdeburg, Universität Platz 2, 39106 MAGDEBURG, Deutschland vajna@mb.uni-magdeburg.de
P. HORÁK	Department of Machine and Product Design Budapest University of Technology and Economics horak.peter@gt3.bme.hu H-1111 Budapest, Műegyetem rkp. 9. MG. ép. I. em. 5.
K. JÁRMAI	Department of Materials Handling and Logistics University of Miskolc H-3515 Miskolc-Egyetemváros, Hungary altjar@uni-miskolc.hu
L. KAMONDI	Department of Machine- and Product Design University of Miskolc H-3515 Miskolc-Egyetemváros, Hungary machkl@uni-miskolc.hu
GY. PATKÓ	Department of Machine Tools University of Miskolc H-3515 Miskolc-Egyetemváros, Hungary patko@uni-miskolc.hu
J. PÉTER	Department of Machine- and Product Design University of Miskolc H-3515 Miskolc-Egyetemváros, Hungary machpj@uni-miskolc.hu

CONTENTS

<i>János Bihari</i> : Pneumobile Competition and Education	5
<i>Ádám Döbröczöni–Csaba Dömötör–József Péter</i> : TRIZ and Nature	15
<i>Csaba Dömötör–József Péter</i> : Natural Analogies and TRIZ	23
<i>Csaba Dömötör–József Péter</i> : Design Principles in Nature.....	33
<i>Zsuzsa Drágár–László Kamondi</i> : Asymmetrical Teeth Meshing near General Centre Distance	43
<i>György Hegedűs–György Takács–Gyula Patkó</i> : Collision Detection between Toolholder and Workpiece on Ballnut Grinding	57
<i>László Kelemen–József Szente</i> : Analysis of Gear Meshing for Gear Coupling.....	67
<i>Géza Németh–József Péter–Ádám Döbröczöni</i> : Helical Springs in Epicyclic Traction Drives.....	81
<i>Géza Németh–József Péter–Ádám Döbröczöni</i> : Ensuring of the Clamping Force in Epicyclic Traction Drive by a New Sun Wheel Design	93
<i>József Péter–Géza Németh– Csaba Dömötör</i> : Natural Analogies – Creative Principles of the Nature and the Product Designer	101
<i>Attila Szilágyi–Gyula Patkó–Tibor Csáki–Balázs Barna</i> : Dynamical Investigation of a Superfinishing Device	115
<i>Renáta Szűcs–László Kamondi</i> : Analytical Model to Determine Meshing Stiffness of Spur Gears	123
<i>Renáta Szűcs–László Kamondi</i> : Determination of Backlash for Gear Dynamic Analysis	137
<i>Ágnes Takács</i> : Environmentally Friendly Design Tools – Possibilities of the Application	149

PNEUMOBILE COMPETITION AND EDUCATION

JÁNOS BIHARI

Department of Machine and Product Design, University of Miskolc
H-3515 Miskolc-Egyetemváros
machbj@uni-miskolc.hu

Abstract. Those students who study at the University of Miskolc at the Faculty of Mechanical Engineering have a lot of possibilities that improve their experience during the university-years. Usually the companies are entrusted simple tasks to the trainee. Pneumobile competition was initiated by Bosch Rexroth and they have organized it fifth times this year. Those students who participated this competition have to solve complex tasks are needed to know a lot of areas of the technical sciences. Pneumobile competitions are described and introduced by this paper through an example that confirms what kind of practical development it was for those students who attended this program.

Keywords: Pneumatic vehicle, compressed air, competition, education

1. INTRODUCTION

Frequent problem is in our University that some students do not find practical place in the industry where they could use and improve their knowledge and skills. Pneumobile competition was organised fifth times this year, which is particularly a good chance for us. They need a lot of knowledge to the successful preparation. This knowledge is deepening during the vehicle design and build. Especially important it is that they have to document their activities. As the documentation is one of the most important tasks of the mechanical engineer practicing it is indispensable within the education. These competitions are international so many participants come from the Czech Republic, Poland and Rumania. The aim of this paper is to increase the reputation of the Pneumobile competitions. The students can build relationship with each other and learn a lot during the competition.

2. THE PNEUMOBILE COMPETITION

The Pneumobile competition is announced for students who come from the higher education. The task of the students is to design and build a kind of vehicle, which is driven only by compressed gas (air or nitrogen). The announcement of this year competition [1] includes the task detailed.

3. THE PNEUMOBILE COMPETITION FROM THE VIEWPOINT OF THE UNIVERSITY OF MISKOLC

During the design and produce of the vehicle the following knowledge/skills are needed.

3.1. Designing of the elements

3.1.1. Frame – mechanical engineering studies, CAD, FEM

The driver's weight, effects of motor forces and forces that are resulted from the movement are loaded the frame. As the performance of the motor is small the minimal mass should be reached, but in the interest of driving inflexibility is also important.

3.1.2. Suspension – additional researches, CAD

Our students have not got any information about the suspension when they start to design the vehicle, because they do not learn such type of subjects during their studies. They have to look for the suspension in the required literature and on this basis they have to design it. They have to take into consideration what kind of elements they can buy in the shop after all to produce the wheels and brakes are beyond quote of budget. They have to use the CAD to fit the suspension and the frame together.

3.1.3. Steering – knowledge of the mechanical engineering, CAD

Mechanism of the steering has to ensure the movement of the wheels so the steering-force will not be too high.

To the calculations of steering-force mechanical engineering knowledge needs. CAD software is suggested to use to fit it into the system.

3.1.4. Pneumatic system – mechanical engineering or mechatronic engineering studies

It is basically a mechanical engineering task to define force-effects of the pneumatic system. According to the documentation the students who learn on other special mechanical engineering fields can approximately calculate the forces too. The control is a very important element of the system. Operation of valves is able to be mechanical or electrical. Setting up the system that works with electrical valves is easily, but electronic control is needed.

3.1.5. Electronic system – mechatronic engineering or electrical engineering studies

Electronic control can be used for controlling the valves. The mechatronic engineering students learn PLC programming at our University; the electrical engineers are able to build controls with microcontrollers when they are in their second-year. Colleagues of the Bosch Rexroth gladly help using the PLC.

3.1.6. Powertrain system – mechanical engineering studies

Characteristically powertrain system combines the special elements of the bicycle and unique torque converter. Sizing of them is very important from the point of view of safety.

3.2. Racing team

The racing team consists of four persons. The practical benefits of the competition can really succeed if these members are able to develop according to their own territory and the vehicle is suitable for physical implementation. The team has to obtain suitable skills at work. According to our experiences students participating in the challenge it is usually succeed, after the race the need for further development evolves in them.

3.2.1. Responsible team leaders

The responsible team leader's tasks are the coordination, checking the work and handle the occasional conflicts. She/he Examines the design and manufacturing process steps, check the plans and construction. Sometimes self-control is needed to responsible team leader do not force their ideas to students, because the competition is primarily to serve the development of students. She/he also have to provide of distributing the tasks among the students according to their capabilities. The responsible team leader is responsible for the safety work in the workshops of the university.

3.2.2. Other persons

In the Hungarian educational system students are not allowed to use certain machines still not with supervisor because of security reasons. Therefore turning, milling and welding of aluminium in the university workshop leader's job.

If there is a missing skill in the team members they can use outer helper, for example for designing the electrical system or programming. It is also a principle at our university that such helpers can only be students.

3.2.3. Sponsors

Vehicle building needs money and raw materials that the university cannot ensure.

The largest sponsor of the competition is the Bosch Rexroth. Typically the pneumatic system components are the most expensive parts of the vehicle.

It is a good thing that this competition is gladly supported by different companies. According to the education it is particularly useful that those companies give not only financial, but professional help for our students as well. Since student get in contact with many companies the help of these companies is might be more comprehensive than students can access during their university studies.

4. DEVELOPMENT OF A TEAM AND A VEHICLE

4.1. The first race in 2008



Figure 1. First Pneumobile at the Department of Machine- and Product Design

The first race was organized on the yard of the factory in Eger, the ready vehicles were measured in two categories by the competitors. These categories were the fastest lap and the longest distance. There were three teams from the University of Miskolc and one team from the Department of Product- and Machine Design.

The team was consisted of only Bsc. mechanical engineering students who did not have some certain skills at the moment of the entry. They were able to use CAD and VEM software but only at basic level, two of them have a basic knowledge of pneumatics as well. The vehicle was not ready in time for the race and was not working properly in this year. This vehicle was a simple construction, but they were seeking for demanding design.

The vehicle (see *Figure 1*) was made of large (and weak) bicycle wheels, the suspension was stiff and steering was elementary. The motor was a three-cylinder engine, cylinders were driving the planets of a planetary gear by crank tap. The sun gear was the driven element. The pneumatic control is electrical, but only a simple reed sensors connected to relays control the valves (see *Figure 2*).

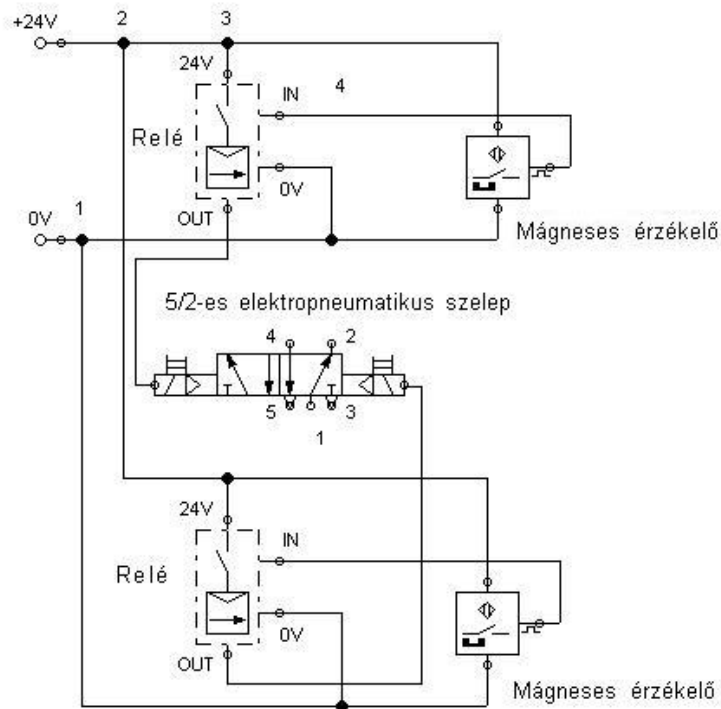


Figure 2. Pneumatic scheme of the first Pneumobile

The lessons and benefits of the competition for students:

- The development of individual components should be carefully done.
- To start work in time, so there is time to handle the problems as well.
- The selection of ready parts is also a serious job.

- The team members learned to work together, to handle different personalities of each other.
- Students began independently to explore the potentials of the pneumatic system.
- They have thoroughly studied bearings in order to reduce the friction.
- They have learned to use basic machine tools, tried to design according to correct production, as they soon faced with the failures of the design during the manufacture of the components.

4.2. 2009 – The second race.

Two team members left, two members remained of them to continue their studies at MSc. level. Two new members were joined. They have already paid attention to the team's work. It was recognized that planning is only in consequence of precise knowledge of the case is worth, so they began to work by searching for sponsors. The engine was retooled on the basis of their experiences and researches, so it seemed to be excellent without any physical changes. They concentrated to modify the suspension. Due to the modifications the vehicle was able to reach higher cornering speeds and was able to safely break from higher speed as well (*Figure 3*). This vehicle each event carried out in the first half of the field and it was second in the event of original construction.



Figure 3. The modified Pneumobile

The lessons and benefits of the competition for students:

- They have improved their communication skills, learned how to present their activities to the sponsors.
- They have become capable of independent work, not waiting for constant confirmation.
- They recognized the need for careful documentation.
- They have obtained new knowledge on the field of pneumatics and bearings.

4.3. 2010 – a brand new vehicle

Two members left the team again, because they have finished their studies. Two new members arrived, one of them was beginner and the other one was experienced, because he was also the racer of the last two years but his team was closed down. I decided as the responsible team leader that they have to build a new vehicle that is much more difficult than the earlier ones because they were to graduate as MSc students. The engine had to be capable of expansion mode; it was unique and was designed with tottering disk (*Figure 4*). Very careful design was essential in case of this vehicle, the usage of CAD, VEM and the computer modelling. The control could not work without electronics, the students prepared control computer is based on microcontroller; so all-new skills were needed. The design and the production of this vehicle was such a higher level job that is neither given to a beginner in the industry. They could apply their previous experiences that they had to share with the new team members. Some pictures probably say more about the development of the vehicle as the text. All of the following figures are made by our students.

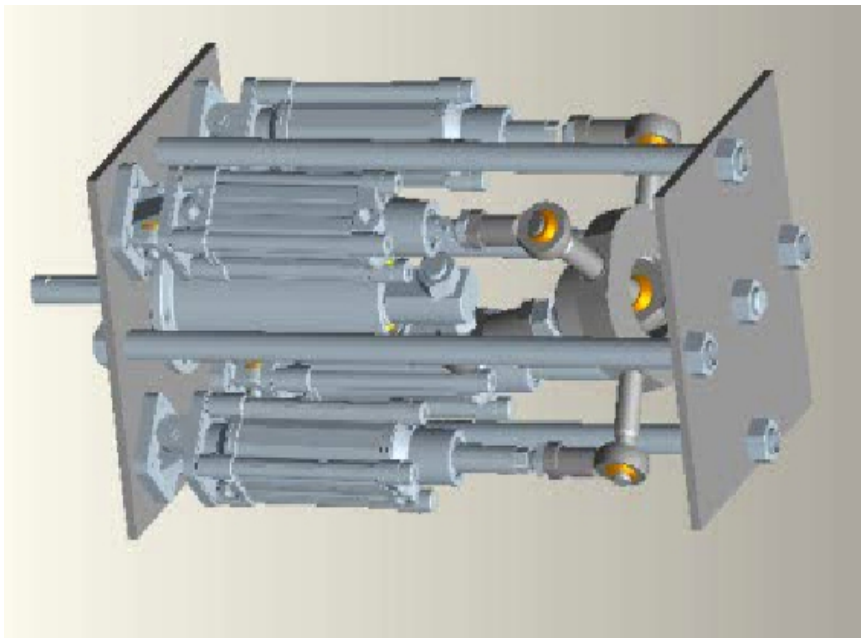


Figure 4. Tottering disk pneumatic motor (2 kW & 10 bar and 95 l/min)

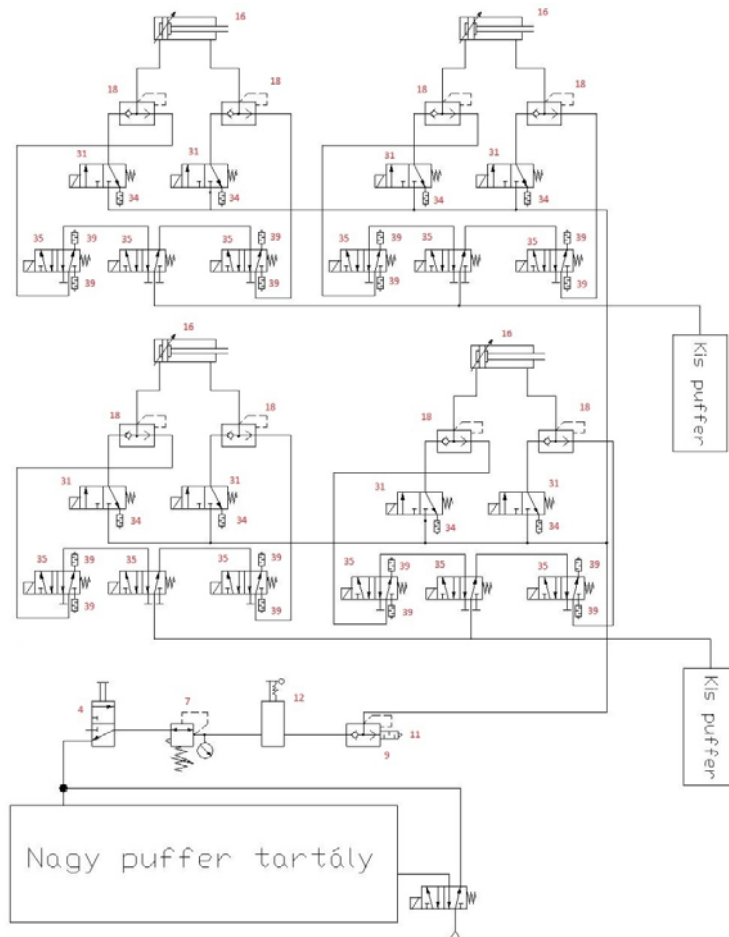


Figure 5. Pneumatic scheme of the motor

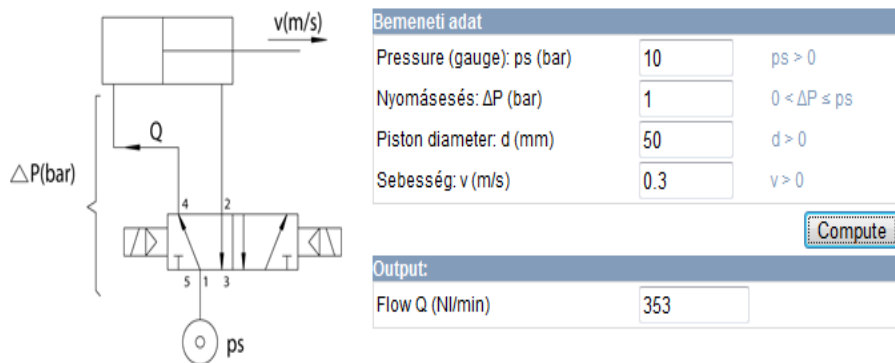


Figure 6. Computer aided calculation of the cylinder speed

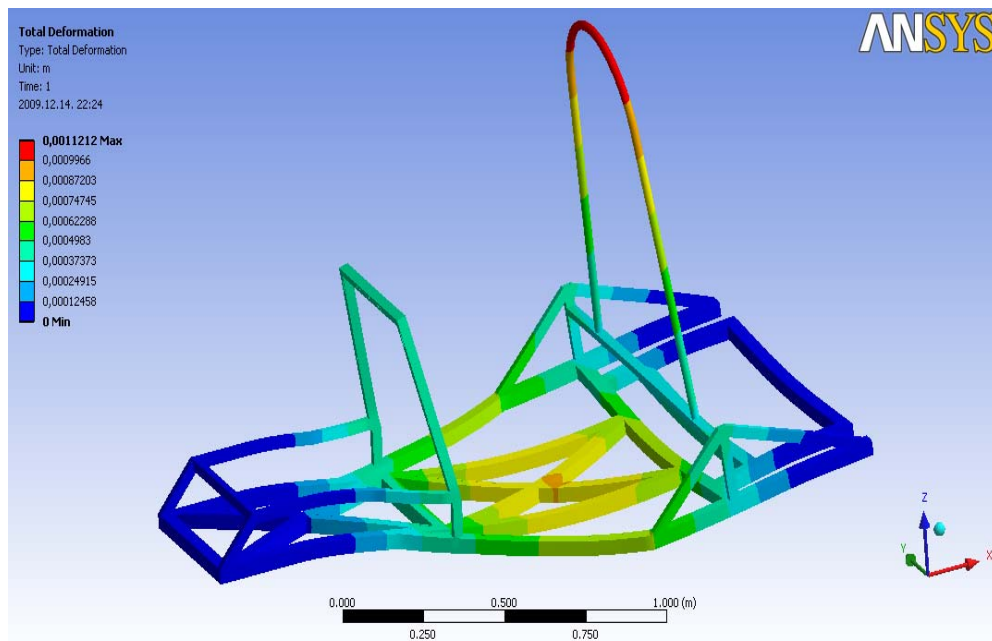


Figure 7. Deformations of the main frame

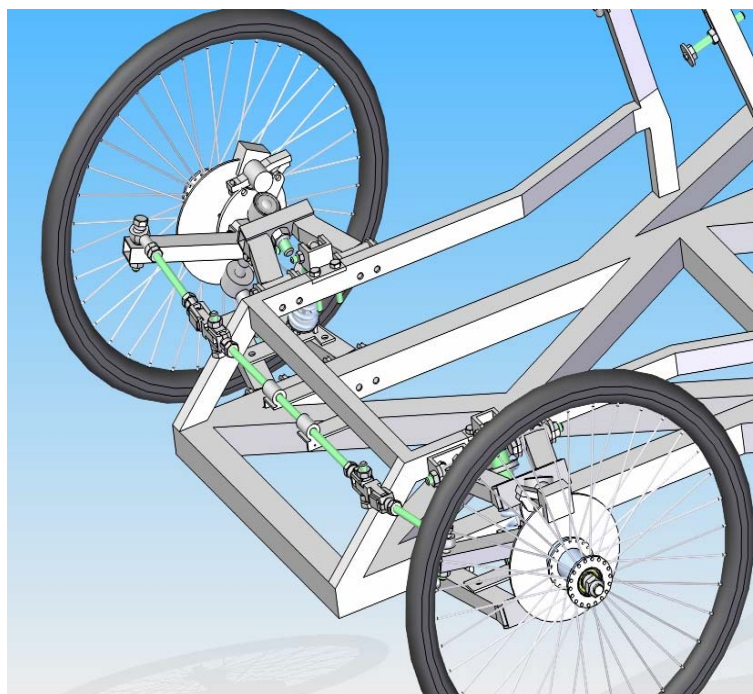


Figure 8. Front suspension and steering system of the vehicle

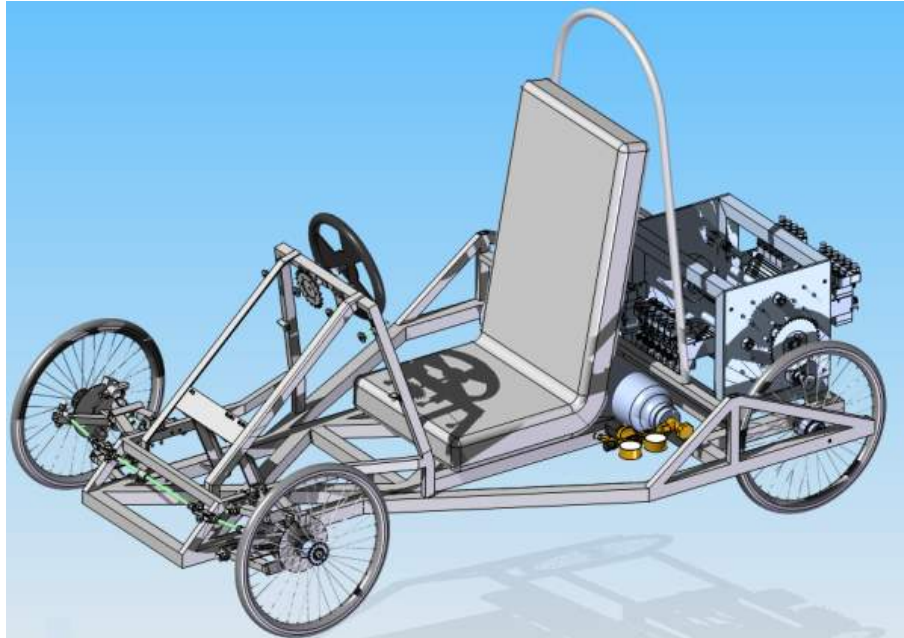


Figure 9. CAD model of the vehicle



Figure 10. The vehicle

The lessons and benefits of competition for students:

- It showed that four of them together are able to plan and carry out a complex automated industrial system.
- They got acquainted with the possibilities and limitations of electro-pneumatic systems.
- All students finished their studies with an excellent qualification.
- All four students immediately found job after graduation.

5. TEAM MEMBERS

Members of the team Keszkosz (2008)

László Attila Kelemen (BSc. mechanical engineering, 3rd year)
Tamás Koncsik (BSc. mechanical engineering, 3rd year)
Gábor Szenczi (BSc. mechanical engineering, 3rd year)
László Szűcs (BSc. mechanical engineering, 3rd year)

Members of the team Keszkosz 2 (2009)

Tamás Faragó (MSc. mechanical engineering, 1st year)
László Attila Kelemen (MSc. mechanical engineering, 1st year)
Gábor Szegedi (BSc. mechanical engineering, 3rd year)
László Szűcs (MSc. mechanical engineering, 1st year)

Members of the team Szélhámosok (2010)

Zsolt Bodnár (MSc. mechanical engineering, 2nd year)
Tamás Faragó (MSc. mechanical engineering, 2nd year)
László Attila Kelemen (MSc. mechanical engineering, 2nd year)
László Szűcs (MSc. mechanical engineering, 2nd year)

Helpers of the team Szélhámosok in 2010 and members of the team Entrópia in 2011

Zsombor Kiss (BSc. electrical engineering, 3rd year)
Péter Magyar (BSc. electrical engineering, 3rd year)

Acknowledgement

“This research was carried out as part of the TÁMOP-4.2.1.B-10/2/KONV-2010-0001 project with support by the European Union, co-financed by the European Social Fund.”

References

[1] http://en.pneumobil.hu/pneumobile_2012/announcement_for_a_competition

TRIZ AND NATURE

ÁDÁM DÖBRÖCZÖNI–CSABA DÖMÖTÖR–JÓZSEF PÉTER
Department of Machine and Product Design, University of Miskolc
H-3515 Miskolc-Egyetemváros

machda@uni-miskolc.hu, machdcs@uni-miskolc.hu, machpj@uni-miskolc.hu

Abstract. One of the significant representatives of design methods known from design science is the TRIZ. The present article compares some of the 40 principles defined by this method with the solutions in nature. This comparison is also beneficial from the point of view that the systematization of effect principles and effect bearer found in nature on the basis of an existing design method will increase their later adaptability.

Keywords: TRIZ, natural structures, inventive problem solving

1. INTRODUCTION

While solving and engineering (or other) task we can often face a problem that the optimal solution falls beyond our field of science or at least it is far away from our narrow field of research. Handling such a problem means extra burden in all cases, which can turn the elaboration of the solution uneconomical considering the unduly long working hours spent on it. The TRIZ theory brings solution to cases like that, with the help of which the developing process may be faster and more efficient.

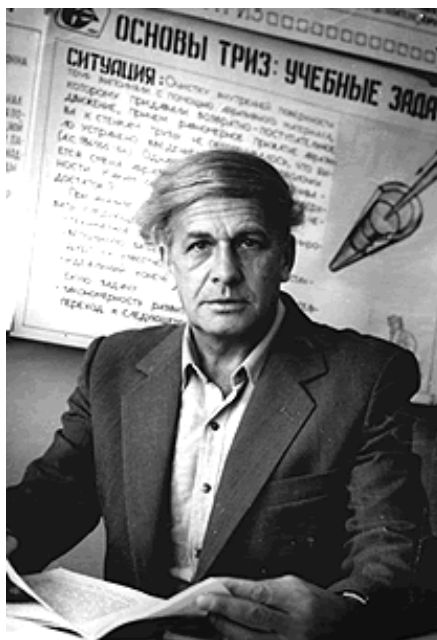


Figure 1. Genrich Altshuller created TRIZ [12]

2. WHAT IS TRIZ?

One of the significant representatives of design methods known from design science is the TRIZ, which was developed by Genrikh Saulovich Altshuller, an Uzbek clerk in the middle of the 20th century. Altshuller studied the patents as an employee of the patent office, trying to find a kind of regularity

After the survey with representative samples, Altshuller divided patents into five categories according to novelty, which can be seen in *Table 1* [16]. On the basis of these data it can be stated that new ideas are rarely taken, therefore it is always worth finding the solution for a special engineering problem among existing effect principles as well as effect bearers.

Table 1.

The classification of patents studied by Altshuller according to the value of novelty

Level	Description	Percentage of studied patents
1	already existing solutions	32%
2	smaller development of an existing system	45%
3	basic development of existing system with the help of known solutions	18%
4	application of new principles with an idea from science	4%
5	developing a new system on the basis of a rare scientific invention	1%

Relying on this, in the 1970s Altshuller created his design method called TRIZ, which comes from the Russian acronym of *Теория Решения Изобретательских Задач*, (*Teoriya Resheniya izobreatatelskikh Zadach*). In the literature it is often called IPS, which stands for the English “*Theory of Inventive Problem Solving*”. The method barely taught at universities starts up from the hypothesis that a special constructional task (or something similar to it) has already been resolved somewhere. Creativity means nothing else but to find this solution and adapt it to the actual task. [5]. The problem solving flowchart of this general problem is presented in *Figure 2*.

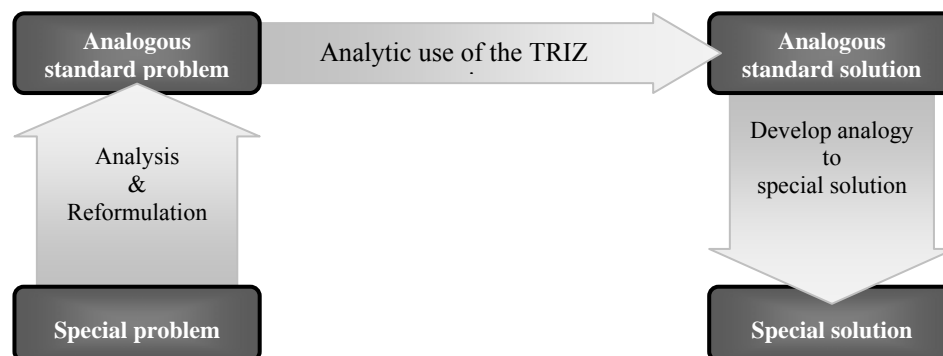


Figure 2. General problem solving model with TRIZ [8]

Assuming that the tasks are essentially built on contradictions, the method looks for solution by resolving them. To achieve this, it defines 40 basic governing principles of problem solving and a two-dimensional contradiction matrix with a size of 39×39. The rows of the square matrix contain the features of a certain developing task considered to be improving, while its columns parallelly have the necessarily worsening features. According to this concept the engineering task is in fact the resolution of the principle according to which the improvement of one parameter results in the the worsening of another one.

Altshuller gives at best 4 pieces of suggestion out of 40 principles (with codes) on each possible conflict as guidance. The order of principles offered as solutions is also important since the principle of the most frequently given solution for the task based on patent statistics stands in the first place of element e_{ij} in the contradiction matrix. Studying the same contradictory functions, but exchanging their "improving" and "worsening" features (i.e. the column and row indices), the matrix offers other principles with other preferences, i.e. $e_{ij} \neq e_{ji}$. (Figure 3).


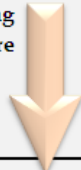
Worsening Feature  Improving Feature 		Weight of moving object	Weight of stationary object	Length of moving object	Length of stationary object	Area of moving object	Area of stationary object	Volume of moving object	Volume of stationary object
		1	2	3	4	5	6	7	8
1	Weight of moving object	-	-	15, 8, 29,34	-	29, 17, 38, 34	-	29, 2, 40, 28	-
2	Weight of stationary object	-	+	-	10, 1, 29, 35	-	35, 30, 13, 2	-	5, 35, 14, 2
3	Length of moving object	8, 15, 29, 34	-	+	-	15, 17, 4	-	7, 17, 4, 35	-
4	Length of stationary object		35, 28, 40, 29	-	+	-	17, 7, 10, 40	-	35, 8, 2,14
5	Area of moving object	2, 17, 29, 4	-	14, 15, 18, 4	-	+	-	7, 14, 17, 4	
6	Area of stationary object	-	30, 2, 14, 18	-	26, 7, 9, 39	-	+	-	
7	Volume of moving object	2, 26, 29, 40	-	1, 7, 4, 35	-	1, 7, 4, 17	-	+	-

Figure 3. A part of the contradiction matrix defined by TRIZ

3. TRIZ PRINCIPLES AND BIOLOGICAL MODELS

Since the theory of TRIZ looks for the solution of a task among already existing principles, it is obvious to widen their scope. Taking into consideration that the living and non-living

world has provided well-adaptable analogy for numerous engineering problems so far, it is worth combining the two fields. First of all, it is practical to parallel the 40 principles of TRIZ and the solutions in nature, if it is possible. The comparison is also useful because integrating the effect principles and effect bearers to be found in nature in an already existing design method, as well as its appropriate systematisation increase the application of these analogies.

First, let us look at the 40 principles of TRIZ.: **1.** Segmentation, **2.** Taking Out, **3.** Local Quality, **4.** Asymmetry, **5.** Merging, **6.** Universality, **7.** Nested doll (Matryoshka), **8.** Anti-Weight, **9.** Preliminary anti-action, **10.** Preliminary Action, **11.** Beforehand Cushioning, **12.** Equipotentiality, **13.** Inversion, **14.** Spheroidality – Curvature, **15.** Dynamicity, **16.** Partial or Excessive Action, **17.** Another Dimension, **18.** Mechanical Vibration, **19.** Periodic Action, **20.** Continuity of Useful Action, **21.** Skipping, **22.** Convert Harm into Benefit, **23.** Feedback, **24.** Intermediary, **25.** Self-Service, **26.** Copying, **27.** Cheap Short-Living Objects, **28.** Mechanics substitution, **29.** Pneumatics or Hydraulics, **30.** Flexible shells and thin films, **31.** Porous Materials, **32.** Colour Changes, **33.** Homogeneity, **34.** Discarding and Re-covering, **35.** Parameter Changes, **36.** Phase Transitions, **37.** Thermal Expansion, **38.** Strong Oxidants, **39.** Inert Environment, **40.** Composite Materials. [1]

The adaptation of these basic principles of engineering approach with the analogies of nature can be a complex and sometimes impossible task. However, if changing the basic principles and conflicts of the TRIZ method or just extending it means that the TRIZ can also be used in other promising fields as a problem solving method, the method can be adapted to natural analogies in a flexible way at a later stage of research.

3.1. Principle 14: Spheroidality – Curvature

The main point of this principle is that straight lines are replaced by curves. This principle can be a solution to a technical problem both on a flat surface and in space. Besides, we can use the principle statically or dynamically. For instance, in many cases, flying seed-corns replace the quick straightforward path to the ground by a much more complicated and longer 'journey'. The aim is assisting to the more efficient spread of the species by having the seeds gone as far as possible. The method is simple, the sail-shaped surface developed on the seed starts rotating with the seed due to the drag, this way slows the landing process. If wind supports this, a seed might even get several kilometres far from the original plant (*Figure 4*).

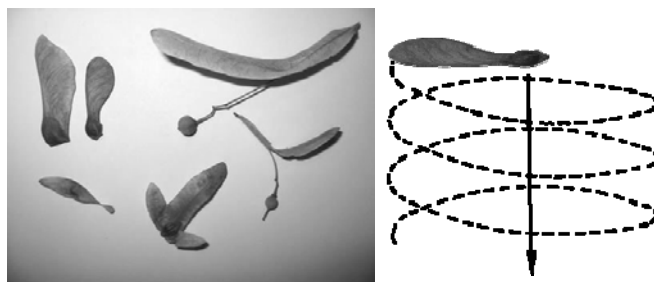


Figure 4. Flying seed-corns

3.2. Principle 15: Dynamicity

Principle 15 suggests creating a system that is able to cope with the environment changes and needs with the help of separating parts or flexible connections. Finding the optimal operating conditions of a structure also belongs to it. The airfoil in birds' wing structure can perfectly be related to the field of engineering. The cross-section of the wing set up by the triad of bones-muscles-and-feathers is perfectly analogous with the airfoil section used in engineering practice. Birds are able to change the inclination of their wings, the density of their feather as well as the size of aerodynamic lift in accordance with the flying destination.



Figure 5. Aerodynamic body of birds and streamlined shape of airplanes [6]

3.3. Principle 22: Convert Harm into Benefit

Koalas live almost entirely on eucalypt leaves. These animals take advantage of an otherwise unfilled ecological niche, because the almost indigestible leaves of eucalypt are low in protein and contain compounds toxic to most species. This is why the koala has a very low metabolic rate and sleeps most of the day. So koalas turn the harmful environment to benefit of easy food. The compromise of this solution is the slow lifestyle in the spirit of energy-saving. (Figure 6. a)

It is not too hard to discover the parallelism between koalas and new cars based on hybrid technologies. These products draw profit from expensive fossil energy resources in the way of efficient marketing of hybrid technology. Nowadays there are a few compromises in it such as low effective range, expensive accumulators, low-built infrastructure or not as low fuel usage as we should wait. But maybe after all it will be the future. (Figure 6. b)



a)



b)

Figure 6. a) Koalas eat eucalyptus,

b) Hybrid vehicles use alternative fuel

3.4. Principle 25: Self-Service

One important element of self-service is using waste resources, energy or substances instead of wasting. Animals - out of their volition, it is true - use their waste as fertilizer in pasture this way help the plants growing.

This Self-Service principle is realized by relieving and amending the tissues in plants and animals too. On this basis scientists from the University of Southern Mississippi developed a new polyurethane film, which generates the self-healing car bodies. Scientists add 0.01 per cent in either a four-molecule oxetane ring or a long rod of chitosan into standard polyurethane. This layer works when exposed to sunlight and the scratch will be gone in an hour. Chitosan is like the chitin known from shells of lobsters and crabs. (*Figure 7*)

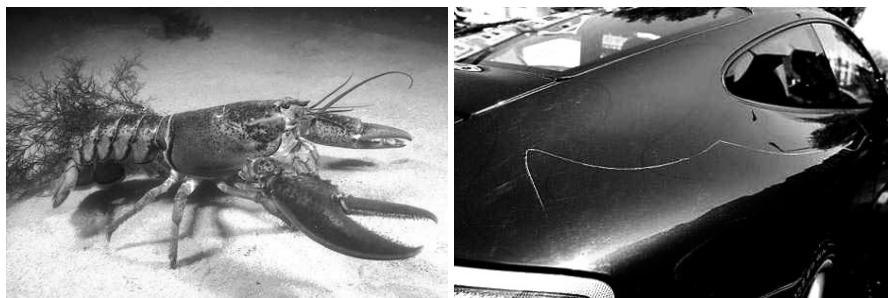


Figure 7. Crabs chitin helps to discover the new self-healing car paint

3.5. Principle 11: Beforehand Cushioning

Practically it means beforehand compensation for the relatively low reliability of an object. For example, preparing things that may fail or go wrong. In nature - and in technical practice - it is a popular principle called the concept of redundancy. In case of the living creatures it is realized as paired organs. Another good sample is the several lines of shark teeth. If one tooth is broken, a new one turns into its place as *Figure 8* shows.

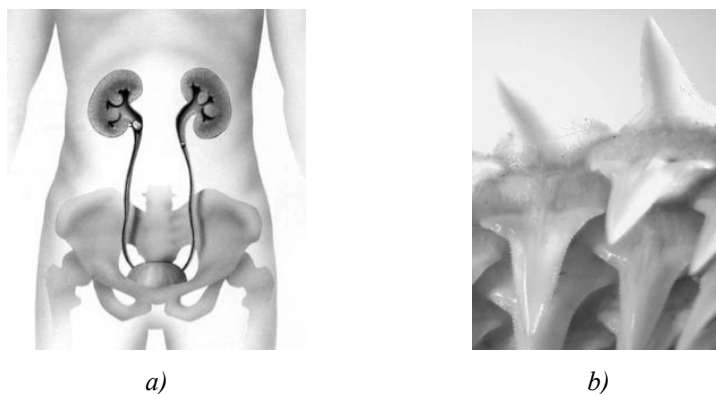


Figure 8. a) Paired organs in human body

b) Shark teeth with several lines of teeth

3.6. Principle 27: Cheap Short-Living Objects

When a designer replaces an expensive object with a cheap one it is a good way to save cost and time. By this principle use engineers breaking piece as safeguard in expensive devices to save it from damages because of overload.

It exists in nature, too. As a defensive strategy the lizard may drop its tail, leaving it writhing on the ground. The writhing tail is intended to distract a predator. The loss of the tail does not harm the lizard. It will grow back once in life of this reptile (*Figure 9*).



Figure 9. Lizard can drop its tail while defending

3.7. Principle 26: Copying

In nature or human practice often arises the demand for trying to use a simple, cheap copy instead of a difficult or expensive structure. The most popular ones are optical copies. Eyes of mammals are really typical and for the luck of insects it is easy to copy. Using eyespots is a general defensive attitude of small animals. When the peacock butterfly detects danger, suddenly open its wings and the flash eyespots. Ordinarily the predator stops the attack. (*Figure 10. a*) Fish also try to deceive the prey or aggressor, because at the first moment it is hard to verify, which is the front of the fish so it wins some time to attack or defend. Additionally there is another function of eyespots in case of fish. They defend their very sensitive and important organs because enemies may attack this spot instead of their real eyes (*Figure 10. b*).



a)



b)

Figure 10. Eyespots a) on wings of butterfly, b) on back of fish

4. CONCLUSIONS

Biological engineering with natural adaptations is the valuable discipline of learning useful structures from nature. We can find several highly effective ideas in both the non-living and living world so we should admit that nature had enough time to perfect its creations, so it is strongly recommended to use this endless free source of ideas.

Acknowledgements

“This research was carried out as part of the TAMOP-4.2.1.B-10/2/KONV-2010-0001 project with support by the European Union, co-financed by the European Social Fund.”

References

- [1] Altshuller, G. S.: *And Suddenly the Inventor Appeared: TRIZ, the Theory of Inventive Problem Solving*. Technical Innovation Center, 1996.
- [2] Altshuller, G. S.: *40 Principles: TRIZ Keys to Technical Innovation*. Technical Innovation Center, 2002.
- [3] Altshuller, G. S.: *Creativity as an Exact Science: the Theory of the Solution of Inventive Problems*. New York, Gordon and Breach Science Publishers, 1984.
- [4] Altshuller, G. S.: *Innovation Algorithm: TRIZ, systematic innovation and technical creativity*. Technical Innovation Center, 2007.
- [5] K. Barry–E. Domb–M. S. Slocum: *TRIZ – What Is TRIZ?* The TRIZ Journal, November, 1996 http://www.triz-journal.com/archives/what_is_triz/
- [6] Glenn Mazur: *Theory of Inventive Problem Solving (TRIZ)*. University of Michigan College of Engineering, 1995.
- [7] A. R. Mansoorian–F. H. Naini: *40 Inventive Principles and Biological Models*. The TRIZ Journal, September 2004, <http://www.triz-journal.com/archives/2004/09/07.pdf>
- [8] A. R. Mansoorian–F. H. Naini: *Integrating TRIZ and Bionical Engineereeng*. The TRIZ Journal, March 2005, www.triz-journal.com/archives/2005/03/07.pdf
- [9] A.R Mansoorian.: *Comparing Problem Solving in Nature and TRIZ*. The TRIZ Journal, April 2007.
- [10] Don B. DeYoung: *Discovery of Design*. Creation Matters, Volume 9, Number 5 September/October 2004 pp. 1, 5, 8.
- [11] Harun Yahya: *Design in Nature*. Ta-Ha Publishers Ltd., United Kingdom
- [12] Gábor Lantos: *Az innováció algoritmusa*. Magyar Grafika 2010/5, pp. 28–32.
- [13] Dr. Donald De Young–Derrick Hobbs: *Discovery of Design – Searching Out the Creator’s*. Secrets Master Books, 2009.
- [14] S. D. Savransk: *Engineering of Creativity Introduction to TRIZ Methodology of Inventive Problem Solving*, CRC Press, 2000.
- [15] J.F.V. Vincent–D.L.Mann (2002): *Systematic Technology Transfer from Biology to Engineering*. Philosophical Transactions of the Royal Society of London Series, Mathematical, Physical and Engineering Sciences, 360: 159–173.
- [16] Á. Takács: *Termékek számítógéppel segített koncepcionális tervezési módszereinek kutatása*. Ph.D. értekezés, Miskolc-Egyetemváros, 2009.
- [17] J. Péter–Cs. Dömötör.: *Principles of the design theory and the nature*. XXVI. MicroCAD International Scientific Conference, Miskolc, 2012. March 29–30.
- [18] Péter, J., Dömötör, Cs.: *Industrial design in development*, Lecture notes, Miskolc-Egyetemváros, 2011.
- [19] Cs. Dömötör–J. Péter: *Natural analogies and TRIZ*. Advanced Engineering, Vol. 6 (2012) No. 1.

NATURAL ANALOGIES AND TRIZ

CSABA DÖMÖTÖR–JÓZSEF PÉTER

Department of Machine and Product Design, University of Miskolc

H-3515 Miskolc-Egyetemváros

machdcs@uni-miskolc.hu, machpj@uni-miskolc.hu

Abstract. From the discipline of design science there are several design methods. One of this is the TRIZ (Theory of Inventive Problem Solving). It is a very important method, because this so popular that man use this not only for technical problems but for agriculture, business, management, economic, marketing, social relations or any other human problems. This paper draws a parallel between TRIZ principles and nature analogies.

Keywords: TRIZ, inventive problem solving, natural analogy, adaptation, bionics

1. INTRODUCTION

When engineer design or develop a product often find the conflict that the optimal solution is out of his or her speciality or simple searching of this may require extreme financial or time input in comparison to starting mission. This may make the development so uneconomical. TRIZ was invented for these situations and making the design process faster and more efficient.

2. BASICS OF TRIZ

TRIZ is one of the most popular design methods that consulting firms teach and many industrial companies use. It was developed in the middle of the 20th century by Genrich Saulovich Altshuller who was born in 1926 and was a patent officer. The acronym comes from the first characters of the Russian name of his theory: Теория Решения Изобретательских Задач (Teorija Resheniyja Izobreatatylskih Zadach). In English we should use “Theory of Inventive Problem Solving” or IPS acronym, too.



Figure 1. Genrich Altshuller, the father of TRIZ [12]

Its hypothesis that there are universal principles of creativity and the creative innovations should be the basis for advance technology. If these principles could be identified and codified, they could be taught people to make the process of creativity more predictable. Otherwise a similar problem of ours has probably solved somewhere so the mission of our creativity is just finding that solution and adapting it to our particular problem. [5]

TRIZ concept supposes that tasks practically based on contradictions so the process tries to eliminate it and this way finds one or more creative solutions. TRIZ research has identified 40 principles that solve the technical contradictions. In the 39×39 contradiction matrix which contain 39 engineering parameters the constructor define the main conflict of special problem and choose from 4 recommended principles as a solution. [2]

But when we have a particular problem in a special field of science or industrial sector, first of all we have to translate it to the language of TRIZ. So we compose the conflicts of our special problem, than make it matched with 39 TRIZ features in the contradiction matrix. The seeking process will give us a standard solution, which is able to be transformed back to special solution. This general pattern of problem solving procedure is shown in the *Figure 2*.

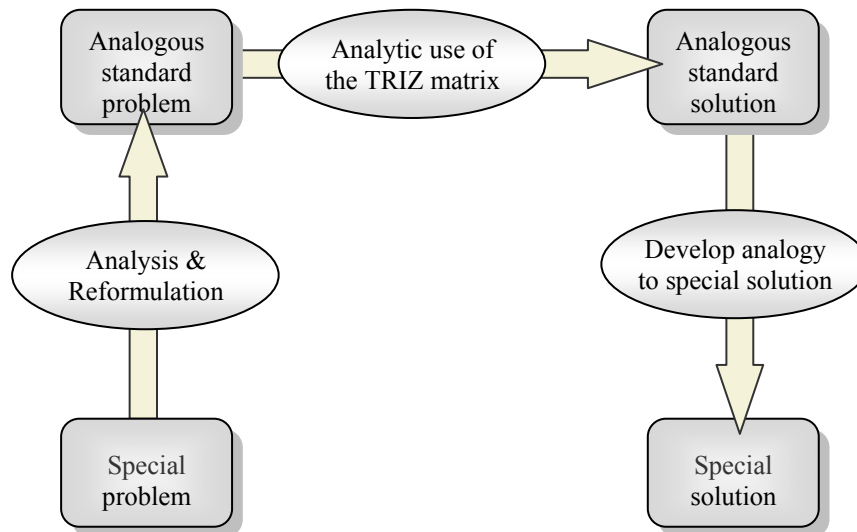


Figure 2. General problem solving model with TRIZ [8]

3. CONNECTION OF TRIZ AND NATURE

Theory of Inventive Problem Solving searches for the solution of special technical problem in existing categorized principles and it is logical to use the biggest database. Unquestionable the largest free mass of principles is in the nature, but we have to make contact between TRIZ and bionical engineering.

At first it is suitable to apply 40 principles of TRIZ, because integrate natural analogies to a popular design method is make the development faster, cheaper, more effective and more enjoyable in fact. Integrate the natural effect-principles or effect-carriers to system of TRIZ increase the adaptability of these analogies. The further parts of the paper present several examples about this potential.

4. ADAPTATION FROM NATURE

First of all shot a glance at the list of TRIZ principles from which few will be discussed on the following pages.

TRIZ principles: **1.** Segmentation, **2.** Taking Out, **3.** Local Quality, **4.** Asymmetry, **5.** Merging, **6.** Universality, **7.** Nested doll (Matryoshka), **8.** Anti-Weight, **9.** Preliminary anti-action, **10.** Preliminary Action, **11.** Beforehand Cushioning, **12.** Equipotentiality, **13.** Inversion, **14.** Spheroidality – Curvature, **15.** Dynamicity, **16.** Partial or Excessive Action, **17.** Another Dimension, **18.** Mechanical Vibration, **19.** Periodic Action, **20.** Continuity of Useful Action, **21.** Skipping, **22.** Convert Harm into Benefit, **23.** Feedback, **24.** Intermediary, **25.** Self-Service, **26.** Copying, **27.** Cheap Short-Living Objects, **28.** Mechanics Substitution, **29.** Pneumatics or Hydraulics, **30.** Flexible shells and thin films, **31.** Porous Materials, **32.** Colour Changes, **33.** Homogeneity, **34.** Discarding and Recovering, **35.** Parameter Changes, **36.** Phase Transitions, **37.** Thermal Expansion, **38.** Strong Oxidants, **39.** Inert Environment, **40.** Composite Materials. [1]

It is apparent, that engineering principles cannot be created simply analogically with natural principles. There is an extra task to find connect between natural analogies and TRIZ principles.

4.1. Principle 11: Beforehand Cushioning

Practically it means that beforehand to compensate for the relatively low reliability of an object. For example preparing such things that may fail or go wrong. In nature - and in technical practice 2 – it is a popular principle called concept of redundancy. In case of the living creatures it is realized as twin organs. Another good sample is the several lines of shark teeth. If one tooth broken a new one turn into its place as *Figure 3* shows.



Figure 3. Shark teeth with several lines of teeth

4.2. Principle 14: Spheroidality – Curvature

In many instances size of linear object should be extreme large but it is able to minimize dimensions with replacing linear to a curve or a sphere at least one direction. For example in the shell of snails [Figure 4. a)] or long slender tube called proboscis of butterflies (Figure 4. b) are utilized this principle in their organs. Mention must be made gliding how birds execute linear upward with circular gliding in rising air flows as the Figure 4. c) shows.

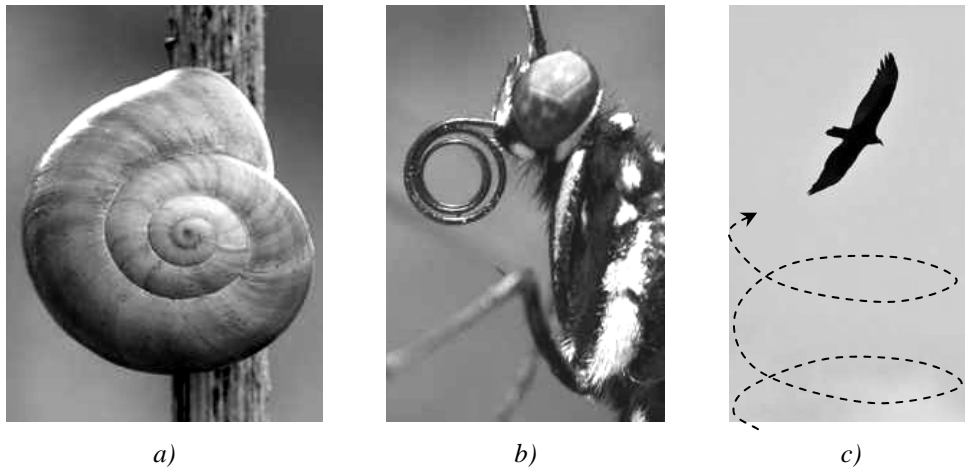


Figure 4. Instead of using linear form use curvilinear ones
a) snail shell, b) proboscis of butterfly, c) gliding of birds

4.3. Principle 15: Dynamicity

Dynamicity in TRIZ also means to design the characteristics of an object, external environment, or process to change to be optimal or to find an optimal operating condition. The octopus also uses flexible connections between its arms and the prey by sucking discs. If the animal expels the water under sucking discs and the pressure under these become less than outside so the pressure strongly compresses together the objects (Figure 5).



Figure 5. Sucking disc of octopus and its adaptation

4.4. Principle 22: Convert Harm into Benefit

Koalas live almost entirely on eucalypt leaves. These animals take advantage of an otherwise unfilled ecological niche, because eucalypt almost indigestible leaves are low in protein and contain toxic compounds to most other species. This is why the koala has a very low metabolic rate and sleeping most of the day. So koalas turn the harmful environment to benefit of easy food. The compromise of this solution is the slow lifestyle in the spirit of energy-saving. [Figure 6. a)]

It is not too hard to discover the parallelism between koalas and new cars based on hybrid technologies. These products draw profit from expensive fossil energy resources in that way of efficient marketing of hybrid technology. Nowadays there are a few compromises in it such as low effective range, expensive accumulators, low-built infrastructure or not as low fuel using as we should wait. But maybe after all this will be the future [Figure 6. b)].



Figure 6. a) Koalas eat eucalyptus, b) Hybrid vehicle use alternative fuel

4.5. Principle 25: Self-Service

One important element of self-service is using waste resources, energy or substances instead of wasting. Animals - out of their volition, it is true - use their waste as fertilizer in pasture this way help the plants growing.

This Self-Service principle is realized with relieving and amending of tissues in plants and animals too. On this basis scientists from the University of Southern Mississippi developed a new polyurethane film, which generates the self-healing car bodies. Scientists add 0.01 per cent is either a four-molecule oxetane ring or a long rod of chitosan into standard polyurethane. This layer works when exposed to sunlight and the scratch will be gone in an hour. Chitosan is like the chitin known from shells of lobsters and crabs (Figure 7).

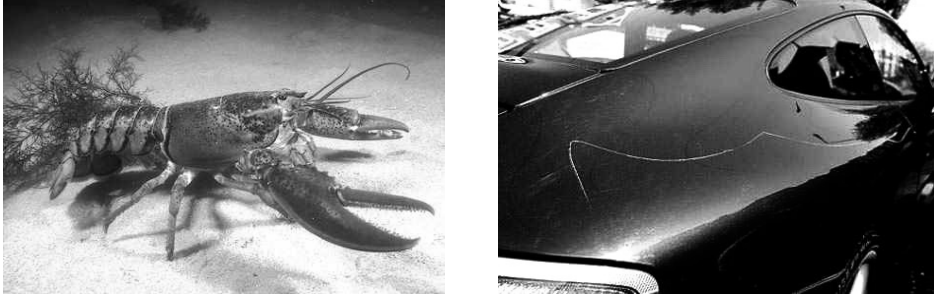


Figure 7. Crabs chitin helps to discover the new self-healing car paint

4.6. Principle 26: Copying

In nature or human practice often arises the claim trying to use a simple, cheap copy instead of a difficult or expensive structure. The most popular ones are optical copies. Eyes of mammals are really typical and for the fortune of insects easily copyable. Using eyespots is a general defensive attitude of small animals. When the peacock butterfly detects danger, suddenly open its wings and the flash eyespots. Ordinarily the predator stops the attack [Figure 8. a)]. Fishes also try to deceive the prey or aggressor, because at the first moment it is hard to verify, which is the front of the fish so it win a short time to attack or defend. Additionally there is another function of eyespots in case of fishes. They defend their very sensitive and important organs because enemies will attack this spot instead of their real eyes [Figure 8. b)].

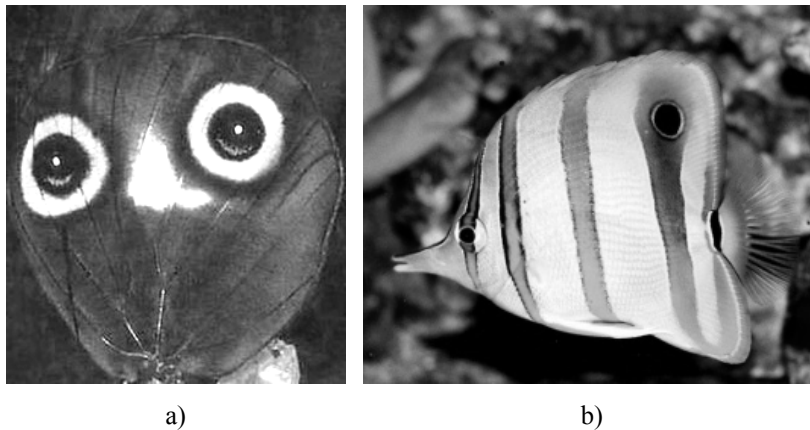


Figure 8. Eyespots a) on wings of butterfly, b) on back of fish

4.7. Principle 27: Cheap Short-Living Objects

When designer replace expensive object with a cheap one it is a good possibility to save cost and time. By this principle use engineers breaking piece as safeguard in expensive devices to save it from damages because of overload.

It exists in nature, too. As a defensive strategy the lizard may drop its tail, leaving it writhing on the ground. The writhing tail is intended to distract a predator. The loss of the tail does not harm the lizard. It will grow back once in life of this reptile [Figure 9].



Figure 9. Lizard can drop its tail while defending

4.8. Principle 28: Mechanics Substitution

In the principle 28 TRIZ proposes that replace a mechanical system with electric, magnetic or electromagnetic fields to interact with the object. Hammerhead shark and duckbilled platypus perfectly utilized this concept. These animals search their food on the bottom of oceans or rivers, but they do not sweep the bed because they have special electric field sensors with that they can detect their prey under the sand or slime.

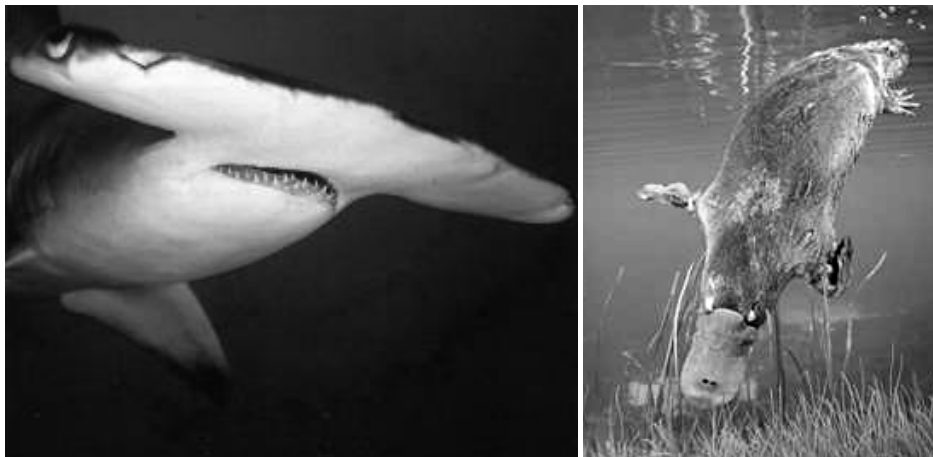


Figure 10. Hammerhead and platypus detect electric signals

4.9. Principle 32: Colour Changes

The simplest way to change optical properties is to highlight or hide components, to pay attention to danger or develop saleability of a product. Chameleon, octopus or sepia found individual solution for keeping them hide or to signify their feelings.

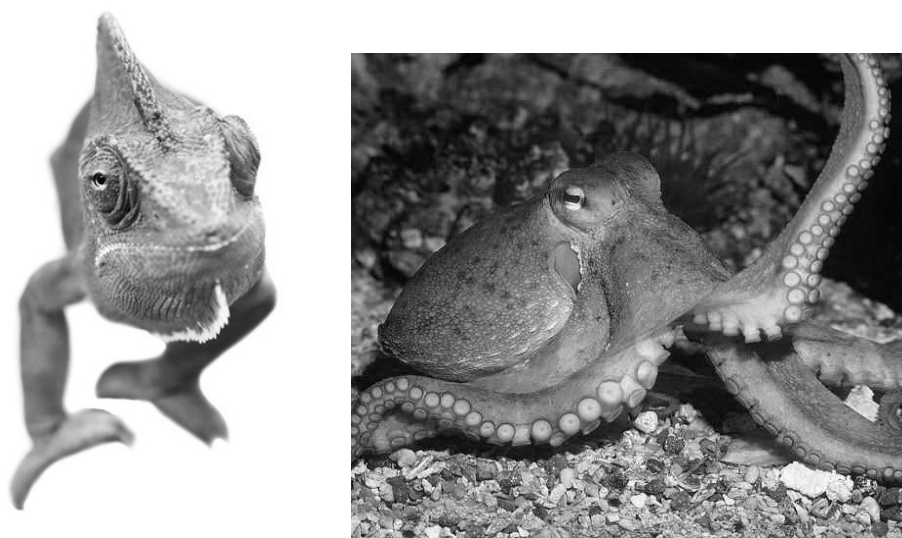


Figure 11. Chameleon and octopus are the artists of colour changing

5. CONCLUSION

Biological engineering with natural adaptations is the valuable discipline of learning useful structures from nature. We can find several highly effective ideas in both the non-living and living world so we should admit that nature had enough time to perfect its creations, so it is strongly recommended to use this endless free source of ideas.

Acknowledgements

“This research was carried out as part of the TAMOP-4.2.1.B-10/2/KONV-2010-0001 project with support by the European Union, co-financed by the European Social Fund.”

References:

- [1] Altshuller, G. S.: *And Suddenly the Inventor Appeared: TRIZ, the Theory of Inventive Problem Solving*. Technical Innovation Center, 1996.
- [2] Altshuller, G. S.: *40 Principles: TRIZ Keys to Technical Innovation*. Technical Innovation Center, 2002.
- [3] Altshuller, G. S.: *Creativity as an Exact Science: the Theory of the Solution of Inventive Problems*. New York, Gordon and Breach Science Publishers, 1984.
- [4] Altshuller, G. S.: *Innovation Algorithm: TRIZ, systematic innovation and technical creativity*. Technical Innovation Center, 2007.

-
- [5] K. Barry–E. Domb–M. S. Slocum: *TRIZ – What Is TRIZ?* The TRIZ Journal, November, 1996 http://www.triz-journal.com/archives/what_is_triz/
- [6] Glenn Mazur: *Theory of Inventive Problem Solving (TRIZ)*. University of Michigan College of Engineering, 1995.
- [7] A. R. Mansoorian–F. H. Naini: *40 Inventive Principles and Biological Models*. The TRIZ Journal, September 2004, <http://www.triz-journal.com/archives/2004/09/07.pdf>
- [8] A. R. Mansoorian–F. H. Naini: *Integrating TRIZ and Bionical Enginereeng*. The TRIZ Journal, March 2005, www.triz-journal.com/archives/2005/03/07.pdf
- [9] A.R Mansoorian.: *Comparing Problem Solving in Nature and TRIZ*. The TRIZ Journal, April 2007.
- [10] Don B. DeYoung: *Discovery of Design*. Creation Matters, Volume 9, Number 5 September/October 2004 pp. 1, 5, 8.
- [11] Harun Yahya: *Design in Nature*. Ta-Ha Publishers Ltd., United Kingdom
- [12] Gábor Lantos: *Az innováció algoritmusá*. Magyar Grafika 2010/5, pp. 28–32.
- [13] Dr. Donald De Young–Derrick Hobbs: *Discovery of Design – Searching Out the Creator’s*. Secrets Master Books, 2009.
- [14] S. D. Savransk: *Engineering of Creativity* Introduction to TRIZ Methodology of Inventive Problem Solving, CRC Press, 2000.
- [15] J.F.V. Vincent–D.L.Mann (2002): *Systematic Technology Transfer from Biology to Engineering*. Philosophical Transactions of the Royal Society of London Series, Mathematical, Physical and Engineering Sciences, 360: 159–173.
- [16] Á. Takács: *Termékek számítógéppel segített koncepcionális tervezési módszereinek kutatása*. Ph.D. értekezés, Miskolc-Egyetemváros, 2009.
- [17] J. Péter–Cs. Dömötör,: *Principles of the design theory and the nature*. XXVI. MicroCAD International Scientific Conference, Miskolc, 2012. March 29–30.
- [18] Péter, J., Dömötör, Cs.: *Industrial design in development*, Lecture notes, Miskolc-Egyetemváros, 2011.

DESIGN PRINCIPLES IN NATURE

CSABA DÖMÖTÖR–JÓZSEF PÉTER

Department of Machine and Product Design, University of Miskolc

H-3515 Miskolc-Egyetemváros

machdcs@uni-miskolc.hu, machpj@uni-miskolc.hu

Abstract. The form-shaping elements, the proportion and the rules of nature have been present in the machine and product design since their beginning. The main reason of this is that the message conveyed by a product design may often become the key to the overall success of the product, thus the designer should return to natural forms rooted deeply in the back of customers' minds. These forms undergo constant changes, yet they carry reliability recalling the living world that carries stability of the existence. This paper focuses on its outstanding role, potentials hidden in the form design and the opportunities of form bearing elements that have already been proved to operate in the nature.

Keywords: natural structures, bionics, design principles, natural adaptation, form, pattern, colour

1. INTRODUCTION

Defining the product's design forms in product development has become of increasing importance in the planning process in the past few years. The main objective of profit-oriented companies is to make profit by designing a product which is appealing to consumers, meets their needs or is likely to do so and sells well. In order to have a constant revenue, novelty should be maintained for the sake of appearances. This is achieved by a completely new design and not by further developing the functions that have a technical content.

2. NOVELTY FAKE

The “facelift” that has widely been used in the automobile industry is a good example of novelty fake when car models that have been on the market for several years undergo a facelift. This facelift trick does not involve any considerable technical changes, but just prolongs the life cycle time of products to some extent.



Figure 1. Renault Mégane II a) Before facelift: 2003–2006, b) After facelift: 2006–2009

It is clearly seen from *Figure 1* that Renault Mégane II has undergone a facelift since both the front grille and the bumper have been redesigned. As for the version of Clio II manufactured since 1998, the changes in its form are even more exciting. Despite the fact that the assessment of the third generation of Clio is about to finish and the launch of Clio IV has already started, the manufacturer of Clio launches Clio II in South America retaining the old techniques without performing any changes in the form. It is quite common in the automobile industry to prolong the life cycle time of cars this way. What is extraordinary is that a relatively old model receives design elements of a new Renault image, which is about to be launched on the market. In order to achieve economic efficiency and to maximize the utilisation of the production line, only a few product attributes have been redesigned such as the bonnet, the boot lid, the bumper and the lights. Other elements and the technical content remained unchanged.



Figure 2. Renault Clio II a) After first facelift: 2001–2006, b) Post facelift: 2012

3. THE ROLE OF FORMS IN THE PRODUCT LIFE CYCLE

In the broad sense of the word, the product life cycle is the period of the time the product is available on the market. Similar to the life cycle of living beings, the product life cycle has several stages where the form plays an important role and has a considerable impact on sales. In the *introduction stage* when the product is introduced to consumers, the form acts as novelty and bears basic dimensions, thus this is the best time for making the public accept the product. In the second stage, the *growth stage*, the product already generates profit the amount of which depends on the form. This is highly influenced by the image shaped about the product. The reliability or even its appearance arising from form is sometimes more important than real and value increasing functions. In the *maturity stage* minor changes in form may delay the beginning of the last stage of the product life cycle, namely the decline stage discussed in the previous chapter. The performed changes will result in gaining some valuable time that can be spent on designing new products, whose developing process may be finished by the time the old product is withdrawn from the market.

The role of design strategy is becoming more and more important so that it can meet the consumer's increasing need for novelty. Since consumers' demand changes more rapidly than in previous years, both the life cycle of a product and the time to be spent on designing

a new product gets considerably shorter depending on the market segments. It is more economical, easier and simpler to redesign the product form, colour and appearance than to invent new functions, materials and technologies or to further develop the available ones.

4. TIMELESS DESIGN FORMS

When a design form of a product is created, referring to “the always fashionable nature” is a good idea in almost all cases, not depending on the prevailing fashion trends. This can be a simple pattern or a combination of colours, a stereotypical design form element or a conventional dimension. The success of products designed this way lies in the fact that these natural design form creating elements acting as well-established form and function carriers that exist in consumers’ mind consciously or unconsciously represent reliability and durability. Since they represent values that most consumers are looking for while purchasing a product, it is worth copying the nature and learning from it.

The act of copying the nature should not be considered as if the consumers were cheated. When the use-value of a product is assessed, it is common and fundamental to take into account the users’ needs, body structure or movements required to perform functions. A right-handed tool or device is adapted to the size of users’ right hand or possible movements (*Figure3*).

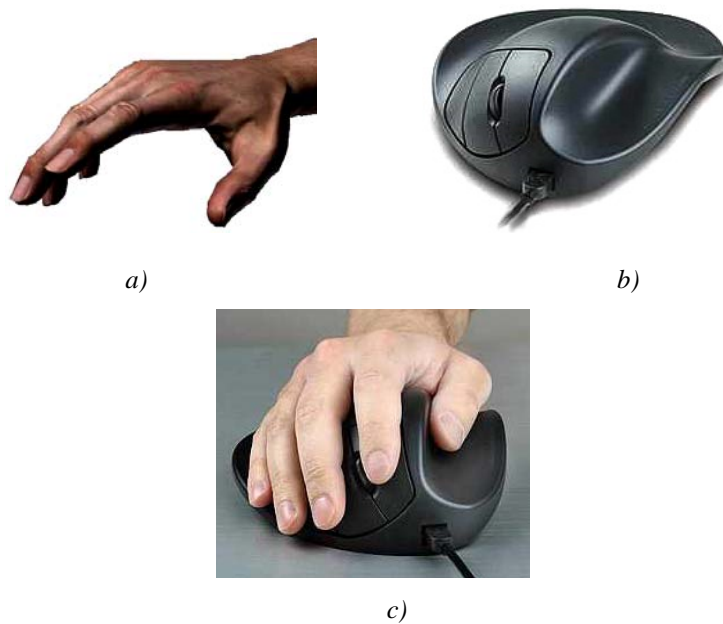


Figure 3. a) Model of the right hand, b–c) Handshoe Mouse manufactured by Hippius

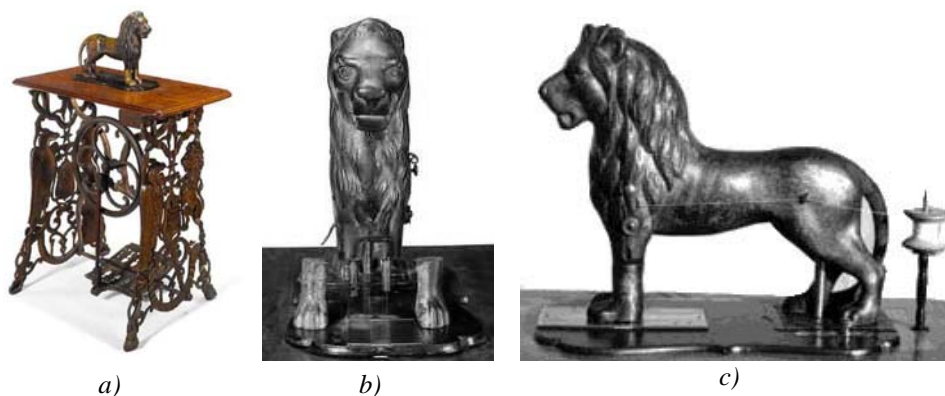
There is also a psychological approach to target groups when a product is designed so that users can identify themselves with it as soon as they see it. Consumers are pleased to purchase and use products that are able to trigger positive feelings in them, which results in accepting shortcomings or technical functions of these products.

The colours and materials of the table resembling the shape of a flower illustrated in *Figure 4* recalls nature. Its simple organic forms attract the target audience that appreciates innovative objects. Another peculiarity of this table is that it consists of five similar elements that are supported by an ordinary wooden structure without any glue or fixing elements and a simple glass surface.



Figure 4. Wood-and-glass coffee table design by Shige Hasegawa

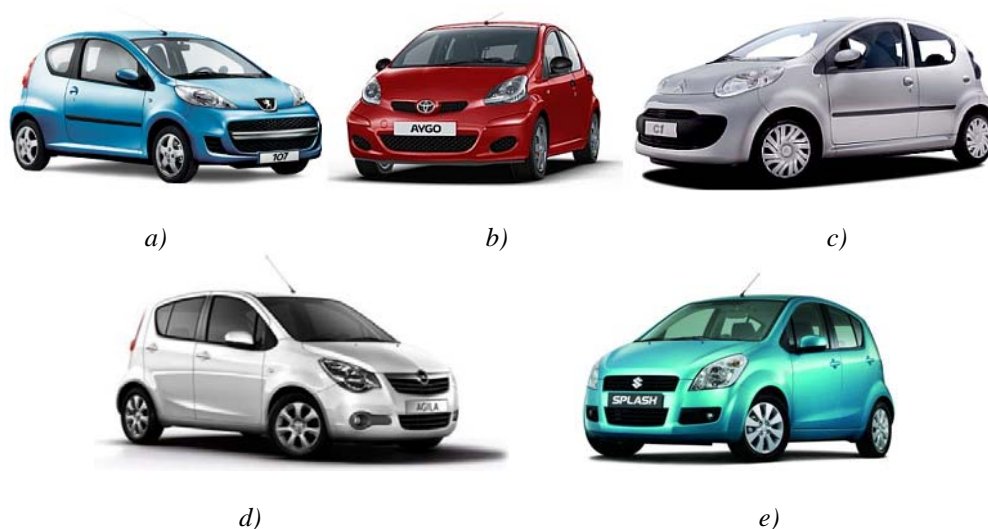
In some cases designers both draw inspiration from the nature and attempt to produce an exact replica of it. Instead of simple design form elements, he moulds complex formations or structures of living beings and pays special attention to precise description of details. The lion-shaped sewing machine shown in *Figure 5* is not used. It serves as a decoration in the room, but can be easily transformed in to a sewing machine. This is rather applied arts than organic design.



*Figure 5. a) “Lion Singer” sewing machine from 1868 by Kimball and Morton Company
b–c) Operating-board of the “Lion” treadle lock-stitch sewing machine*

5. PSYCHOLOGICAL ROLE OF FORMS

There are very few innovative and technical solutions both in the down and middle market products in the automotive industry that differ from competitors. Nevertheless, consumers prefer particular brands to others. Products of different manufacturers differ only in design forms in many cases. Moreover, only logos are different in some down market products. It is obvious that buyers make decisions on the basis of their emotional attachment when purchasing products like that and gives preference to a brand and a design form which is more appealing than the competitors'. That is the reason why manufacturers conduct product development with other brands and even with potential competitors. They appear on the market with products having similar technical solutions developed in cooperation, but different built-in materials. They build on the loyalty of established consumers, on the company's name and brand specific design forms. Companies manage to decrease development costs significantly when developing a product in cooperation and generate profit by well positioning the members of a product family. *Figure 6* illustrates the results of two valuable co-operations. It is clearly seen that the basic dimensions, the main lines of the doors and windows are similar, but the lights, the bumpers and the mud-guards are quite different and belong to different brand images of down market small cars that target different audience.



*Figure 6. a–b–c) Family of Peugeot 107, Toyota Aygo and Citroën C1
d–e) Opel Agila and Suzuki Splash twins*

6. DESIGN AS A SOURCE OF INFORMATION

When users get into contact with a product, they create their first impression based on the product appearance. Consequently, the impression created by forms and colours is of great importance, since it may have an impact on the image of the product function in the future.

6.1. Forms

Design forms may market the product *as high-tech, modern, conventional and retro*. It may illustrate the applied technology or highlight the quality of used materials. The *symmetry* of main elements may carry information transmitted by forms, which suggests reliability. An element placed asymmetrically raises attention to one of the main functions by highlighting it visually, whereas dissection may highlight particular units of different parts. By careful selection of straight and curved lines and surfaces form contrasts can be achieved, which can also be dissected. By using repeating regular form elements, rhythmical appearances create the feeling of considerateness and order in customers.

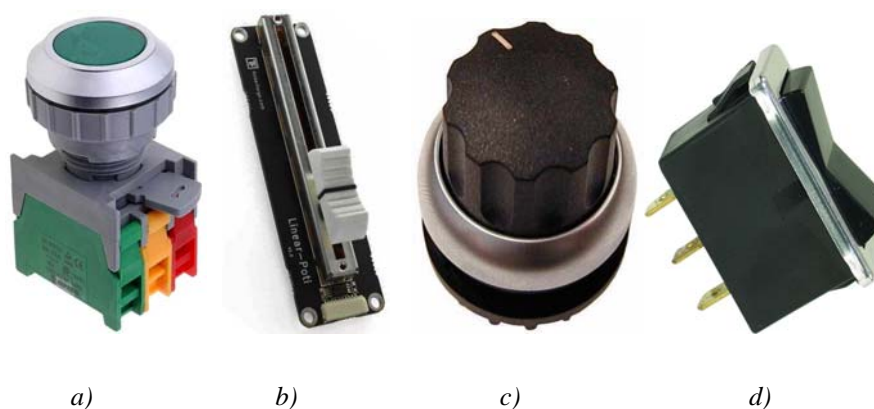


Figure 7. Handling operators:

a) press-button, b) puller, c) rotary switch, d) tumbler switch

Using these design principles we can achieve, for example, to draw a conclusion on the basis of the shapes and striations of different buttons about the movements needed for usage. These are very important pieces of information that should be available during the usage independently from the product description. The shapes of press button, puller, rotary switch and tumbler switch can be recognized easily and they serve the above mentioned aim (Figure 7).

6.2. Colour scheme

Beside the shape, colour scheme is also the part of the design, since the designer is able to express information in the same way as colours have outstandingly important signalling and warning functions. Association of ideas are instinctive in people, because they are deeply coded in them. If fire is mentioned, for instance, the so called luminous flame (having the shades of orange and red depending on the proportion of oxygen, coal and hydrogen, but within a relatively narrow range of colour) occurring at burning materials rich in coal, comes to most people's mind. Contrary to this, ice as the most common cold medium, appears in the shades of blue. This way we consider the shades of red to be hot and the shades of blue are considered to be cold. Even the fact that nowadays we more frequently see the

blue flame in gas appliances (which forms at the perfect burning of methane) would not change this attitude.

According to this, if a surface is hot and we want it to be felt hot, the most appropriate thing is to use the shades of red. People's mood can be influenced by the basic principles of colour dynamics, or we can even compensate the sense of heat, noise and smell occurring due to environmental effects. For instance, the shower with blue and red LED lights in *Figure 8*, affects not only the user's mood, but the sense of heat can also be increased by a few degrees if we use the appropriate colours.

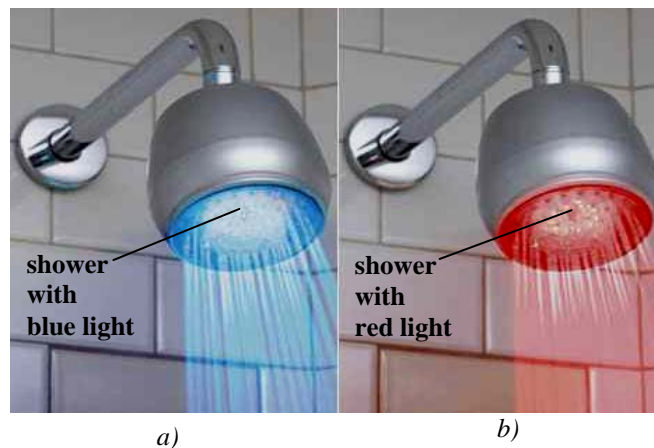


Figure 8. LED shower a) with BLUE light, b) with RED light

The use of full colours suggests dynamism or the wish to play. The most important functions can be highlighted by bright colours in a colour scheme with grey. The combination of yellow and black is one of the most appropriate options used for drawing attention to something. Since the living world also uses it due to its outstanding colour contrast for warning, it is also suitable for drawing attention to artificially developed engineering objects (*Figure 9*).

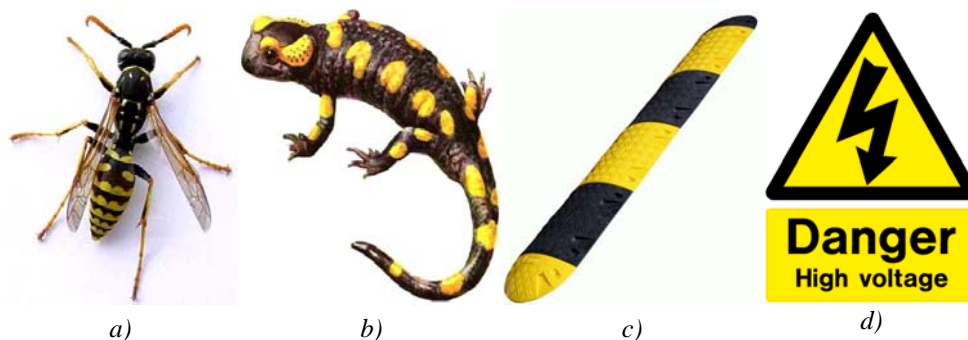


Figure 9. Black and yellow signs:

a) wasp, b) salamander, c) speed bump, d) caution board

While studying the contrast of different colours we should not forget about the phenomenon of the simultaneous contrast effect, which was one of the greatest observations made by Leonardo da Vinci. Its main point is that “*an object seems to be less light among the same light objects if its surroundings are the most white and that is the object to seem more white if the background is darker.*” It can be said about the whole spectrum that in reality all colours are considered to be different due to the background.

Using this phenomenon we can compensate a discoloration or difference in shades appearing due to technology with a well chosen background colour. The other scope of application of this phenomenon occurs, for example, when the same medium grey buttons are used with dark or light background. This way significant cost saving can be realized by decreasing the number of spare tools despite the product’s several, even strikingly different colour scheme. In certain cases colours and shapes are used similarly to animals for hiding away in the environment. The main point is that we choose the colour of a spare part so that it would assimilate with the environment. For example, wires, cables and other equipment of a room or machine can optically be hidden.

6.3. Design as marketing

An important feature of the information package behind the design is that it gets to the user in a nonverbal way, and the user feels it much more authentic as he does not read about it in a description popularizing the product, but he finds it out by himself. Therefore, certain data of the product description serve to enforce the impressions based on the shape and colour. That is why we should make an effort to achieve the harmony between the functions and design, because without this the product will promise something else by its design not the things that it can offer to the user.

During the product designing process it is emphasized that signals transmitted by the design should be clear for the widest range of consumers. It is important that the clear message of design elements bearing information would depend – to the least extent – on the sex, age, education, social and cultural or geographical sense of belonging. It is obvious that it offers a firm solution to such a design task if we start with coded impressions instinctively developing in people.



Figure 10. a) Shape of falling drop b) “Las Crono 2011” long tear drop shaped aero helmet

In Figure 10 a helmet having the shape of a falling waterdrop can be seen. It is not only streamlined, but its extra shape elements and dynamic paint makes this property even more

visible. This aerodynamically perfect shape was inspired by nature. Its developers found the solution of minimum function of drag coefficient in the dynamically deforming shape of the falling plastic liquid drop.

7. SHAPE ELEMENTS

Forms most often consist of basic geometric shapes: *point, straight line, flat surface, circle, square, cube, prism, pyramid, cone, sphere, cylinder* etc. All of these shapes can easily be interpreted, they are regular, and these features result in a shape suggesting reliability. However, amorphous and complicated shapes are recurrent motifs, which are used by the designer to suggest movement, creativity, ease, or naturalness, since geometric shapes are rarely clear in nature. Despite this fact basic geometric shapes can also be used effectively, unless we forget about the messages of *proportion, rhythm, symmetry, orientation, articulation, or shape contrasts*.

The build, proportions, size or even colours are subjected to the functionalism needed for sustainment. The minimum usage of material and energy appears to be an important subtask beyond basic functions. Similarly to the living world, expediency is a primary aspect in the case of everyday objects, this way basic proportions are also defined by functions. Within it, the designer still has the opportunity to create the final shape of the product with eye-catching proportions.

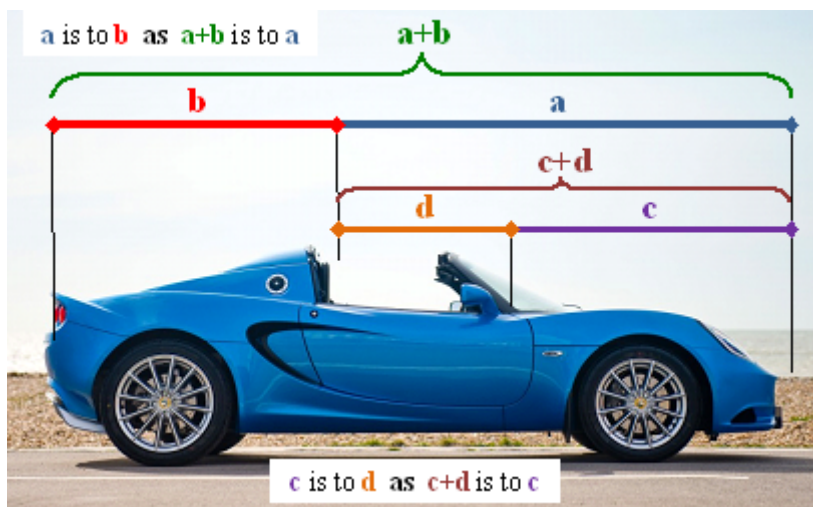


Figure 11. Lotus Elise and golden section

Ancient scientists determined beauty according to the proportion of the human body, i.e. the golden section, in which the ratio of shorter and longer parts corresponds with that of the longer part and the whole. An object built on principles like that makes the viewer feel the lasting beauty and reliability due to its natural proportion. The proportions of the body of the *Lotus Elise* sports car built on the basis of golden section are shown in *Figure 11*.

Another basic element appearing in nature and engineering practice is the hexagon. As these two-dimensional figures can be put next to each other optimally without any dead

space, the length of walls surrounding the cells projected to the area unit can be minimized alongside with maximizing the usage of space on a flat surface. Therefore, the honeycomb structure in the case of bees and wasps perfectly exemplifies the intention for the principle of minimum material and energy in the living world. The other advantage of this kind of construction is the structure, which is rigid despite the thin walls – and this is one of the most important conditions of engineering tasks (*Figure 12*).



Figure 12. Hexagonal alveole structure

8. CONCLUSIONS

Although it falls into oblivion, mankind has spent much more time close to nature than far away from it. Despite new impulses, social effects or changed behaviour patterns earlier experience gained by our ancestors instinctly come up to the surface. In the subjective science of design it is worth finding stable guidelines that are related to these associations of ideas coded in our mind. This way we can develop products with design accepted more and more widely.

Acknowledgement

“This research was carried out as part of the TÁMOP-4.2.1.B-10/2/KONV-2010-0001 project with support by the European Union, co-financed by the European Social Fund.”

References

- [1] J. Péter– Cs. Dömötör: *Principles of the design theory and the nature*. XXVI. MicroCAD International Scientific Conference, Miskolc, March, 2012.
- [2] J. Péter–Cs. Dömötör: *Industrial design in development*. Miskolc-Egyetemváros, 2011.
- [3] T. Szentpéteri: *Design fogalommeghatározások*. Zsennye, 1983, p. 27.
- [4] Gy.Lissák: *A formáról*. Láng Kiadó és Holding Rt., Budapest, 1997.
- [5] G. Pahl–W. Beitz: *A géptervezés elmélete és gyakorlata*. Műszaki Könyvkiadó, Budapest, 1981.

ASYMMETRICAL TEETH MESHING NEAR GENERAL CENTRE DISTANCE

ZSUZSA DRÁGÁR–LÁSZLÓ KAMONDI

Department of Machine and Product Design, University of Miskolc

H-3515 Miskolc-Egyetemváros

machdzs@uni-miskolc.hu, machkl@uni-miskolc.hu

Abstract. In propulsion technique applied in every day practice the load of gears is usually one directional or two directional, but the stresses on the tooth flanks are not the same degree. Numerous researches verify that departing from standard symmetric toothed wheels, the load carrying capacity of gears can be increased by asymmetric teeth. Effects of deviation from standard have numerous consequences, which have to be examined. For example geometric results, especially, when the gear pair is not fitted in elementary centre distance, but general centre distance. We would like to answer that, what kind of addendum modifications have to be applied to ensure backlash-free engagement.

Keywords: tooth shape, tooth root curve, tooth root stress, asymmetrical teeth, general teeth, backlash-free engagement.

1. APPLICATION OF GEARS

Functional units and gear drives, which modify parameters of movement, take a great part in energetic chain realized in mechanical products. In gear drives continuous one-directional rotation of the toothed element pairs can be ensured by a suitably integrated rotation reversing facility. These transmission elements of movement realize either exact map of movement or large load transfer. The tooth shape plays a great role in the determination of transmission parameters. Deviation from symmetric tooth shape generates questions about design, manufacturing and certification (dimensioning, reliability) [3]. The most important function of gear drives applied in driving mechanisms is steady transmission of movement during working [1]. Considering the single forms of motion, rotation would be changed, for example by the reduction of revolutions.

Gearings can essentially be divided into two groups, kinematical and load transfer drives [1]. These functions mean different requirements for the teeth. Kinematical drives have to ensure precise angle rotation. These drives are characterized by small backlash. In load transfer drives the backlash is larger, which helps accommodation to the fluctuation of temperature and reliability of gears during working respectively.

In the drive train of mechanical systems there is a usual functional claim, where the energy in a unit of time, which is the source of power, should be available for any working machine. This availability taking the energy components into consideration can be changed discreetly or continuously in a range. These functional units are the driving mechanisms.

One element of the system is denoted functionally by the structure element in *Figure 1*, which can be examined from inside as if it would be an unknown construction.

The input is described by the power $P_1(t)$, with its components in the energy chain that are the moment $M_1(t)$ and the angular speed $\omega_1(t)$. This characterizes the source of energy at the same time.

The output is marked by the power $P_2(t)$, which due to the construction of the system element depends on the system controller information. These are the stage contact (i), which can be discrete or time controlled - it gives the system transmission - and the functional δ , which denotes the direction of rotation inside the system.

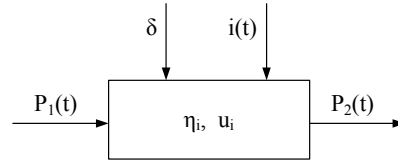


Figure 1. Functional unit describing driving mechanism

Based on the above mentioned it can be written that

$$P_1(t) = M_1(t) \cdot \omega_1(t), \quad (1)$$

$$P_2(t) = M_2(t) \cdot \omega_2(t), \quad (2)$$

$$\frac{\omega_2(t)}{\omega_1(t)} = u_i = f(i), \quad (3)$$

together with the appropriation of the formulas (1), (2), (3)

$$M_2(t) = \eta_i \cdot M_1(t) \cdot u_i, \quad (4)$$

where η_i is the efficiency which belongs to the controlled settings (stages) of the system element. Examining the system so that in point $\omega_1(t)$ regulated rotating movement should be mapped as well, from formula (3) it follows that

$$\omega_2(t) = \delta \cdot u_i \cdot \omega_1(t), \quad (5)$$

where δ is a $\{-1, 0, 1\}$ -value function, which is a further directional input and defines the rotation direction character of the input (given direction, stillness, change of direction). To the outgoing moment of the system generally it can be written that

$$M_2(t) = \delta \cdot \eta_i \cdot M_1(t) \cdot u_i. \quad (6)$$

It can be concluded from the above that improving the strength of asymmetric teeth, their geometrical examination has to be performed, too. The question is raised so that what kind of geometry can be applied, and how it can be changed and controlled in order that the meshing conditions, the teeth margins can be completed.

2. GENERALIZATION OF THE TOOL BASIC PROFILE

In order to study of effects of asymmetry, one of the first steps is to determine the basic profile of the tool, which generates the gear teeth [4]. Later changing possibilities of the meshing characteristics can be examined with this [2]. Points of the basic profile are arranged in an xy orthogonal coordinate-system in such a way that the middle line of the basic profile overlaps with the x axis of the coordinate-system, the y axis divides longitudinal the tooth of the basic profile into halves. This arrangement was shown in *Figure 2*.

The basic profile is constituted by straights and curves connected to one another, equations determining them must be described in the xy coordinate-system. The straights construct the edges at the sides, head and at foot line of the basic profile. The curves are the roundings between the straight parts. The rounding between the side edge and the head edge has a great influence on the shape of the tooth root profile [1]. The equations of the straights can be given as a function of x in the xy coordinate-system. These straights are marked I. and II. in *Figure 2*. The straight I. which forms the edge at the side of the tool basic profile crosses the point P_3 on the x axis in a given direction. The straight I. encloses $(90^\circ + \alpha)$ with the x axis, where α means profile angle. The coordinates of the point P_3 (7) can be read from *Figure 2* and by this the equation of straight I can be written (8).

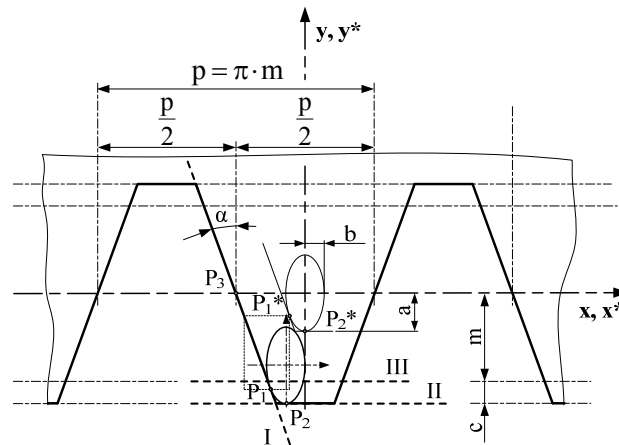


Figure 2. Tool basic profile with ellipse curve [4]

$$P_3(x_3; y_3) = P_3\left(-\frac{\pi \cdot m}{4}; 0\right), \quad (7)$$

$$y_1 = -\frac{1}{\tan \alpha} \left(x + \frac{\pi \cdot m}{4}\right). \quad (8)$$

The straight II, which defines the straight part of the tool basic profile, is parallel with the x axis, and the distance between them is equal to the sum of clearance and module. The equation of the straight II. can be given by formula (9).

$$y_{II} = -(m + c) = -(m + c \cdot m) = -m \cdot (1 + c^*) . \quad (9)$$

To the rounding of the head edge and the side edge for example an arch of a round or an ellipse can be taken. Another curve can be used as well, which is attached to a suitable reference point. Another x^*y^* coordinate-system can be used to write down the equation of the curve. The origin of this new coordinate-system overlaps the origin of the xy coordinate-system. As an example, let the rounding of head edge and side edge be an ellipse arch, whose major axis (2a) is fitted to the y axis while its minor axis (2b) is fitted to the x axis. From well known equation of the ellipse value of y can be expressed (10).

$$y^* = \sqrt{\left(1 - \frac{(x^*)^2}{b^2}\right) \cdot a^2} . \quad (10)$$

After tangents of the curve are defined (11) on the understanding that gradients of the tangents be equal with gradients of the straights I. and II. Thus the tangents are parallel with the straights I. and II. The tangents on the points P_1^* and P_2^* are tangential to the curve (12). After differentiation formula (13) is offered.

$$\frac{dy^*}{dx^*} = (y^*)' , \quad (11)$$

$$\frac{dy^*}{dx^*} = \frac{dy_{I,II}}{dx} \rightarrow P_{1,2}^* (x_{1,2}^* ; y_{1,2}^*) , \quad (12)$$

$$\frac{dy^*}{dx^*} = (y^*)' = \frac{-\frac{a^2}{b^2} \cdot 2x^*}{2 \cdot \sqrt{a^2 - \frac{a^2}{b^2} \cdot (x^*)^2}} , \quad (13)$$

If the formula (13) equals with gradient of the straight I. and x^* is expressed from the equation, then formula (15) is given. From the result of the extraction of root the negative value is considered. This equals to the coordinate x_1^* of the usual point P_1^* later.

$$(y^*)' = -\frac{1}{\tan \alpha} , \quad (14)$$

$$x^* = -\frac{1}{\sqrt{\frac{1}{b^2} \left(\frac{a^2}{b^2} \cdot \tan^2 \alpha + 1\right)}} . \quad (15)$$

After this the origin of the ellipse curve is moved (shifting in the direction of x and y) in the xy coordinate-system so that the tangents and the straights I. and II. are covered with one another. This time the rounding between the head edge and the side edge which are

By exact description of the tool basic profile definite teeth can be generated. In the course of generalization by changing the parameters of the basic profile for example the profile angle, the rounding of the head edge, the combination of the rounding curves, in different ways on the two sides of the profile, rows of asymmetric non standard teeth can be originated.

3. PROFILE CHARACTERISTICS OF ASYMMETRIC TEETH FOR MESHING NEAR GENERAL CENTRE DISTANCE

In gear pair design the tooth shape has a great importance. On the one hand it has its importance in the precision of the movement mapping, on the other hand in the determination the load carrying capacity. The base profile parameters do not have an effect on kinematic precision, it is affected by the boundaries of the production technology possibilities.

Beside kinematic movement mapping the dynamic behaviour of the driving has a significant role. Because of the changing tooth stiffness the meshing process oscillates periodical vibration. In the consequence of the oscillation the contacting surfaces in mesh can separate, which causes that not the functional surfaces are touching. This time the meshing continuity is broken, which can be regulated by the degree of backlash release.

However the load carrying capacity depends largely on the geometric determination of the contacting surfaces, which influences the tooth surface fatigue. The fatiguing stress forming in the tooth root is defined by the tooth root geometry – namely, at a how large degree the nominal tooth root stress is increased by the stress correction factors from geometry. The tooth root geometry depends on the tooth generating base profile. Departure from the symmetry can prosperously influence the geometry of the tooth surface and the tooth root.

The meshing gears determine elementary teeth from the basic geometrical data. In the event when the axis distance of the driving is not elementary but general then addendum modification is needed for the backlash-free engagement. In case of symmetric tooth shape known calculation methods are available [1]. By non-symmetric tooth shape relations like this are not yet disposable. In order to determine the addendum modifications some basic geometrical ideas must be introduced.

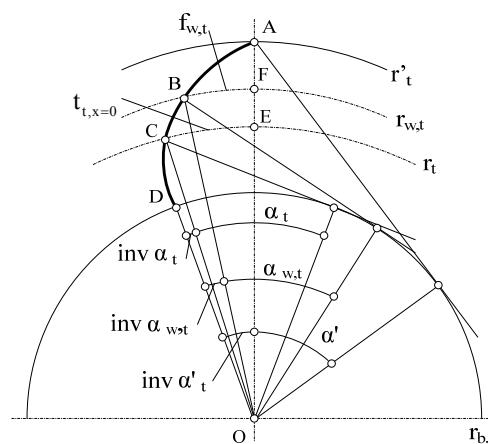


Figure 4. Explanation the tooth profile part thickness belonging to the tooth

3.1. The tooth thickness of the asymmetric teeth

The condition of backlash-free engagement is that the pitch on the rolling circle and the sum of the tooth thickness on the rolling circle are the same. The tooth thickness on the rolling circle can be determined with the help of the two tooth profiles. See *Figure 4*, which explains for a non-symmetric case one tooth profile side. This side is on the basis of indexing the coast one (t). The tooth thickness part belonging to the tooth profile is $f_{w,t}$. In order to define $f_{w,t}$ it can be reached by the following way.

The arch on the pitch circle between the points C and E can be determined from the pitch (p) explained on the base profile. First of all the pitch p has to be divided half-and-half between the tooth and the tooth space (groove) defined on the basic profile (19)

$$s_{x=0} = \frac{m \cdot \pi}{2}. \quad (19)$$

The different arched tooth profiles can be placed on the pitch circle so that the tooth thickness (19) is divided between the arches. The proportion is expressed by the factor λ , which suitably be now 0,5. Thus the tooth thickness belonging to the coast side without addendum modification ($t_{t,x=0}$)

$$t_{t,x=0} = \lambda \cdot s_{x=0} = \frac{m \cdot \pi}{4} \quad (\lambda = 0,5). \quad (20)$$

Take the profile displacement (21) into consideration, the tooth thickness on the coast side ($f_{w,t}$) can be written by formula (22), then developing it relation (23) is got

$$t_{t,x \neq 0} = t_{t,x=0} + m \cdot x \cdot \operatorname{tg} \alpha_t = \frac{m \cdot \pi}{4} + m \cdot x \cdot \operatorname{tg} \alpha_t, \quad (21)$$

$$f_{w,t} = \left(\frac{t_{t,x \neq 0}}{r} + \operatorname{inv} \alpha_t - \operatorname{inv} \alpha_{w,t} \right) \cdot r_w, \quad (22)$$

$$f_{w,t} = m \cdot \frac{\cos \alpha_t}{\cos \alpha_w} \left(\frac{\pi}{4} + x \cdot \operatorname{tg} \alpha_t + \frac{Z}{2} (\operatorname{inv} \alpha_t - \operatorname{inv} \alpha_{w,t}) \right). \quad (23)$$

The tooth thickness part on the drive side ($f_{w,m}$) on the pitch- and rolling circles can be written in a similar way, only the signs of the indexes change. The two tooth thickness parts express the real tooth thickness, namely

$$s_w = f_{w,t} + f_{w,m}. \quad (24)$$

3.2. Special circles of the tooth profiles

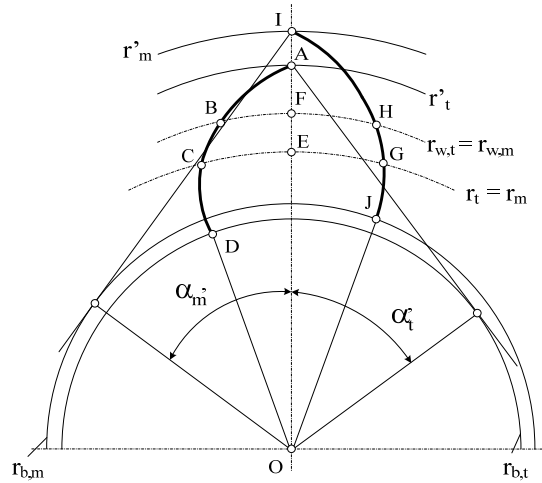


Figure 5. Positions of the drive and the coast tooth profiles

The tooth thickness parts have to be determined on optional circles, because at the teeth margin examination the top land thickness is necessary. It can be given by the sum of the tooth thickness parts. The determination the tooth thicknesses, within the tooth thickness parts on an optional circle is the condition of that the permissive mark of the addendum modifications to the general centre distance be definable. At the same time for the construction it is similarly important that the top land thickness on the addendum circle be determinable as a condition inside the teeth margin.

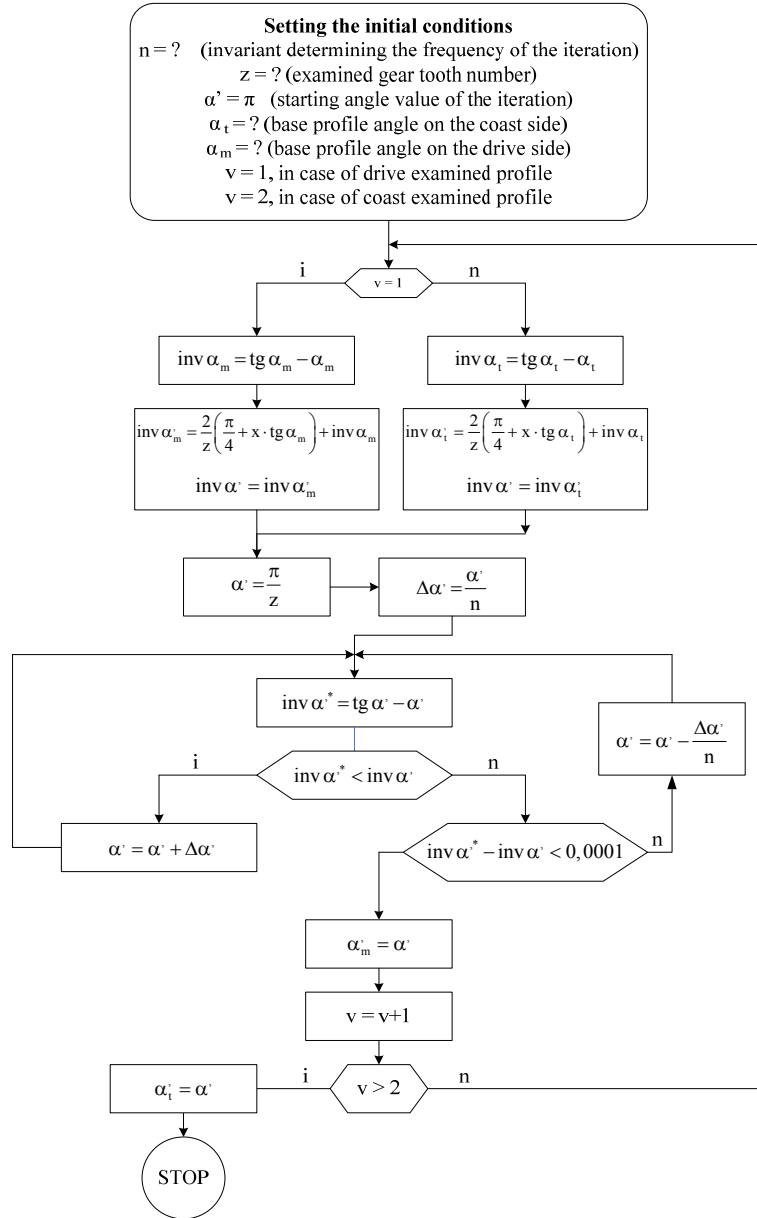


Figure 6. Angles belonging to the closing of the tooth profile sides

The tooth profile on the drive side has similar structure, but because of the basic profile angle deviation its base circle is different, so its arch is dissimilar, too (Figure 5). Both tooth profiles intersect the virtual tooth centre line passing the points O and A. These points of intersection determine one-one radius (r'_t, r'_m). For the examination of the teeth compliance

condition we need to know the radiuses belonging to the intersections A and I on the straight OA (virtual centre line).

The radiuses can be determined only by the knowledge of the angles α'_m and α'_t . On these radiuses the dimension of the tooth thickness parts is zero. The tooth thickness is written on the coast side and the

$$f'_t = m \cdot \frac{\cos \alpha_t}{\cos \alpha'} \left(\frac{\pi}{4} + x \cdot \operatorname{tg} \alpha_t + \frac{Z}{2} (\operatorname{inv} \alpha_t - \operatorname{inv} \alpha') \right) \quad (25)$$

relation is given, on which the zero value solving, then it is expressed to $\operatorname{inv} \alpha'_t$

$$\frac{\pi}{4} + x \cdot \operatorname{tg} \alpha_t + \frac{Z}{2} (\operatorname{inv} \alpha_t - \operatorname{inv} \alpha'_t) = 0, \quad (26)$$

$$\operatorname{inv} \alpha'_t = \frac{2}{Z} \left(\frac{\pi}{4} + x \cdot \operatorname{tg} \alpha_t \right) + \operatorname{inv} \alpha_t \quad (27)$$

equation is received. From this formula and the known data the involute angle can be determined. To the determination of the involute angle the formula (28) is available,

$$\operatorname{inv} \alpha'_t = \operatorname{tg} \alpha_t - \alpha'_t, \quad (28)$$

which contains the value of the α'_t in implicit form. We have worked out an iteration algorithm for the determination of α'_t and α'_m , which can be seen in *Figure 6*. In the knowledge of α'_t and α'_m the radiuses r'_m and r'_t belonging to the points A and I can be given

$$r'_m = \frac{r_{b,m}}{\cos \alpha'_m}, \quad r'_t = \frac{r_{b,t}}{\cos \alpha'_t}. \quad (29)$$

4. FEATURES OF NON-SYMMETRIC TOOTH PROFILE FROM THE MESHING CONDITIONS

In case of non-symmetric teeth the important condition of the mesh is the identity of the pitch on the rolling circle. While supposing symmetric teeth the rotation direction can be left out of consideration, in case of asymmetric teeth this can not be done. However, the pitch on the rolling circle has to be the same regardless of the rotation direction, this can be obtained from the meshing conditions. *Figure 7* with the different base circles shows, that the meshing near rotation reversing connection can be established among the pitches on the rolling circle, on the pitch circle and on the base circle.

From the permanence of the base circle radius between the pitches on the pitch circle and on the rolling circle it can be written on the drive side that

$$p_w \cdot \cos \alpha_{wm} = p \cdot \cos \alpha_m, \quad (30)$$

and on the coast side that

$$p_w \cdot \cos \alpha_{wt} = p \cdot \cos \alpha_t. \quad (31)$$

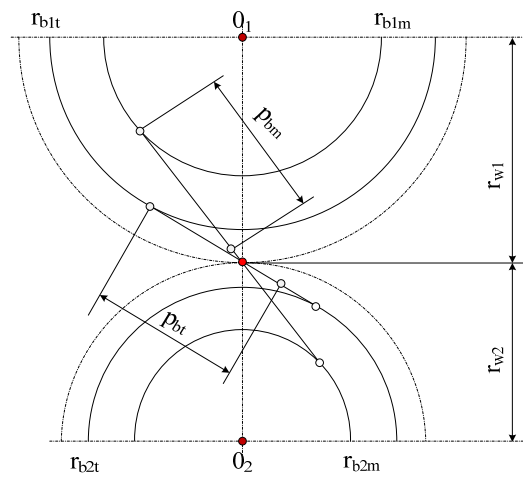


Figure 7. Connection of the base circles and the pitch on the rolling circle

On the ratio of the pitches on the rolling circle and on the pitch circle it is true that

$$\frac{p_w}{p} = \frac{\cos \alpha_m}{\cos \alpha_{wm}} = \frac{\cos \alpha_t}{\cos \alpha_{wt}}. \quad (32)$$

Relation (32) is suitable to guarantee the backlash-free condition referring to the meshing for the backlash release of the engaging teeth.

5. TOOTH THICKNESS DETERMINATION FROM THE BASE PROFILE ANGLE VALUES

When gears are in mesh one essential is that they engage without backlash clearance. Naturally this does not mean that there cannot be any gap between the tooth pairs at all. The minimal thickness of the grease, the demand for the gap originating from teeth deformation appears in the regulation of the base tangent length tolerance. Deviating from symmetric tooth shape at the asymmetric teeth the involute arches building up the tooth flanks are determining the tooth thickness belonging to the given circle of the wheel. The base tangent length between not identical tooth flank measurable determined intercepted teeth gives a

measurable distance. The tooth thickness is a determining component of the base tangent length.

With the help of the initiated relations in *Figure 4* at non-symmetric tooth shape the tooth thickness consists of two parts. One part is an arch belonging to a given circle, which is between the drive side and a seeming symmetry line dividing the tooth. Another part is an arch belonging to a given circle too, which is between the coast side and the seeming symmetry line of the tooth.

The tooth thickness part belonging to the drive side is marked by $f_{i,m}$, the tooth thickness part belonging to the coast side is marked by $f_{i,t}$, where i means the optional radius. In case of rolling circle instead of index i index w is used. On the rolling circle the drive sided tooth thickness part applying relation (21)

$$f_{w,m} = \frac{r_w}{r} \left\{ \frac{m \cdot \pi}{4} + r (\operatorname{inv} \alpha_m + x \cdot \operatorname{tg} \alpha_m - \operatorname{inv} \alpha_{wm}) \right\} \quad (33)$$

can be written. The coast sided tooth thickness part can be written in a similar way as well.

$$f_{w,t} = \frac{r_w}{r} \left\{ \frac{m \cdot \pi}{4} + r (\operatorname{inv} \alpha_t + x \cdot \operatorname{tg} \alpha_t - \operatorname{inv} \alpha_{wt}) \right\} \quad (34)$$

The tooth thickness on the rolling circle can be given by the sum of the drive sided (33) and the coast sided (34) tooth thickness parts.

$$s_w = \frac{r_w}{r} \left\{ \frac{m \cdot \pi}{2} + r [\operatorname{inv} \alpha_t + \operatorname{inv} \alpha_m + x \cdot (\operatorname{tg} \alpha_t + \operatorname{tg} \alpha_m) - (\operatorname{inv} \alpha_{wt} + \operatorname{inv} \alpha_{wm})] \right\} \quad (35)$$

6. SUM OF THE PROFILE DISPLACEMENT FACTOR FOR ANTI-BACKLASH GEARS

To the backlash-free engagement the sums of the tooth thicknesses on rolling circle have to correspond to the pitch on the rolling circle

$$p_w = s_{w1} + s_{w2} \quad (36)$$

The pitch on the rolling circle independently from the rotation of direction must be equal. The equation (32) makes a connection among the pitch (p) explained on the basic profile, the asymmetry angles (α_t , α_m) explained on the basic profile, and the pressure angles ($\alpha_{w,t}$, $\alpha_{w,m}$) depending on the direction of rotation. It gives the left side of the relation (36). The tooth thicknesses, which are interpreted on the rolling circles of the meshing gears, can be written as the sum of the relations (33) and (34) referring to the given tooth, then the sum relating to the meshing teeth. The simpler form can be seen as follows

$$p_w = (f_{w,m,1} + f_{w,t,1}) + (f_{w,m,2} + f_{w,t,2}) \quad (37)$$

In the knowledge of the referred formulas relation (37) can be written, then simplified. After reducing and expressing the sum of the addendum modification shifts it can be given as

$$\sum_{i=1}^{i=2} x_i = x_1 + x_2 = \frac{z_1 + z_2}{2} \cdot \frac{\text{inv } \alpha_m + \text{inv } \alpha_t - (\text{inv } \alpha_{w,m} + \text{inv } \alpha_{w,t})}{\text{tg } \alpha_m + \text{tg } \alpha_t}. \quad (38)$$

On the basis of relation (38) it can be laid down that in case of asymmetrical teeth near general centre distance the sum of the addendum modification coefficients accordance with the direction of rotation can be determined by a simple calculation method.

The sum of the addendum modification defined this way shows that coefficients can be divided between the gear pairs, by the possession of the knowledge of the expected properties from the gear pairs.

7 CONCLUSION

In propulsion chain of mechanical constructions the toothed element pairs, mainly gear pairs with involute tooth profile play an important role. Constructional solving come to foreground increasingly tending to fulfil the function. Now that the one directional energy transfer (there is no rotation direction change) is in the centre of interest, it proposed the request how tooth shapes can be deviated from the symmetrical form. This study presents the generalization of the deductive base profile to mapping the non-symmetrical teeth. It introduces the calculation method of the tooth thickness and the determination of the profile displacement factors, which ensure the backlash-free engagement near general centre distance working.

Acknowledgement

“This research was carried out as part of the TÁMOP-4.2.1.B-10/2/KONV-2010-0001 project with support by the European Union, co-financed by the European Social Fund.”

References:

- [1] Gy. Erney: *Fogaskerekék*. Műszaki Könyvkiadó, Budapest, 1983.
- [2] Zs. Drágár–L. Kamondi: *Questions about design of gears generated by non-symmetric racks*. Géptervezők és Termékfejlesztők XXVII. Szemináriuma, Miskolc, Hungary, November, 2011. GÉP, LXII. Volume I, 2011/7–8., Scientific Society of Mechanical Engineering, Budapest, 2011. pp. 35–38.
- [3] Zs. Drágár–L. Kamondi: *Design questions of gears with non-symmetric teeth*. 13th International Conference on Tools, Miskolc, March 2012; Department of Production Engineering, University of Miskolc, 2012. pp. 329–332.
- [4] Zs. Drágár–L. Kamondi: *Determination of general tool basic profile for gears using analytical geometry*. XX. International Conference on Mechanical Engineering, OGÉT 2012, Cluj, Romania; Hungarian Technical Scientific Society of Transylvania, Cluj 2012. pp. 105–108.

COLLISION DETECTION BETWEEN TOOLHOLDER AND WORKPIECE ON BALLNUT GRINDING

GYÖRGY HEGEDŰS–GYÖRGY TAKÁCS–GYULA PATKÓ

Machine Tools Department, University of Miskolc

H-3515 Miskolc-Egyetemváros

hegedus.gyorgy@uni-miskolc.hu, takacs.gyorgy@uni-miskolc.hu,

patko@uni-miskolc.hu

Abstract. This paper presents a numerical method for the determination of collision detection of toolholder (quill) and workpiece on ballnut grinding. Beside the collision detection the method is capable of the determination of proper grinding angle with the prescribed safety gap between the toolholder and workpiece. The applied Newton-Raphson and Broyden numerical algorithms were executed with MATLAB computation software.

Keywords: ballscrew, ballnut, grinding, collision, numerical method

1. INTRODUCTION

Gothic-arc profile ballscrew motion transforming mechanisms are widely used in machine tools and the demand for high-lead ballscrews is increasing due to the high-speed manufacturing. The gothic-arc is a symmetrical combined curve of two arcs with equal radius and distance between their centres. These types of ballscrews are manufactured by form grinding, where the grinding tool has corresponding profile [1], ultra-precision ballscrews sometimes lapped after grinding process [2], [3]. In case of long and high lead threaded ballnut the grinding wheel is not tilted at the lead angle of the thread to avoid the collision between the quill and workpiece. *Figure 1* shows the real manufacturing process on conventional thread grinding machine.

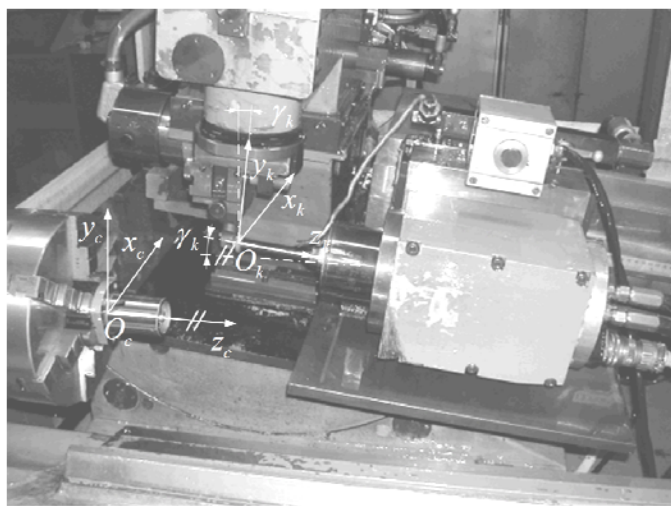


Figure 1. Ballnut thread grinding on conventional machine

Due to these conditions the profile obtained is not gothic-arc, because the grinding wheel tends to overcut the thread surface. The problem is well known in gear and worm manufacturing, different methods had been worked out to solve this task [4], [5], [6]. In case of long threaded ballnut the setting of optimum tilt angle is not possible due to the collision of quill and workpiece. This angle parameter has to be determined for the real manufacturing process. In this paper a numerical method will be presented for the determination of grinding wheel tilt angle on cylindrical and conical toolholders.

2. COLLISION DETECTION BETWEEN QUILL AND BALLNUT

Collision detection between cylindrical bodies is widely used in three dimensional mechanical systems, for example machine tools, robots, different mechanisms. There are different software package for collision detection, for example I-Collide, V-Collide, Rapid, Solid. In this work collision detection is only determined between cylindrical–cylindrical and conical–cylindrical bodies without using of third party developed software.

In case of the ballnut and the quill the determination of collision is equivalent with a minimum distance computation between cylinders or conical and cylindrical surfaces. Detecting of collision between cylindrical rigid bodies were developed using line geometry by Ketchel and Larochelle [8]. Distance computation between cylinders has four different types according to their three dimensional positions in space. Fast and accurate computation method was developed by Vranek [7]. To determine the maximum tilt angle for the grinding the minimum distance determination is required between the tilted quill axis and the edge of the ballnut represented as a circle (see *Figure 2*, where γ_k is tilt angle, φ lead angle – optimal tilt angle – of the ballnut, L_n length of the ballnut, p_h pitch of the ballnut).

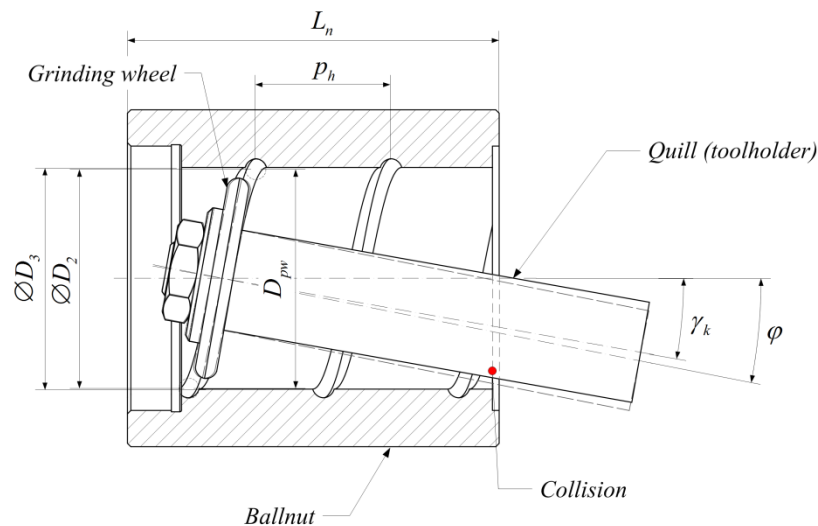


Figure 2. Schematic figure of collision between cylindrical quill and ballnut

2.1. Collision detection between cylindrical quill and ballnut

Determination of minimum distance between the quill and the ballnut is equivalent with the computation of the distance between the quill axis and the circular edge of the ballnut.

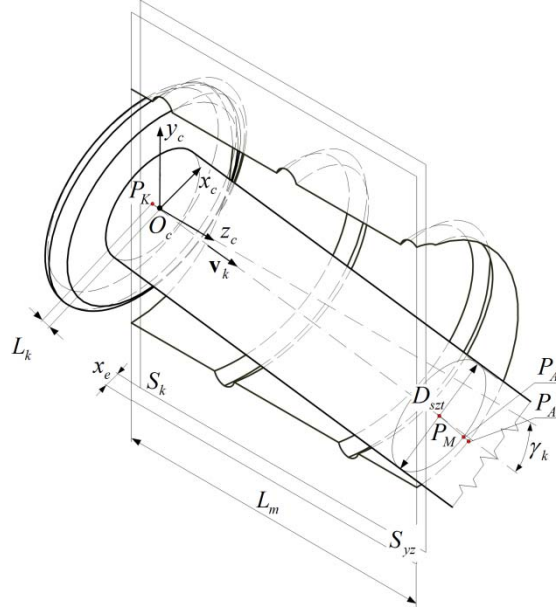


Figure 3. Spatial position of quill-workpiece

Applying notations of *Figure 3* the circle equation described by

$$\mathbf{P}_A = \mathbf{C} + \frac{D_{szt}}{2} (\cos(\phi)\mathbf{u} + \sin(\phi)\mathbf{v}), \quad (1)$$

where $\phi \in [0, 2\pi]$, \mathbf{P}_A is point of the circle, \mathbf{C} is centre of the circle, D_{szt} is diameter of the quill and \mathbf{u} and \mathbf{v} are unit vectors in the plane containing the circle. The minimum distance between the quill axis and the circular edge is

$$D = \left(\frac{D_{szt}}{2} \right)^2 + |\mathbf{C} - \mathbf{P}_M|^2 - D_{szt} \frac{\mathbf{Q} - \mathbf{C}}{|\mathbf{Q} - \mathbf{C}|} \cdot (\mathbf{C} - \mathbf{P}_M), \quad (2)$$

where \mathbf{P}_M is a point on the quill axis and \mathbf{Q} is the projection of \mathbf{P}_M on the circle plane. Applying the expressions from [9] a nonlinear equation system can be formulated for the unknown parameters. The equation for the minimum distance between the quill and the edge of the ballnut using the notations of *Figure 3* is written by

$$\frac{D_{szt}}{2} + b_h - \left[\left(\frac{D_3}{2} \right)^2 + x_e^2 + \sin^2(\gamma_k)t^2 + (L_m + L_k - \cos(\gamma_k)t)^2 - D_3 \sqrt{x_e^2 + \sin^2(\gamma_k)t^2} \right]^{\frac{1}{2}} = 0, \quad (3)$$

where b_h is a safety gap between the quill and the ballnut, and γ_k is the tilt angle from the \mathbf{v}_k direction vector of the quill axis. Minimizing (2) a quartic equation can be formulated [9]

$$d_4 t^4 + d_3 t^3 + d_2 t^2 + d_1 t + d_0 = 0, \quad (4)$$

where

$$\begin{aligned} d_0 &= \cos^2(\gamma_k)(L_k + L_m)^2 x_e^2, \\ d_1 &= -2(L_k + L_m)x_e^2 \cos(\gamma_k), \\ d_2 &= \cos^2(\gamma_k)(L_k + L_m)^2 + x_e^2 - \left(\frac{D_3}{2}\right)^2 + 2\cos^2(\gamma_k)\left(\frac{D_3}{2}\right)^2 - \\ &\quad - \cos^4(\gamma_k) \cdot (L_k + L_m)^2 - \cos^4(\gamma_k)\left(\frac{D_3}{2}\right)^2, \\ d_3 &= -2(L_k + L_m)\cos(\gamma_k)\sin^2(\gamma_k), \\ d_4 &= \sin^2(\gamma_k). \end{aligned} \quad (5)$$

The roots of the nonlinear equation system from (3) and (4) are found by root finder algorithm. In this work *Newton-Raphson* and *Broyden* numerical algorithms are used for the solving of the nonlinear equation system and the results are compared. Initial values are required for the two unknown parameters on both methods. *Figure 4* shows the quill and the workpiece position for initial value determination.

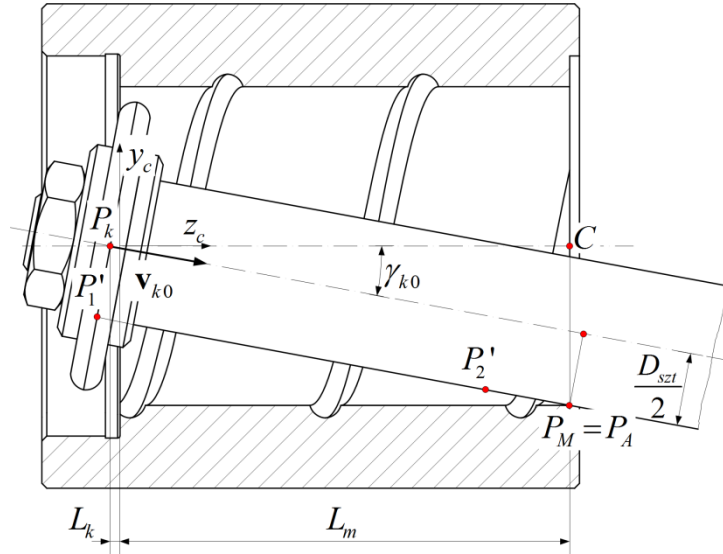


Figure 4. Quill and workpiece position for initial value determination on cylindrical quill

Assuming that the quill and the ballnut axes are in the same $y_c z_c$ plane. The initial γ_{k0} tilt angle and the initial t_0 quill axis parameter are determined by

$$\frac{|(\mathbf{P}_A - \mathbf{P}'_1) \times (\mathbf{P}_A - \mathbf{P}'_2)|}{|\mathbf{P}_2 - \mathbf{P}_1|} = 0, \quad (6)$$

where

$$\mathbf{P}'_i = \begin{bmatrix} 1 & 0 & 0 \\ 0 & \cos(\gamma_{k0}) & -\sin(\gamma_{k0}) \\ 0 & \sin(\gamma_{k0}) & \cos(\gamma_{k0}) \end{bmatrix} \cdot \mathbf{P}_i, \quad (i=1,2) \quad (7)$$

applying the *Figure 4* notations. Solving equation (6) the required initial values for the iterative algorithms are

$$\gamma_{k0} = -2 \cdot \arctan \left(\frac{2 \cdot (L_k + L_m) - \sqrt{D_3^2 + 4 \cdot (L_k + L_m)^2 - D_{szl}^2}}{D_3 + D_{szl}} \right),$$

$$t_0 = L_k \cos(\gamma_{k0}) + \sqrt{L_k^2 \cos^2(\gamma_{k0}) + \left(\frac{D_3}{2}\right)^2 + (L_m + L_k)^2 - D_{szl}^2}.$$

(8)

2.2. Collision detection between conical quill and ballnut

In the previous section the equation system was formulated for the determination of the tilt angle of the quill, where the quill was cylindrical. In certain cases conical quills are used in grinding process. The determination of the conical quill tilt angle is similar to the cylindrical case, but equation (3) has to be modified according to the taper angle of the quill (see *Figure 5*).

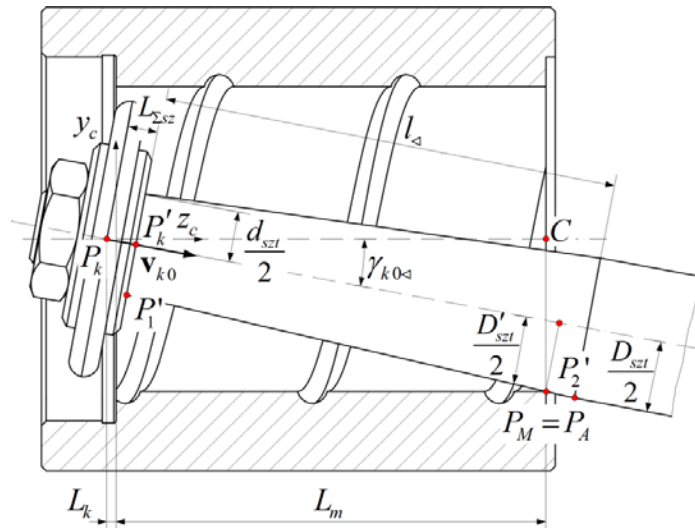


Figure 5. Quill and workpiece position for initial value determination on conical quill

The modified expression is

$$\left[\frac{d_{szt}}{2} + \sqrt{\sin^2(\gamma_k)t^2 + \left(\cos(\gamma_k)t - \frac{b_{sz}}{2} - b_j \right)^2} \tan(\kappa) + b_h \right] - \left[\left(\frac{D_3}{2} \right)^2 + x_e^2 + \sin^2(\gamma_k)t^2 + (L_m + L_k - \cos(\gamma_k)t)^2 - D_3 \sqrt{x_e^2 + \sin^2(\gamma_k)t^2} \right]^{\frac{1}{2}} = 0, \quad (9)$$

where d_{szt} is the smaller diameter of the quill, b_{sz} is the grinding wheel width and b_j is the width of additional parts. Solving equation (6) similarly the initial values are,

$$\gamma_{k0\triangleleft} = 2 \arctan \left[\frac{4l_{\triangleleft} (L_k + L_m) - D_3 d_{szt} - a + D_3 D_{szt}}{2 \left(D_{szt} \left(b_j + \frac{b_{sz}}{2} + (L_k + L_m) \right) - l_{\triangleleft} (D_3 + d_{szt}) - d_{szt} \left(L_k + L_m + b_j + \frac{b_{sz}}{2} \right) \right)} \right],$$

$$a = \left[4 \left((D_{szt} - d_{szt})^2 + l_{\triangleleft}^2 \right) (L_k + L_m)^2 + D_3^2 \left((D_{szt} - d_{szt})^2 + 4l_{\triangleleft}^2 \right) + D_{szt}^2 (4b_j b_{sz} - 4b_j^2 + b_{sz}^2) - d_{szt}^2 (4b_j (L_{\Sigma sz} + 2l_{\triangleleft}) + b_{sz}^2 + 4l_{\triangleleft} (b_{sz} + l_{\triangleleft})) + 2D_{szt} b_{sz} d_{szt} (b_{sz} + 2l_{\triangleleft}) + 8D_{szt} b_j d_{szt} (L_{\Sigma sz} + l_{\triangleleft}) \right]^{\frac{1}{2}}, \quad (10)$$

$$t_{0\triangleleft} = L_k \cos(\gamma_{k0\triangleleft}) + \sqrt{L_k^2 \cos^2(\gamma_{k0\triangleleft}) + \left(\frac{D_3}{2} \right)^2 + (L_m + L_k)^2 - D_{szt}^2},$$

$$D'_{szt} = \frac{2 |(\mathbf{P}_A - \mathbf{P}_k) \times (\mathbf{P}_A - \mathbf{v}_{k0})|}{|\mathbf{v}_{k0}|},$$

where $\mathbf{P}_1 = [0, d_{szt}/2, L_{\Sigma sz}]$ and $\mathbf{P}_1 = [0, D_{szt}/2, L_{\Sigma sz} + l_{\triangleleft}]$ (see *Figure 5*).

3. DETERMINATION OF QUILL TILT ANGLE

In the previous section the collision detection has been described to cylindrical and conical quill by a quartic nonlinear equation system. There are different root finding methods for solving nonlinear equation [10]. In this work the Newton-Raphson and Broyden methods have been applied to solve the equation systems (numerical computations made by MATLAB software). Tab. 1. shows the computed tilt angles when the initial guesses were zeros, where i is the iteration number and ε is the absolute relative approximate error. The predefined tolerance for the absolute relative error was $\varepsilon = 10^{-6}$, the run-out of the tool was $L_k = 1\text{mm}$ (see *Figure 3*) and the safety gap between the quill and workpiece was $b_h = 1\text{mm}$ on both numerical methods.

Table 1

Computed tilt angles at $\gamma_{k0}=0$ and $t_0=0$

Dimension	Numerical algorithm	γ_k [°]	i	ε [°]
32 x 25	Newton-Raphson	$-4,788076 \cdot 10^5$	11	$1,016858 \cdot 10^{-9}$
	Broyden	$-1,853271 \cdot 10^6$	51	$1,426114 \cdot 10^{-8}$
40 x 20	Newton-Raphson	$-5,180525 \cdot 10^5$	15	$3,731273 \cdot 10^{-9}$
	Broyden	$3,487852 \cdot 10^6$	139	$9,544611 \cdot 10^{-9}$
40 x 30	Newton-Raphson	$-5,158853 \cdot 10^5$	14	$6,711693 \cdot 10^{-7}$
	Broyden	$-1,789745 \cdot 10^6$	148	$1,672484 \cdot 10^{-7}$
50 x 30	Newton-Raphson	$-4,989719 \cdot 10^5$	5	$2,159759 \cdot 10^{-9}$
	Broyden	$-4,989480 \cdot 10^5$	22	$2,856460 \cdot 10^{-8}$

Table 2

Computed tilt angle at predefined γ_{k0} and t_0

Dimension	Numerical algorithm	t_0 [mm] γ_{k0} [°]	γ_k [°]	i	ε [°]
32 x 25	Newton-Raphson	63,169352	7,653505	5	$7,151210 \cdot 10^{-8}$
	Broyden	10,135615	7,653505	8	$2,708951 \cdot 10^{-8}$
40 x 20	Newton-Raphson	93,147753	6,952097	5	$4,675239 \cdot 10^{-7}$
	Broyden	8,481599	6,952097	7	$4,859574 \cdot 10^{-8}$
40 x 30	Newton-Raphson	102,8418	5,260079	5	$7,800237 \cdot 10^{-8}$
	Broyden	7,180805	5,260079	8	$8,030855 \cdot 10^{-9}$
50 x 30	Newton-Raphson	136,217801	5,651421	5	$3,449851 \cdot 10^{-9}$
	Broyden	7,196824	5,651421	7	$6,958383 \cdot 10^{-9}$

Applying the predefined initial guesses on the Newton-Raphson and Broyden methods the computed quill tilt angle becomes more accurate and number of the iterations is decreased (see Tab. 2.). Computations have been carried out to conical and cylindrical quill as well. In order to control accuracy and reliability of the results a graphical user interface has been developed under MATLAB.

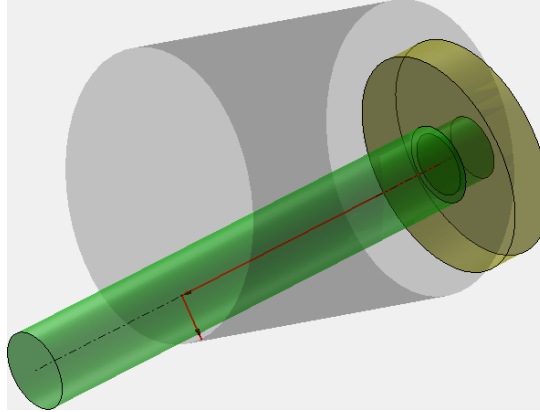


Figure 6. Visual control of computed result

Figure 6 shows result of a ballnut with 50x30 dimensions, where the safety gap between the cylindrical quill and workpiece was 1mm. The ballnut was substituted by a cylinder according to its smallest diameter (gray cylinder on Figure 6).

In order to control the collision on the real ballnut and quill surface further future work would be carried out. There are to method for this purpose, one of them to develop the described algorithm under the proper CAD system in which the ballnut and quill are modelled. Other ways to prepare the ballnut's CAD model in system neutral file format (e.g. STL format) and visualized in the MATLAB graphical user interface.

4. CONCLUSION

This paper presents a numerical method on the collision detection between workpiece and quill. The quill tilt angle is an important manufacturing parameter on ballnut grinding. The Newton-Raphson and Broyden methods were analysed with different initial guesses. One of the disadvantages of iteration algorithms has pointed out, namely inadequate initial guess raises the iteration's number and results inappropriate solutions. Results have become correct, number of iterations have been decreased with predefined initial guesses.

Acknowledgement

“This research was carried out as part of the TAMOP-4.2.1.B-10/2/KONV-2010-0001 project with support by the European Union, co-financed by the European Social Fund.”

References

- [1] H. Harada– T. Kagiwada: *Grinding of high-lead and gothic-arc profile ballnuts with free quill-inclination*. Precision Engineering (28), 2004. pp. 143–151.
- [2] D. S. Guevarra– A. Kyusojin–H. Isobe–Y. Kaneko: *Development of a new lapping method for high precision ball screw (1st report) – feasibility study of a prototyped lapping tool for automatic lapping process*. Precision Engineering (25), 2001. pp. 63–69.

-
- [3] D. S. Guevarra– A. Kyusojin–H. Isobe–Y. Kaneko: *Development of a new lapping method for high precision ball screw (2nd report). Design and experimental study of an automatic lapping machine with in-process torque monitoring system.* Precision Engineering (26), 2002. pp. 389–395.
 - [4] L. Dudás: *New way for the innovation of gear types.* Engineering the Future, L. Dudás (Ed.), Sciyo, Rijeka, November 2010. pp. 111–140.
 - [5] F. L. Litvin–A. Fuentes: *Gear Geometry and Applied Theory.* Second Edition, Cambridge University Press, 2004. p. 801.
 - [6] I. Dudás: *The Theory and Practice of Worm Gear Drives.* Butterworth-Heinemann, 2004. p. 320.
 - [7] D. Vranek: *Fast and accurate circle–circle and circle–line 3D distance computation.* Journal of Graphics Tools, Volume 7 (1), 2002. pp. 23–32.
 - [8] J. Ketchel–P. Laroche: *Collision Detection of Cylindrical Rigid Bodies Using Line Geometr.* Proceedings of the 2005 ASME International Design Engineering Technical Conferences, California, September 2005. pp. 3–13.
 - [9] P. J. Schneider–D. H. Eberly: *Geometric Tools for Computer Graphics.* Morgan Kaufmann Publishers, San Francisco, 2003. p. 1056.
 - [10] J. H. Mathews–K. D. Fink: *Numerical Methods Using MATLAB.* Third Edition, Prentice Hall, 1999. p. 680.

ANALYSIS OF GEAR MESHING FOR GEAR COUPLING

LÁSZLÓ KELEMEN–JÓZSEF SZENTE

Department of Machine and Product Design, University of Miskolc

H-3515 Miskolc-Egyetemváros

kelemen.laszlo@index.hu, machszj@uni-miskolc.hu

Abstract. Gear couplings are mechanical components to connect shaft ends and eliminate the misalignments. Most important elements of the gear coupling are the hub and the sleeve. The hub is an external gear having crowned teeth and the sleeve is an internal spur gear. Both gears have equal number of teeth. In this paper the manufacturing methods are presented for the hub and sleeve and mathematical models are investigated for the tooth surfaces of both components. An approximation is presented to determine the contact points and to analyze the gear meshing.

Keywords: gear coupling, internal gear, crowning, gear hobbing, gear shaping, gear meshing

1. INTRODUCTION

Main components of the gear coupling (*Figure 1*) are the sleeve and the hub. The sleeve is an internal gear and the hub is an external gear which has crowned teeth.

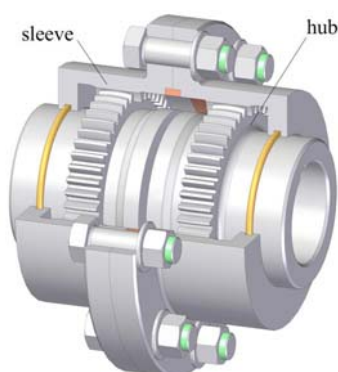


Figure 1. Gear coupling

The two toothed components compose a special gear pair, wherein both number of teeth are the same. The gear coupling is able to compensate the misalignment of the coupled shafts by the tooth crowning and backlash. Using a single hub and sleeve, the effect of angular misalignment may be eliminated. In the practice, generally two hub-sleeve pairs are built up as it is shown in *Figure 1*. In this case the compensation of the offset misalignment is possible in addition to the angular misalignment. Henceforward the possible manufacturing methods of these special gears will be examined. Mathematical models of the tooth surfaces will be set up, which can provide the basis of the further investigation for gear meshing and operation of gear coupling.

2.2. Mathematical model for crowned tooth surfaces

Based on the above-mentioned description, it is found that the resulted tooth surface depend on several parameters. Thus it is influenced by the size of the hob (r_0) and the feed.

In fact, it is also true for hobbing of cylindrical gears, that one gear produced by different hob or different feed has several tooth surfaces. The cylindrical gears with involute tooth surfaces are idealized surfaces.

The idealized tooth surface for crowned gearing will be derived so that involute tooth surfaces having variable profile shifting in parallel transverse planes are assumed (Figure 3).

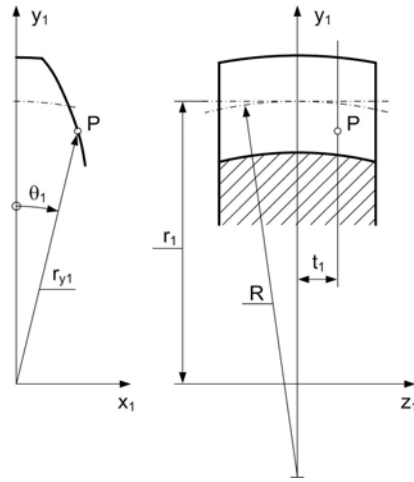


Figure 3. Crowned tooth surface

Equations of the tooth surface are:

$$\left. \begin{aligned} x_1 &= r_{y1} \sin \theta_1, \\ y_1 &= r_{y1} \cos \theta_1, \\ z_1 &= t_1. \end{aligned} \right\} \quad (4)$$

where r_{y1} is the arbitrary radius along the tooth profile, and θ_1 is the tooth angle. To calculate it the following expression is used:

$$\theta_1 = \frac{s}{2r_1} + \text{inv}\alpha - \text{inv}\alpha_{y1} \quad (5)$$

where s is the tooth thickness along the pitch cylinder, r_1 is the pitch radius, α is the standard pressure angle, α_{y1} is the pressure angle at radius r_{y1} . α_{y1} can be determined by the following equation:

$$\cos \alpha_{y1} = \frac{r_{b1}}{r_{y1}}. \quad (6)$$

Here r_{b1} is the radius of base circle. In Eq. (5) the *inv* means the involute function, which is interpreted as $\text{inv } \alpha = \tan \alpha - \alpha$.

The tooth thickness along the pitch cylinder is

$$s = s_0 - 2(R - \sqrt{R^2 - z_1^2}) \tan \alpha, \quad (7)$$

where s_0 is the tooth thickness in the plane $z_1 = 0$.

All these indicate that θ_1 depend on the radius r_{y1} and the coordinate $z_1=t_1$, i.e. in Eq. (4)

$$\begin{aligned} x_1 &= x_1(t_1, r_{y1}), \\ y_1 &= y_1(t_1, r_{y1}). \end{aligned} \quad (8)$$

3. DETERMINATION OF TOOTH SURFACE OF THE SLEEVE

3.1. Manufacture methods for internal gears

Manufacture methods of the internal gears may be classified into two categories, which are the forming and generating procedures. The forming processes include the form milling and broaching.

The form milling is realized by hobbing machine using form milling head and finger type or disk type milling cutter. The teeth are formed one by one without generating motion. Form milling may be used economically for machining the gears which have large diameter and high module. Disk type cutters having carbide bit realize appropriate productivity. The disadvantage of the procedure to be less accurate than the generating methods and large ring gears can be manufactured only. The tip diameter of gear should be many times as large as the milling head. Form milling is not suitable for preparation of helical teeth.

The broaching is the most productive method for manufacture of internal gears, but also the most expensive as well. In consideration of the prime and foundation costs of broaching machines and the high price of the broach, the broaching should only be used economically in quantity production. To produce helical teeth using special machine is possible, but the fabrication and sharpening of tool and the guiding of tool along helical path are very difficult tasks.

The generating processes are the gear shaping, gear skiving and gear hobbing.

The gear shaping was the first generating process which is suitable to produce internal gears too. This procedure is still the best known and most widely used method.

Since the gear shaping has low productivity due to intermittent operation, several attempts have been made to develop efficient production methods. Such methods were the gear skiving and gear hobbing for internal teeth generation.

The gear skiving was created as a special blend of the gear shaping and hobbing. The cutter comes from gear shaping while the movements come from gear hobbing. The productivity of gear skiving is similar to the gear hobbing of external gear teeth. It can be mentioned as an advantage that the helix angle may be set between wide limits, compared to other procedures that are either unsuitable for the manufacture of helical teeth, or just defined helix angle values can be produced. The special tool holder ("flying cutter") did not provide sufficient rigidity, therefore the gear skiving did not come in general use.

Gear hobbing for internal gears can be done on conventional hobbing machine using special tool clamping device. In the course of production barrel-shape hob is used. The spread of procedure was obstructed by the cost of complicated hob geometry, the convenient solution to a rigid tool holder and the size limit, which arises from the fact that the tool holder device must have fit to the internal ring.

Henceforward we consider the gear shaping because it is the only generating process using the manufacture of internal gear, which is widely used, reliable, and has adequate precision.

The gear shaper and shaper cutter were developed and patented by Fellows in 1897. The position of work piece and cutter and the characteristic movements of gear shaping are illustrated in *Figure 4*.

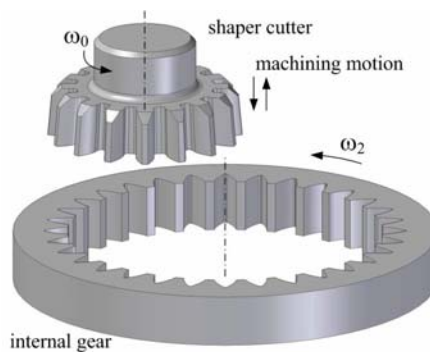


Figure 4. Gear shaping of an internal gear

Axes of work piece and cutter are parallel to each other. The generation is produced by the harmonized rotation between the cutter and gear blank. The relationship between the angular velocities can be expressed as the gear ratio:

$$\frac{\omega_0}{\omega_2} = \frac{z_2}{z_0} = u. \quad (9)$$

The cutting motion is a vertical (at certain types of machine is horizontal) reciprocating movement of the cutting tool. In the machining process there are two type of feed in radial and tangential direction. The radial feed is realized by cam mechanism or threaded spindle. The tangential feed is the rotation in mm referred to one stroke and measured on the pitch circle of cutter. During cutting neither cutting tool nor work piece does not rotate. The generating movement that is a slight rotation is carried out during the return motion of cutter.

By gear shaping spur and helical gears can be generated too. Spur gears are produced by straight-toothed tool and helical gears are manufactured by helical shaper cutter. Since the gear couplings contain spur internal gear, hereafter deal with straight teeth only.

3.2. Mathematical model for tooth surfaces of the sleeve

Theoretical tooth surfaces of the internal gears are involute cylinders. *Figure 5* shows the tooth profile and the parameters of tooth surface.

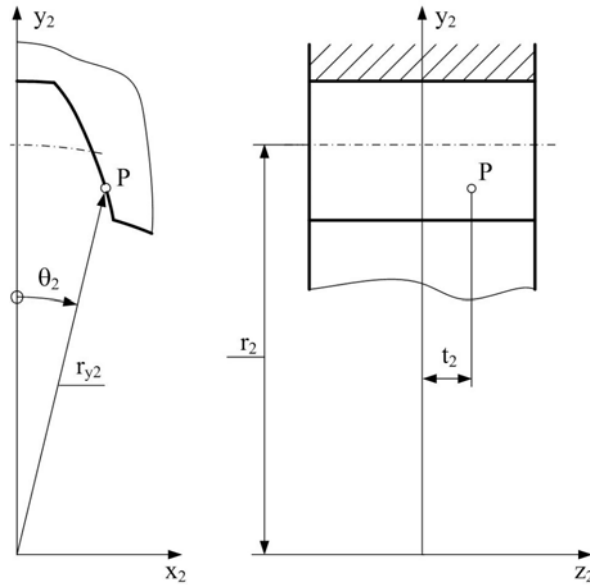


Figure 5. Tooth surface of internal gear

Equations of the tooth surface are:

$$\left. \begin{aligned} x_2 &= r_{y2} \sin \theta_2, \\ y_2 &= r_{y2} \cos \theta_2, \\ z_2 &= t_2. \end{aligned} \right\} \quad (10)$$

Where r_{y2} is the arbitrary radius along the tooth profile, and θ_2 is the angle of tooth space. To calculate this angle the following expression is used:

$$\theta_2 = \frac{e}{2r_2} + \operatorname{inv} \alpha - \operatorname{inv} \alpha_{y2} \quad (11)$$

where e is the tooth width of space along the pitch circle, r_2 is the pitch radius, α is the standard pressure angle, and α_{y2} is the pressure angle at radius r_{y2} . It can be determined by the following equation:

$$\cos \alpha_{y2} = \frac{r_{b2}}{r_{y2}}. \quad (12)$$

Here r_{b2} is the radius of base circle. In Eq. (11) the inv is the involute function, which is interpreted as $\operatorname{inv} \alpha = \tan \alpha - \alpha$.

The tooth surface is described by two independent parameters r_{y2} and t_2 :

$$\left. \begin{aligned} x_2 &= x_2(r_{y2}), \\ y_2 &= y_2(r_{y2}), \\ z_2 &= z_2(t_2). \end{aligned} \right\} \quad (13)$$

4. ANALYSIS OF GEAR MESHING

The gear couplings having angular misalignment compose a special gear pair with intersecting axes (*Figure 6*).

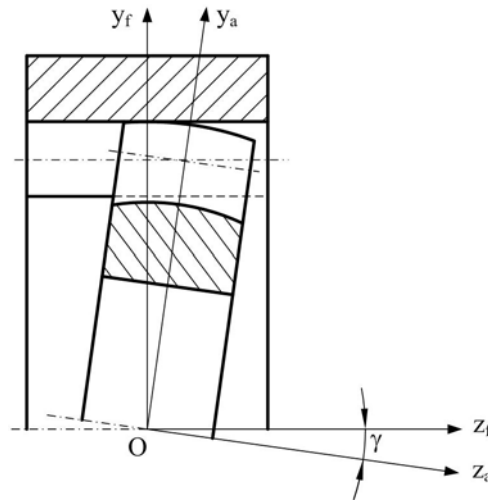


Figure 6. Gear coupling with angular misalignment

The shaft angle of the drive equals the angle of misalignment γ . The number of teeth on the hub equal to the number of teeth on the sleeve. The crowned tooth surface of the hub and the involute spur tooth surface of the sleeve are in point contact. The meshing analysis may be formulated as follows:

- Equations of gear-tooth surfaces and the angle of misalignment are given.
- It is necessary to determine the law of motion, which is the relation between the angles of rotation.

4.1. Coordinate systems

We set up four coordinate systems. $S_1(O, x_1, y_1, z_1)$ and $S_2(O, x_2, y_2, z_2)$ are moving coordinate systems and they are rigidly connected with the hub (gear 1) and the sleeve (gear 2) respectively. $S_f(O, x_f, y_f, z_f)$ and $S_a(O, x_a, y_a, z_a)$ are stationary coordinate systems fixed to the frame. S_f is the global system and S_a is an auxiliary ones. If there is no angular misalignment ($\gamma = 0$) S_a coincides with S_f (*Figure 6*).

All of the coordinate systems have a common origin O.

S_1 rotates in S_a around axis z_a which coincides with z_1 . The turning angle φ_1 is measured between axes x_a and x_1 (Figure 7). When $\varphi_1 = 0$ S_1 coincides with S_a .

Similarly, S_2 rotates in S_f around axis z_f which coincides with z_2 . The turning angle φ_2 is measured between axes x_f and x_2 (see Figure 7). When $\varphi_2 = 0$ S_2 coincides with S_f .

The relationships of transformation among coordinate systems are the following:

$$\mathbf{r}_a = \mathbf{M}_{a1} \mathbf{r}_1, \quad (14)$$

$$\mathbf{r}_f = \mathbf{M}_{f2} \mathbf{r}_2, \quad (15)$$

$$\mathbf{r}_f = \mathbf{M}_{fa} \mathbf{r}_a, \quad (16)$$

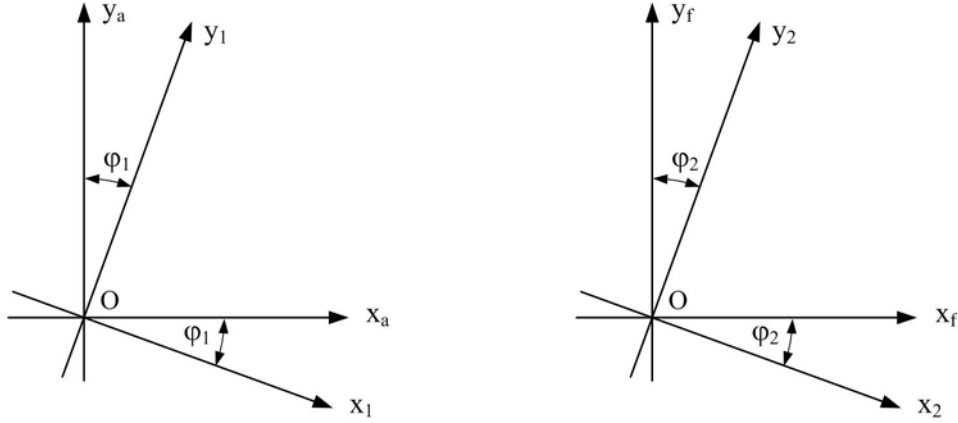


Figure 7. Relation between coordinate systems

where the position vectors in coordinate systems S_1 , S_2 , S_a and S_f are

$$\mathbf{r}_1 = \begin{bmatrix} x_1 \\ y_1 \\ z_1 \end{bmatrix}, \quad \mathbf{r}_2 = \begin{bmatrix} x_2 \\ y_2 \\ z_2 \end{bmatrix}, \quad \mathbf{r}_a = \begin{bmatrix} x_a \\ y_a \\ z_a \end{bmatrix}, \quad \text{and} \quad \mathbf{r}_f = \begin{bmatrix} x_f \\ y_f \\ z_f \end{bmatrix} \text{ respectively.}$$

The transition matrices between coordinate systems are

$$\mathbf{M}_{a1} = \begin{bmatrix} \cos \varphi_1 & \sin \varphi_1 & 0 \\ -\sin \varphi_1 & \cos \varphi_1 & 0 \\ 0 & 0 & 1 \end{bmatrix}, \quad (17)$$

$$\mathbf{M}_{fa} = \begin{bmatrix} 1 & 0 & 0 \\ 0 & \cos \gamma & -\sin \gamma \\ 0 & \sin \gamma & \cos \gamma \end{bmatrix}, \quad (18)$$

$$\mathbf{M}_{f2} = \begin{bmatrix} \cos \varphi_2 & \sin \varphi_2 & 0 \\ -\sin \varphi_2 & \cos \varphi_2 & 0 \\ 0 & 0 & 1 \end{bmatrix}. \quad (19)$$

\mathbf{M}_{nm} means the transformation from S_m system to S_n system.

4.2. Contact points on the tooth surfaces

The contact point between the tooth surfaces of the hub and the sleeve is a point in the coordinate system S_f , at which the position vectors and the surface unit normals coincide with another. Thus

$$\mathbf{r}_f^{(1)}(r_{y1}, t_1, \varphi_1) = \mathbf{r}_f^{(2)}(r_{y2}, t_2, \varphi_2), \quad (20)$$

$$\mathbf{n}_f^{(1)}(r_{y1}, t_1, \varphi_1) = \mathbf{n}_f^{(2)}(r_{y2}, t_2, \varphi_2). \quad (21)$$

Vector equation (20) yields three scalar equations, but equation (21) yields only two independent scalar equations because of the both surface normals are unit vector.

$$|\mathbf{n}_f^{(1)}| = |\mathbf{n}_f^{(2)}| = 1. \quad (22)$$

The tooth surfaces of the hub and the sleeve are represented in coordinate systems S_1 and S_2 respectively by the following equations

$$\mathbf{r}_1 = \begin{bmatrix} x_1 \\ y_1 \\ z_1 \end{bmatrix} = \begin{bmatrix} r_{y1} \sin \theta_1 \\ r_{y1} \cos \theta_1 \\ t_1 \end{bmatrix} \quad (23)$$

and

$$\mathbf{r}_2 = \begin{bmatrix} x_2 \\ y_2 \\ z_2 \end{bmatrix} = \begin{bmatrix} r_{y2} \sin \theta_2 \\ r_{y2} \cos \theta_2 \\ t_2 \end{bmatrix}. \quad (24)$$

The coordinates are known from equations (4) and (10).

Both tooth surfaces rotate about own axis located in the frame. The rotating tooth surfaces are generated in the coordinate system S_f . The locus of these surfaces are determined by the following equations

$$\mathbf{r}_f^{(1)} = \mathbf{M}_{fa} \mathbf{M}_{a1} \mathbf{r}_1 \quad (25)$$

and

$$\mathbf{r}_f^{(2)} = \mathbf{M}_{f2} \mathbf{r}_2. \quad (26)$$

The tooth surface normals in the coordinate system S_f are:

$$\mathbf{n}_f^{(1)} = \mathbf{M}_{fa} \mathbf{M}_{a1} \mathbf{n}_1, \quad (27)$$

$$\mathbf{n}_f^{(2)} = \mathbf{M}_{f2} \mathbf{n}_2, \quad (28)$$

where the surface unit normals are represented as follows:

$$\mathbf{n}_1 = \frac{\frac{\partial \mathbf{r}_1}{\partial r_{y1}} \times \frac{\partial \mathbf{r}_1}{\partial t_1}}{\left| \frac{\partial \mathbf{r}_1}{\partial r_{y1}} \times \frac{\partial \mathbf{r}_1}{\partial t_1} \right|}, \quad (29)$$

$$\mathbf{n}_2 = \frac{\frac{\partial \mathbf{r}_2}{\partial r_{y2}} \times \frac{\partial \mathbf{r}_2}{\partial t_2}}{\left| \frac{\partial \mathbf{r}_2}{\partial r_{y2}} \times \frac{\partial \mathbf{r}_2}{\partial t_2} \right|}. \quad (30)$$

To solve equation system (20, 21) contained five nonlinear scalar equations requires any iterative numerical procedure. It should be based on computer aided solution. The solving is very complex and difficult, so that we present a simplified computing method to determine the locus of contact points and the law of motion.

4.3. An approximate calculation for tooth contact analysis

To simplify the procedure of gear meshing analysis the tooth surface on the hub is divided into several nodes by a grid, which contains curves in radial direction and parallel profiles along the tooth face (*Figure 8*). The curves along the tooth profile are obtained as the intersecting curves between some cylinders having different radii and the crowned surface. The curves parallel to the transverse plane are involute profiles.

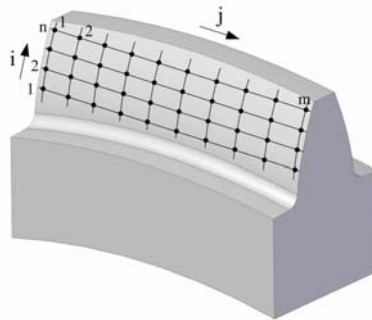


Figure 8. Nodes on the tooth surface of the hub

The number of nodes is n in i direction and m in j direction (see Figure 8). The coordinates of the nodes in the coordinate system S_1 are the following:

$$\left. \begin{aligned} x_{1i,j} &= r_{y1i} \sin \theta_{1i,j}, \\ y_{1i,j} &= r_{y1i} \cos \theta_{1i,j}, \\ z_{1j} &= z_{\min} + j \Delta z, \end{aligned} \right\} \quad (31)$$

where

$$r_{y1i} = r_{\min} + i \Delta r. \quad (32)$$

The nodes on the tooth surface of turning hub in the stationary coordinate system S_a are:

$$\left. \begin{aligned} x_{ai,j} &= r_{y1i} \sin(\theta_{1i,j} + \varphi_1), \\ y_{ai,j} &= r_{y1i} \cos(\theta_{1i,j} + \varphi_1), \\ z_{aj} &= z_{1j}. \end{aligned} \right\} \quad (33)$$

When the gear coupling has an angular misalignment γ , the coordinates of nodes in the coordinate system S_f are:

$$\left. \begin{aligned} x_{fi,j} &= x_{ai,j}, \\ y_{fi,j} &= y_{ai,j} \cos \gamma - z_{aj} \sin \gamma, \\ z_{fi,j} &= y_{ai,j} \sin \gamma + z_{aj} \cos \gamma. \end{aligned} \right\} \quad (34)$$

The position of nodes is characterized by the radius r_{y2} and the angle β in global stationary system S_f as follows:

$$r_{y2i,j} = \sqrt{x_{fi,j}^2 + y_{fi,j}^2}, \quad (35)$$

$$\beta_{i,j} = \arcsin \frac{x_{fi,j}}{r_{y2i,j}}. \quad (36)$$

Contact points on the tooth surface of sleeve are common points with the nodes. These contact points are represented by radii $r_{y2i,j}$, profile angles $\theta_{2i,j}$ and rotation angles $\varphi_{2i,j}$. $\theta_{2i,j}$ may be calculated based on formula (11). Rotation angle is determined by the following expression:

$$\varphi_{2i,j} = \beta_{i,j} - \theta_{2i,j}. \quad (37)$$

In this computing algorithm rotation angle φ_1 is the parameter. If $\varphi_1 = \varphi_0$ is given as a starting value the result to φ_2 gives different values at the different nodes. The contact point between tooth surfaces is that node which gives the maximum of φ_2 from the all $(n \cdot m)$ solutions. Smaller value of φ_2 means clearance at the given nodes.

Maximum value of φ_2 and φ_1 give one point for the law of motion. After that φ_1 is stepped by $\Delta\varphi$ and the new maximum of φ_2 is determined. If φ_1 is stepped from 0 to 2π and

maximum of φ_2 is obtained for all φ_1 the law of motion for gear coupling is generated for one tooth-pair (Figure 9).

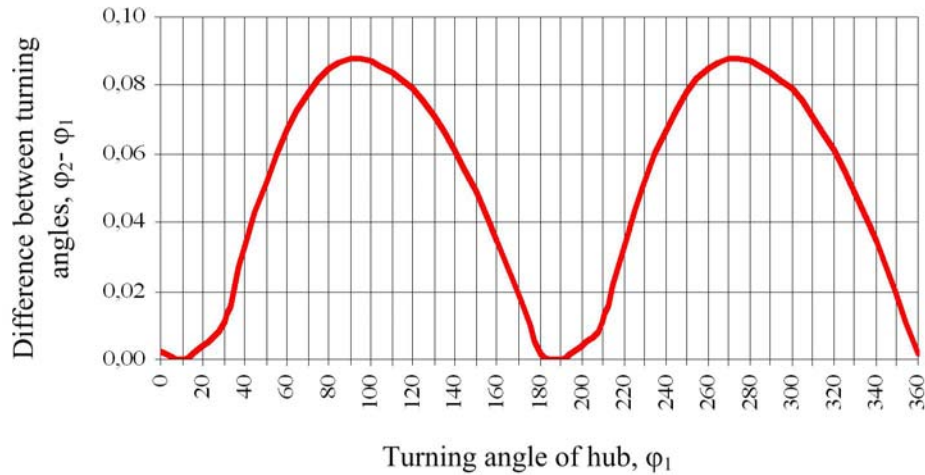


Figure 9. Law of motion in case of one tooth-pair connection

The following figure shows curves from several tooth-pair engagement (Figure 10.).

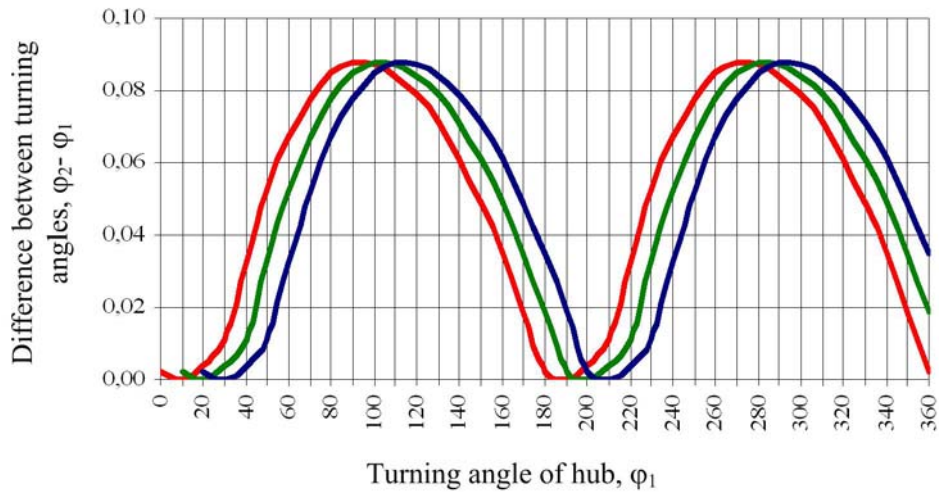


Figure 10. Law of motion in case of more tooth-pair connection

The law of motion for gear coupling contains the upper tips of the curves only, since at intersection points the next tooth-pair receives the driving (Figure 11).

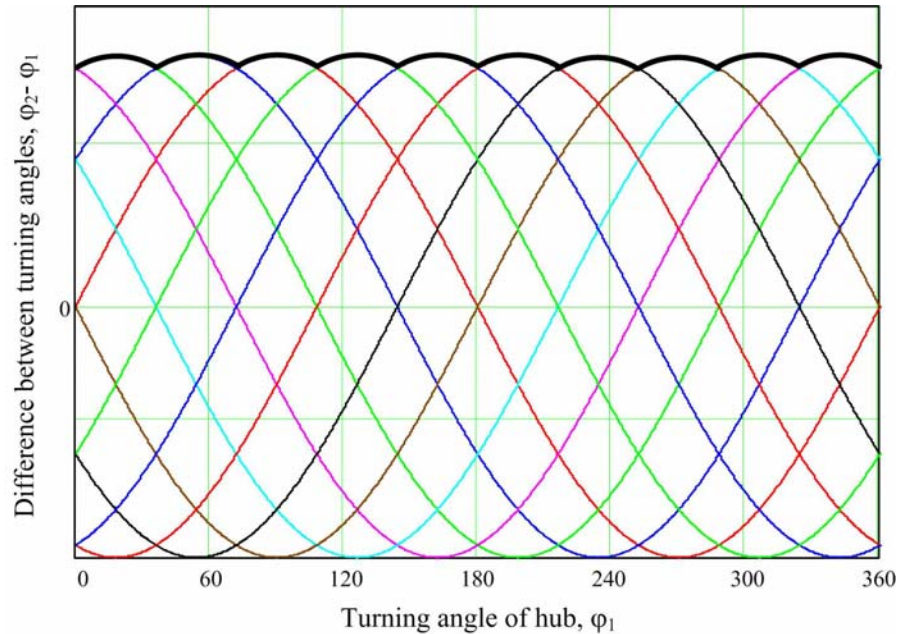


Figure 11. Law of motion for the gear coupling

This calculation method has any approximation, since the common unit normals at contact points of the tooth surfaces are not considered. The real solution is in the neighbourhood of the approximate solution. A consistent grid on the tooth surface of the hub causes smaller difference between the correct and the approximate solution and it gives more precise result.

Acknowledgements

“This research was carried out as part of the TAMOP-4.2.1.B-10/2/KONV-2010-0001 project with support by the European Union, co-financed by the European Social Fund.”

References

- [1] F. L. Litvin (1989): *Theory of gearing*, pp. 1–490, NASA Reference Publication 1212, AVSCOM technical report 88-C-035
- [2] K. Mitome (1981): *Table sliding taper hobbing of conical gear using cylindrical hob*, *Transactions of the ASME*, 103, pp. 446–451.
- [3] I. Moked (1968): *Toothed couplings – Analysis and Optimization*, *Transactions of the ASME Journal of Engineering for Industry*, pp. 425–434.
- [4] P. C. Renzo–S. Kaufman–D. E. De Rocker (1968): *Gear couplings*, *Transactions of the ASME Journal of Engineering for Industry*, pp. 467–474.
- [5] Yi Chuan-yun (2005): *Analysis of the meshing of crown gear coupling*. *Journal of Shanghai University*, pp. 527–533.
- [6] M. A. Alfares– A. H. Falah– A. H. Elkholy (2006): *Clearance distribution of misaligned gear coupling teeth considering crowning and geometry variations*. *Mechanism and Machine Theory* (41), pp. 1258–1272.

HELICAL SPRINGS IN EPICYCLIC TRACTION DRIVES

GÉZA NÉMETH–JÓZSEF PÉTER–ÁDÁM DÖBRÖCZÖNI
Department of Machine and Product Design, University of Miskolc
H-3515 Miskolc-Egyetemváros

machng@uni-miskolc.hu, machpj@uni-miskolc.hu, machda@uni-miskolc.hu

Abstract. The paper tries to introduce an epicyclic traction drive containing one or more helical springs as basic element. Our goal is to assure the necessary normal forces between the contacting surfaces, proportionally to the external loads. Some suitable mechanical models were used to obtain the solution of the elasticity problem with the necessary accuracy.

Keywords: helical torsion spring, epicyclic traction drive, strain energy, pressure device, deflection

1. INTRODUCTION

At the Department of Machine and Product Design in the University of Miskolc the epicyclic gear drive took up a great deal of room ever since its foundation. By the leading of Professor Zénó Terplán the researches generated a scientific school in which numerous theses were born. Beside the dimensioning and strength calculations of the epicyclic drives, the selection of drives on the basis of high efficiency, the analysis of load distribution among the planet gears and along the face width the research field was widened by new domains. Practical results were arisen in the scopes of research, design, production and measurement of harmonic gear drives, and also in the design area of coupled epicyclic drives and the continuously variable drives. Both the changed needs and possibilities influenced the newly coming into view of the epicyclic traction drives. The new needs are the high speed, the noiseless operation, the variable transmission ratio, the clamping force proportional to the load, low production costs and the simple design. The new possibilities are the high surface hardness, the precise machining accuracy, the traction lubricants and the high power density. This paper tries to join to the research tradition of our department with an originally developed epicyclic traction drive instead of gear drive.

After collecting some example for the flexible elements on the area of planetary drives and the antifriction bearings, the common operation states of the rolling bearing and the planetary drives is detected. The helical springs should be classified to select the proper type for our purpose. It is installed into an io type (containing one inner and one outer connection) frictional planetary drive. It is investigated how can be assured the necessary clamping force and a mechanical model for the sun gear should be suggested. The creation of the model is followed by the dimensioning and strength calculation of a kinematic drive (low power drive). At last the results are summarized and the direction for further research is charted.

2. FLEXIBLE MACHINE PARTS IN EPICYCLIC DRIVES

Flexible basic parts in epicyclic drives are not unprecedented at all. Let us just think about the harmonic gear drive. The operational interference in inner mesh having small difference in number of teeth of the pair of gears, can be avoided only with flexible, high elastic deformation elements [1]. The originally cylindrical, cup-shaped flexspline and the originally circular rings of flexible wave generator bearing are capable of large elastic deformation, as shown in *Figure 1*. The principle of harmonic drives is applicable for frictional drives, too. However the flexibility of the flexspline does not contribute to the clamping force of the force-locking connection. In the epicyclic traction drive there is an effort made to assure a clamping force proportional to the external load of the drive. Both axial and radial force-closing clutches, self tightening wedge roller are applicable. One of their common disadvantages is the danger of sliding of the rollers when the operating torque is changing, that needs a special care to prevent them. The well known solutions were reviewed in one of our previous papers [2]. In one of the planetary drive patents of the Timken Bearing Company the only planetary wheel is a sufficiently flexible ring [3]. Two functions in one machine element are united in this solution – one of the elements of the frictional pair and the initial tensioning element.

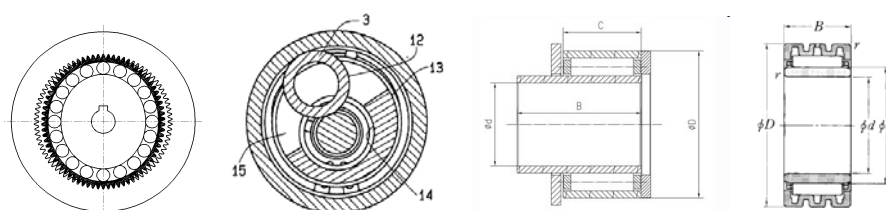


Figure 1. Harmonic gear drive, planetary traction drive [3], spring roller bearing and needle roller bearing with clearance adjustment

The application of flexible elements at the area of the rolling bearings is not unprecedented either. The rollers and/or rings of the spring roller bearing, are helical springs made of steel strip. The radial clearance of some needle roller bearings is reduced to the proper value by compressing axially the outer ring, similar to the Spieth-type clamping sleeve. Hydrodynamic radial slide bearing sleeves inserted in Spieth-type ring are also made by the radial clearance adjustment [4].

The rollers of a roller bearing make planetary motion. When the cage of this bearing is jointed to an output shaft, an io type epicyclic drive is obtained. The bearing also may be a spring roller bearing. *Figure 2* shows the mentioned roller bearing, spring roller bearing and epicyclic drive having the same radial dimensions. The main goal of the application of spring elements in roller bearings is to prevent the bearing against getting stuck, caused by unequal thermal expansion. That of in epicyclic traction drive is to assure the necessary clamping force. By the latter sample we would like to introduce an epicyclic traction drive having high efficiency, using the well known design principle and using basic elements of helical springs.

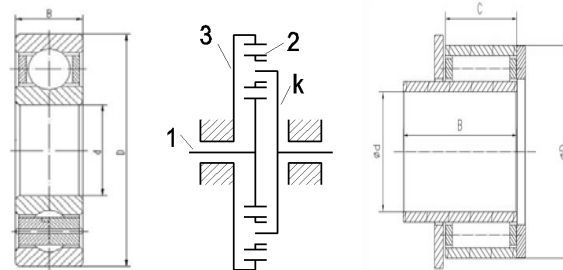


Figure 2. Epicyclic traction drive (io type) as a possible model of roller bearings

3. HELICAL SPRINGS

3.1. Characteristics, loads, production technologies

One type of the mechanically operating springs, made of steel is the cylindrical helical spring, which characteristic is approximately linear. The main load of each cross-section of the working threads of helical compression and helical tension springs, acting the external loads only at their ends, is an approximately constant torque, and that of the helical torsion spring is an approximately constant bending moment. Due to the loads there is a shear stress in the compression and tension springs and a normal stress in the torsion spring. The location of maximum stress is in the sections at the inner diameter. The slightly increment of the diameter of helical compression springs due to load should be mentioned. It requires attention when the compression spring is lead in hollow cylinder to avoid buckling. The helical torsion springs are designed for torque that increases their curvature and decreases their mean diameter. When the torsion spring is lead by a pin to decrease the danger of buckling or because of insufficient end clamping, the decrement in diameter and the friction on the pin should be also considered. The effect of frictional torque to the stiffness, relatively to the frictionless condition is an increase when loading the spring and decrease when unloading the spring. Their manufacturing technologies are forming (winding), machining (turning, milling, wire EDM, laser cutting) or both of them. The residual stresses after machining are much less than after forming, so the ideal characteristics of springs is assured by machined springs. There is a chance to make multiple coil spring which compensate the additional radial loads. The end forms are more versatile, and the load can transfer not only at the ends but anywhere along its length.

3.2. Additional deformations

There are some areas of application where instead of the large deformation caused by the load, the additional deformation is used for our purpose. This principle is used in certain force-locking connections, where an axial load produces the necessary radial increment of the elastic body diameter (ring spring, Belleville spring, or other springs). Helical springs are also applied in non-conventional areas. In the wrap spring clutch the friction torque is

produced by a similar manner than in the rope drive. The decrease in diameter of a helical torsion spring provides the additional deformation.

3.3. The shapes of helical springs

The shape of cross-sections of the springs may be circle, square, rectangle, or other, and the situation of rectangle may be standing or lying. The cross section of spring wire is constant (prismatic bar) or continuously variable. The spring forms a cylinder, cone or other solid of revolution. When one of the rolling elements of an epicyclic traction drive should be substituted by helical torsion spring, the rectangular cross section spring is suggested for our purpose. Not only is the size of cross section variable but the magnitude and sense of lead along the length of spring, and also the size of gap between the coils. The type of spring and production method is chosen to a current task.

4. THE EPICYCLIC TRACTION DRIVE DESIGN

4.1. Locations of helical springs

An io type epicyclic drive contain one inner and one outer connection, the load is distributed between more planet wheel. Any wheel (sun, planet or ring) can be rigid or highly elastic spring. All of the rolling elements of the drive may be rigid wheels and all of them may be helical springs. The number of all the variants is eight considering the two types of all the three rolling elements. *Figure 3* shows the kinematic and velocity diagram of the mentioned epicyclic drive containing sun- (1), planet- (2) and annular wheel (3) and a planet carrier (k). The small lead angle, α and the clockwise angular velocity vector, ω are the two important characteristics of the helical torsion spring having right hand helix, which can substitute the sun wheel. The relative relationship of the sense of rotation and direction of helix is important, because the spring can transmit torque only in one way. The last diagram of *Figure 3* shows a variant where both the rigid sun wheel and rigid annular wheel were substituted by right-hand helix helical torsion springs. The annular wheel is fixed to the frame, the sun wheel joined to the input shaft and the planet carrier to the output shaft.

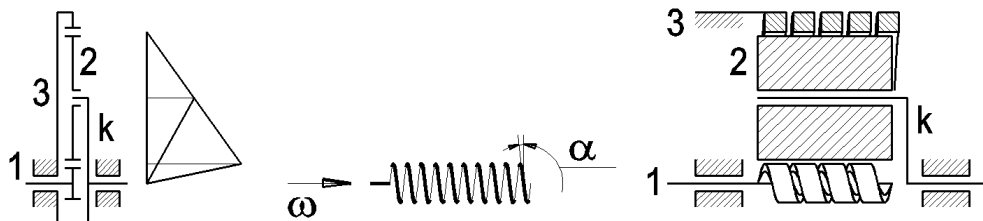


Figure 3. An io type epicyclic drive containing two helical torsion springs as basic elements

4.2. Operation of pressure device

The usual method, to assure the proper clamping force at the friction pairs, is the installation of one or more pressure devices. At the analysed drives where some of the basic elements are substituted by helical torsion spring elements, the detached pressure device is unnecessary. The springs perform the functions of both one element of the friction pair and the pressure device. As it visible in *Figure 3* the wires of springs have rectangular cross-sections and are prismatic, with small gap between the coils. The number of planet wheels is $Q = 3$, e.g. The planet wheels are fixed to the carrier with clearance, the outer diameter of the unloaded sun spring is greater, and that of the annular spring is less, than the current circle diameter determined by the rigid planet wheels. The condition of operation is the initial tensioning of the springs. The greater the external load, the greater the twist angle and the greater the clamping force acting between the mated rolling elements. This is the basis of the proper service of the pressure device. The clamping force is proportional to the external load (to the torque acting at the output shaft). The drive is unidirectional, but the direction of power flow is changeable.

5. THE MECHANICAL MODEL OF THE SUN WHEEL

5.1. Assumptions and simplifications

The previous train of thought and the study of the suggested traction drive design lead to a hopefully sufficiently accurate, usable mechanical model of a helical torsion spring with special loading. The common helical springs are loaded only at their ends, but the load of spring installed into the epicyclic traction drive as a sun gear, is more complicated. The input torque is supplied through one end of the spring, which has a relatively small lead angle, and when this helical spring having the number of coils, n , is in contact with Q piece of planet wheels, the torque is forwarded to the planet wheels through $n \cdot Q$ points. Instead of the other end, the input torque is forwarded along the spring through $n \cdot Q$ points. Another assumption is, that all the contact points are equally loaded, i.e. the radial and tangential reactions are equal to each other. Due to the small lead angle the spring can be modeled by a circular, prismatic beam with rectangular cross-section. The original shape of the spring that can produce an equally loaded circular beam at all the contact point, which are located on the surface of a perfect cylinder, yet is not interesting for us. Due to the small value of traction coefficient, μ_t the tangential components of the contact forces (reactions) are much less than that of the radials.

5.2. Arc-shaped flat beam model with radial and tangential loads

The arc coordinate, s is started at the free end of the beam. The mean radius of the beam is ρ_0 . The angular coordinate, φ at point j of the beam, is

$$\varphi_j = \frac{s_j}{\rho_0}, \quad (1)$$

and
$$(j-1)\frac{2\pi}{Q} + 2k\pi \leq \varphi_j \leq j\frac{2\pi}{Q} + 2k\pi, \quad (2)$$

where $k = 0, 1, 2, \dots, \text{ent}(n)$ and $j = 1, 2, \dots, Q$.
$$(3)$$

The radial forces and consequently the tangential forces, due to the Coulomb friction law, are supposed to be equal, so

$$F_1 = F_2 = \dots = F_j = F \text{ and } F_{t1} = F_{t2} = \dots = F_{tj} = F_t. \quad (4)$$

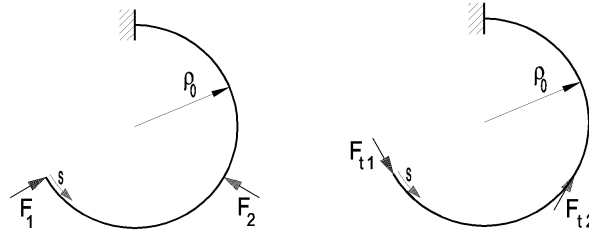


Figure 4. Arc-shaped flat beam model with radial and tangential loads

The normal load N , shear load S and the bending moment M_b along the beam, when radial loads F_j are acting, is changing as

$$N_j = -F \sum_{i=1}^j \sin \left[\varphi - (i-1) \frac{2\pi}{Q} \right], \quad (5)$$

$$S_j = F \sum_{i=1}^j \cos \left[\varphi - (i-1) \frac{2\pi}{Q} \right], \quad (6)$$

and
$$M_{bj} = \rho_0 F \sum_{i=1}^j \sin \left[\varphi - (i-1) \frac{2\pi}{Q} \right], \quad (7)$$

respectively. The normal load, N , shear load, S and the bending moment M_b along the beam, when tangential loads, F_{tj} are acting, is changing as

$$N_j = -F_t \sum_{i=1}^j \cos \left[\varphi - (i-1) \frac{2\pi}{Q} \right], \quad (8)$$

$$S_j = -F_t \sum_{i=1}^j \sin \left[\varphi - (i-1) \frac{2\pi}{Q} \right], \quad (9)$$

$$\text{and} \quad M_{bj} = -\rho_0 F_t \left\{ kQ + \sum_{i=1}^j \left[i - \cos \left(\varphi - (i-1) \frac{2\pi}{Q} \right) \right] \right\}, \quad (10)$$

respectively. Due to the radial loads, along the neutral axes of the beam the loads are periodically changing, and due to the tangential loads only the normal and shear loads are periodical, the bending moment is monotonically increasing function, as *Figure 5* shows.

The diagrams consider a helical spring with $n = 2.75$ working coils contacting with $Q = 3$ piece of planet wheels.

5.3. Slope of the circular beam

The radially acting forces along the circular beam increase the curvature. At the free end of the beam ($\varphi = 0^\circ$), when the number of planet wheel is $Q = 3$, the slope is the maximum, i.e.

$$\delta'_{M_01} = \frac{\rho_0^2 F}{I_{red} E} 3n, \quad (11)$$

that was obtained by Castigliano's theorem. The area moment of inertia, I_{red} , the Young module, E and the number of working threads of spring, n is known. The increment of slope is approximately linear along the beam. At any discrete point it is

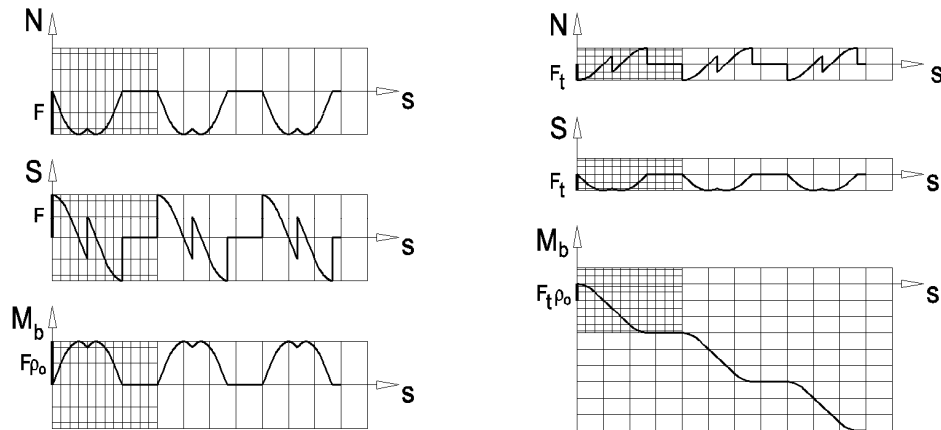


Figure 5. The $N(s)$, $S(s)$ and $M_b(s)$ functions, due to the radial and tangential loads, respectively ($Q = 3$, $n = 2.75$)

$$\delta'_{M_0}(\varphi) = \delta'_{M_0,1} \left(1 - \frac{1}{2\pi n} \varphi \right), \quad (12)$$

where φ is in radian. In an instant the discrete points are expressed by formula (2). The tangential forces are the function of the radial ones. When traction lubricant is used in the drive, a possible value of the traction coefficient, $\mu_t = 0.06$. The tangential forces along the circular beam decrease the curvature. The maximum slope is observed at the free end of the beam, that is

$$\delta''_{M_0,1} = -\frac{\rho_0^2 F_t}{I_{red} E} n(3n+1)\pi. \quad (13)$$

The slope function along the beam is approximately parabolic. Its value at any discrete point is

$$\delta''_{M_0}(\varphi) = \delta''_{M_0,1} \left(1 - \frac{1}{(2\pi n)^2} \varphi^2 \right). \quad (14)$$

The resulting slope, using the superposition principle, is obtained of the sum of the previous slopes, i.e.

$$\begin{aligned} \delta_{M_0}(\varphi) &= \delta'_{M_0}(\varphi) + \delta''_{M_0}(\varphi), \\ \delta_{M_0}(\varphi) &= \frac{\rho_0^2 F}{I_{red} E} \left\{ \mu_t \frac{3n+1}{4\pi n} \varphi^2 - \frac{3}{2\pi} \varphi + n[3 - \mu_t \pi(3n+1)] \right\}. \end{aligned} \quad (15)$$

This resulting slope function has an extreme value at

$$\varphi = \frac{1}{\mu_t} \frac{3n}{3n+1}. \quad (16)$$

The slope per each spring threads are the difference of the slopes at the ends of the stages, so

$$\Delta \delta_{M_0}(k2\pi) = \delta_{M_0}(k2\pi) - \delta_{M_0}((k-1)2\pi), \quad \text{where } k=1, 2, \dots, n$$

$$\Delta \delta_{M_0}(k2\pi) = \frac{\rho_0^2 F}{I_{red} E} \left[\mu_t \frac{3n+1}{n} \pi(2k-1) - 3 \right]. \quad (17)$$

The resulting slope among the threads is changing linearly. This function is negative everywhere. It means that all of the cross-section of the beam turns outwards. However in the case of two adjacent threads, between the points, are at $\Delta s = 2\pi\rho_0$ distance, may occur increase in curvature. This takes place just at the free end of the beam. The change in

the radius of the neutral layer of the circular beam influenced by the loads (F_j, F_{tj}) is negative only until the location of the extreme value (16), i.e.

$$\Delta\rho_{0k} = \rho_0 \left(1 - \frac{2\pi}{2\pi + \Delta\delta_{M_{0k}}} \right), \quad (18)$$

where $k = 1, 2, \dots, n$ and $\Delta\delta_{M_{0k}} = \Delta\delta_{M_0}(k2\pi)$.

The constraints of $F_j = const.$ and $F_{tj} = const.$ loads can be fulfilled if only the outer diameter of the helical spring is changed. The radius of the unloaded circular beam should be increased at the free end, and at the other end, where the input torque is supplied, the diameter should be decreased as shown in the *Figure 6*. In the case of $Q = 3$ and $n = 10$, the extreme value is at $\varphi = 16.13 \text{ rad} \approx 2.5 \cdot (2\pi)$, due to the formula (16).

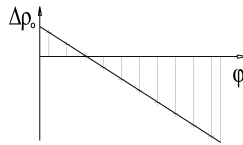


Figure 6. The change of radius of the neutral layer along the whole circular beam

6. LOAD CARRYING CAPACITY OF A TINY DRIVE

6.1. The allowable radial and tangential loads

Simple structure low noise traction drives are frequently used at the area of low power electric motor to modify their speed greatly. Some extremity prosthetics contain io type epicyclic traction drives which both diameter and length are less than 10 mm. Considering the increasing need of the mechatronics, the sample problem introduces a small power drive. Current paper deals with the design questions of sun wheel. The outer diameter of the wheel, that is now a helical torsion spring, is 5 mm. The cross section of the spring steel wire is rectangular, $a \times b$, as *Figure 7* shows. Considering the cross section and the material, the allowable strength, σ_{all} of the spring is selected. The dimensions and material properties are summarized in *Table 1*. The number of working threads, n and each thread is in contact with Q number of planet wheel. The number of contact points is $Q \cdot n$, and at each contact points there are radial and tangential forces acting. Both the radial and tangential forces are supposed to be equal to each other. The location of the maximum stress is at the vicinity of the torque supply (at the end of the n -th thread), at the inner layer of the beam, at distance η of the neutral layer. The beam is considered to be strongly curved, because the quotient of the mean circle radius, ρ_0 and the distance of extreme layer, e_{max} is equal to 4.

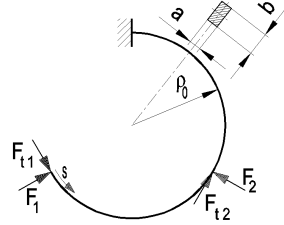


Figure 7. Geometry of the loaded circular beam

The influence of the shear compared to the bending is negligible. Knowing the allowable normal stress, the maximum allowable bending moment,

$$M_{b\max} \approx \frac{\sigma_{all}}{\frac{1}{\rho_0 ab} + \frac{1}{I_{red}} \frac{\rho_0 \eta}{\rho_0 + \eta}} = \dots = -76 \text{ Nmm} , \quad (19)$$

computed by the well known Grashof formula. Knowing the bending moment, the radial forces may be estimated as

$$F_{\max} = \frac{-M_{h\max}}{\mu_t \rho_0 n Q} = \dots = 21 \text{ N} . \quad (20)$$

Table 1

Geometry and material properties of the sum wheel

$Q = 3$	$n = 10$	$\mu_t = 0,06$	$\sigma_{all} = 1100 \text{ MPa}$	$\eta = -\frac{b}{2}$
$F_1, F_2, \dots, F_{(Qn)}$				$E = 2,1 \cdot 10^5 \text{ MPa}$
$F_{t1}, F_{t2}, \dots, F_{t(Qn)}$				$\nu = 0,3$
$\rho_0 = 2 \text{ mm}$	$a = 0,5 \text{ mm}$	$b = 1 \text{ mm}$		
$e_{\max} = \frac{b}{2}$	$\frac{\rho_0}{e_{\max}} = \dots = 4$			
$I_{red} = a \rho_0^3 \left(\ln \frac{2\rho_0 + b}{2\rho_0 - b} - \frac{b}{\rho_0} \right) = \dots = 0,0433 \text{ mm}^4$				

Let the values of radial forces, $F = 20 \text{ N}$ and that of the tangential forces, $F_t = \mu_t F = 1,2 \text{ N}$. The stress distribution in the beam is very unequal.

6.2. The constraints of the proper operation

According to the theoretical model, when constant values of F and F_t forces are acting along the beam, the shape (the meridian curve) of the helical spring at the free end is less than the original, and at the input shaft it is greater than the original, as it derived from the formula (18). Vice versa, the outside diameter of the spring should be modified to obtain the constraints of the original problem. The radial deflection of beam is very small, it is changing between $-6.8 \mu m$ and $+22.4 \mu m$. Let suppose, that in case of so small deflection, relatively to the mean radius, ρ_0 of the beam, the forces generate approximately the same value of deflections, when the unloaded condition deviates of the perfect cylinder, as *Figure 6* shows, and the loaded shape will be a perfect cylinder. The original cylindrical shape of the spring should be modified by grinding, e.g., to get an unloaded spring having $0.0068 mm$ greater radius at the free end and $0.0224 mm$ less at the torque input. The proper operation requires some initial tensioning, that is why the theoretical generatrix of the cone should be shifted farther of the axis of the cone. To develop the accurate deflection in the sun spring, the bearings of planet wheels should be installed into the planet carrier with high accuracy.

6.3. Spring characteristics, assembly of the sun wheel

The maximum input torque can be estimated by

$$T_{\max} = \frac{K \sigma_{all}}{k_0} \approx M_{b_{\max}} = 75 Nmm \quad (21)$$

The maximum distortion of the helical spring, at the maximum torque is

$$\varphi_{\max} = \frac{2\pi\rho_0 n}{I_{red} E} T_{\max} = \dots = 1,07 rad = 61,3^\circ. \quad (22)$$

The decrement of the diameter according to the previous distortion is

$$\Delta d = 2\Delta\rho_0 = 2(\rho_0 - \rho'_0) = 2\rho_0 \left[1 - \frac{n}{\left(n + \frac{\varphi_{\max}}{2\pi} \right)} \right] = \dots = 0,067 mm, \quad (23)$$

and this provide the chance of a convenient assembly process.

6.4. The contact stresses

Knowing the radius and the material properties of the contacting sun wheel (spring) and the planet wheel, and using the symbols of *Figure 3*, the Hertzian contact stress can be computed by the following process.

$$E^* = \frac{E}{2(1-\nu^2)} = \dots = 1,132 \cdot 10^5 \text{ MPa} ,$$

$$r_1 = 2,5 \text{ mm} \quad r_2 = 8,5 \text{ mm} \quad R = \frac{1}{r_1} + \frac{1}{r_2} = \dots = 1,93 \text{ mm} ,$$

$$p_0 = \sqrt{\frac{FE^*}{a\pi R}} = \sqrt{\frac{20 \text{ N} \cdot 1,132 \cdot 10^5 \text{ MPa}}{0,5 \text{ mm} \cdot \pi \cdot 1,93 \text{ mm}}} = 864 \text{ MPa} . \quad (24)$$

The obtained Hertzian stress is allowable in case of usual spring steels.

7. SUMMARY

In the area of epicyclic traction drives an innovative approach was introduced. The clamping force required for the operation was ensured by the flexible design of the traction wheels. In this solution detached pressure device is no longer required. The static model of the sun wheel formed of helical torsion spring was created. The unloaded shape of helical spring, capable for assuring the uniform load distribution along the spring, was calculated. The maximum allowable torque and the maximum angle of twist during the assembly process were calculated. The checking of Hertzian contact stress was also made. Substitution of the annular wheel by helical spring, too, helps us to assure the clamping force proportional to the external load. The possibility of the self aligning of planet wheels hopefully helps the more uniform load distribution. The most sensitive element of the introduced traction drive is the sun wheel that can transmit approximately 75 Nmm torque which is the input torque of the drive.

Acknowledgement

“This research was carried out as part of the TAMOP-4.2.1.B-10/2/KONV-2010-0001 project with support by the European Union, co-financed by the European Social Fund.”

References

- [1] J. Péter: *Fogazott hullámhajtómű kapcsolódásának vizsgálata*. Egyetemi doktori értekezés, Miskolci Egyetem, 1981, 174 p.
- [2] G. Németh– Á. Döbröczöni: *Dörzsolyóhajtások áttekintése*. GÉP, LXII. évf., 11. szám, 2011. pp. 18–21.
- [3] Ai Xiaolan: *Eccentric planetary traction drive transmission with a single planetary roller*. Patent no.: US 6702704 B2, Assignee: The Timken Company, Canton, OH (US), Date of Patent: 9th March, 2004.
- [4] SPIETH Series GLM Radial Slide Bearing, Catalogue no. SN 00.31 e 0409/0000/0409, SPIETH-Maschinenelemente GmbH & Co KG Alleenstrasse 41 73730 Esslingen, p. 20.
- [5] Z. Terplán– G. Nagy– I. Herczeg: *Különleges tengelykapcsolók*. Műszaki Könyvkiadó, Budapest, 1971. p. 680, 769.

ENSURING OF THE CLAMPING FORCE IN EPICYCLIC TRACTION DRIVE BY A NEW SUN WHEEL DESIGN

GÉZA NÉMETH–JÓZSEF PÉTER–ÁDÁM DÖBRÖCZÖNI

Department of Machine and Product Design, University Miskolc
H-3515 Miskolc-Egyetemváros

machng@uni-miskolc.hu; machpj@uni-miskolc.hu; machda@uni-miskolc.hu

Abstract. The paper tries to introduce different designs of helical torsion springs to install them in epicyclic traction drives as basic elements. The goal of the authors is to show some clamping devices collecting ideas among the traction drives, at the areas of free-running clutches and conventional epicyclic traction drives. Helical torsion springs were developed, derived from a split hollow cylinder. A novel traction wheel design was obtained by merging the functions of rolling and clamping. In order to earn a good quality radial clamping force and load symmetry, and an economical design, some innovative technology were joined to the spring production.

Keywords: axial clamping device, free-running clutch, helical torsion spring, epicyclic traction drive, split hollow cylinder

1. INTRODUCTION

The preliminary constraint of the operation of epicyclic traction drives is the proper clamping of the elements which are in force transmitting relation. There are a numerous well known solutions of which one part assures constant clamping force and another part assures a force that proportional to the load. Both the efficiency and the life rating are more favourable in the latter case [1]. *Figure 1* shows three of them, namely wedge ball type, screw-nut type and roller cam type. The case of clamping force proportional to the load is a feature of some clutches e.g. the axial and radial force closing free-running clutches [2]. The slippage of the traction elements during the starting and load changing process should be avoided to save them. A certain degree of preload must be assured by spring, by gravity or by other force.

Both the constant preload and the clamping force which is proportional to the load, depending on the design and location of the drive, and the clamping mechanisms can be axial or radial. The possible sense of rotation and power flow can be unidirectional or bidirectional. The literature of traction drives [1] publishes axial clamping devices and most of them are able to operate undependently of the sense of rotation, and that of the clutches [2] shows free-running clutches with radial force closing which are able to transmit power in one sense of rotation. *Table 1* summarizes the types of free-running clutches.

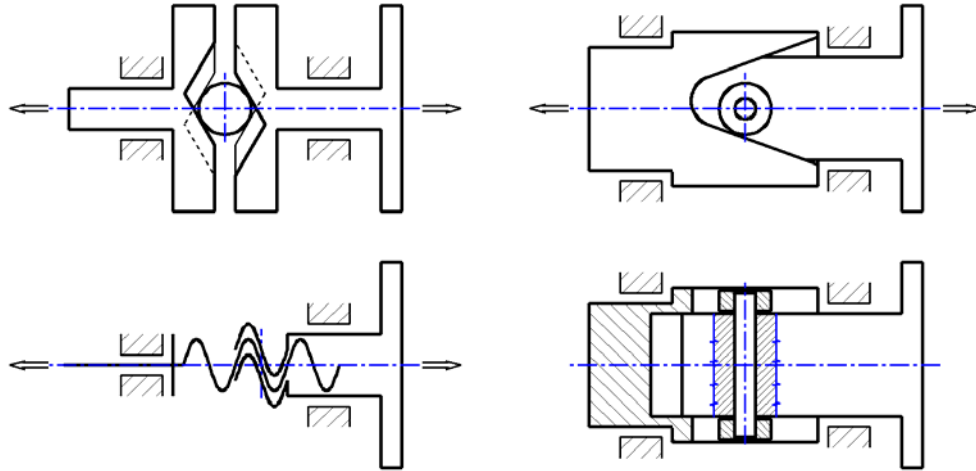


Figure 1. Axial clamping devices [1]

Table 1

Classification of free-running clutches [2]

Shape closing		Shape and force closing	Force closing
Radial	Axial		
ratchet mechanisms	jaw type coupling driven through screw-nut join		
Axial		Radial	
disk or cone type frictional coupling driven through screw-nut join	wedge roller type	locking body type	Other type

The clamping devices but the radial ones are discussed in the literatures in detail. Only a few of the radial types are available which transmit the axial displacement proportional to the load into radial displacement or radial force by a relatively complicated mechanism shown in *Figure 2*. Let's find solutions in the literature of free-running clutches to generate radial force for the clamping devices.

The design of force closing radial free-running clutches may be locking roller type, locking block type or others with elastomer inserts [4], and there are solutions where the shafts are connected to each other by helical torsion springs [5]. The conditions of traction connections are fulfilled only at one of the driving directions in the following ways. The equally rigid driving and driven parts are connected by wedging rigid rollers, closure body, or moulded elastomer disk having wedging elements shown in *Figure 3*. The shafts can be connected by helical torsion spring which coils are tightened rope – like to the cylindrical surfaces shown in *Figure 4*.

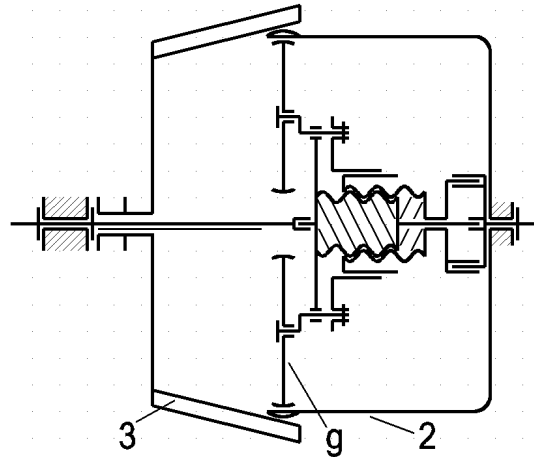


Figure 2. Providing the radial force by pinion-sector gear driven eccentric rollers [3]

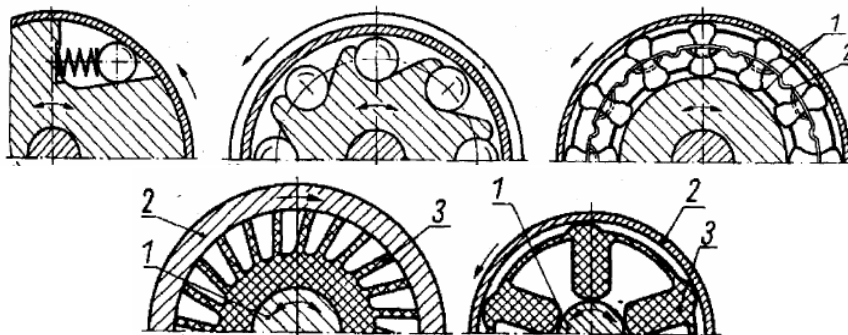


Figure 3. Free-running clutches – wedging rigid roller type, closure body type and elastomer disk type [4]



Figure 4. Free-running clutch – the torque is transmitted by helical torsion spring [5]

2. THE GENERATION OF THE RADIAL FORCE

The free-running clutches of *Figure 3* are force closing types. The degree of wedging of the locking elements between the driving hub and the driven drum depends on the stiffness of the drum. The rigid shape of drum causes large normal clamping force but a more elastic design results less. The elastic design is associated with the greater radial deflection. There are more possible chances to enlarge the flexibility of the drum. The wall thickness of the drum, made of spring steel can be decreased. The original cylindrical shape due to radial force will be changed, formed in polygonal shape. The thin walled cylinder can be split,

too, where the degree of polygonal formation is less and the increase in diameter is greater. The drum can be made of elastomer which can be elongated tangentially, both the large radial increment and the polygonal formation occurs.

In an epicyclic traction drive, in all the rolling relations, a proper clamping force possibly proportional to the load should be made. Let's consider the possible sun wheel designs of an io type epicyclic drive (having one inner and one outer connection) to make the required radial clamping force.

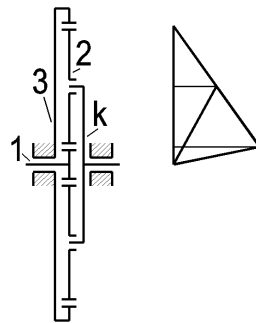


Figure 5. io type epicyclic drive

What kind of drum design of the free-running clutch should be suggested to provide both the function of sun wheel and ensuring the radial clamping force? From the options outlined above the drums made of elastomeric material should be excluded from the scope of studied cases due to its small value of maximum allowable hertzian stress. By similar manner, the very thin walled cylindrical shells, made of steel and tends to large degree of polygonal formation, are also excluded. The split cylinder having greater wall thickness consequently more rigid, retaining the cylindrical shape more accurately, but able to be properly deflected radially, is able to serve the solution which can be refined to find the applicable solution.

3. SUN WHEEL UNIT ENVELOPED BY A SPLIT RING

Let the sun wheel the driving element of the epicyclic drive. The drive receives the driving torque through the hub carrying the locking rollers or locking bodies. The split hollow cylinder increases its diameter due to torque or when the deflection is limited, the radial force is increasing. There are two constraints in relation with the direction of split curve for the proper operation. One of them is the need for the smooth rolling and the other is the unobstructed transmission of the radial clamping force which is proportional to the driving torque.

Considering the symbols of *Figure 6*, when the diameter, d and the with, b of the sun wheel is constant, the smooth rolling can not be assured in case of $\alpha = 0^\circ$ split angle, but the radial clamping force can be transmitted effectively. Increasing the split angle, the rolling of the planet wheels on the sun wheel becomes smoother but the efficiency of the transmission of radial clamping force becomes less. To assure the same contact phases in all the sun wheel – planet wheel engagements with smooth rolling, then using the symbols of *Figure 6* an $\alpha = n \arctan \frac{b}{d\pi}$ split angle should be set, where $n = 1, 2, \dots$ natural number.

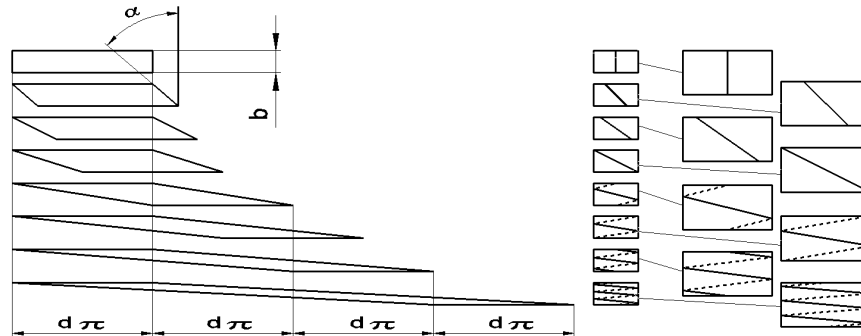


Figure 6. The influence of the split angle, α to the shape of the unfolded split hollow cylinder (d and b are constants)

Choosing $n = 1$, both the smooth rolling and the proper quality driving torque – clamping force transfer can be provided.

From the above mentioned sample it is visible, that a radial clamping force can be generated directly, without any tapered surfaces or axial clamping devices. Figure 7 shows three example for clamping force application with axial forces, on the area of adjusting drives (io), prosthesis of extremities (io) and the power drives (o+i). The sun wheel and/or the ring wheel is conical. At the (o+i) type epicyclic drive, the inner connection is divided in two parts to make load symmetry.

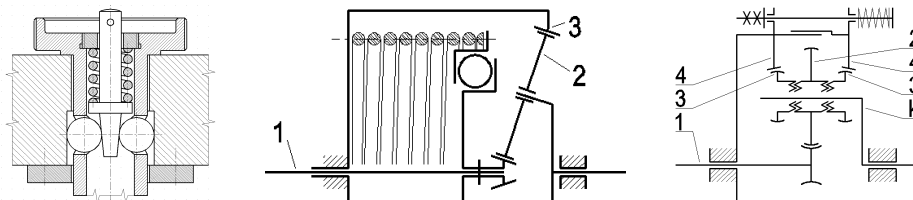


Figure 7. Axial clamping with tapered surfaces [6, 7]

The clamping with radial forces can be made, similarly to the free-running clutches, proportionally to the load. The only difference is in the output element, the thinner ring design and the split ring. The increasing torque at the driving shaft of the epicyclic drive causes the enlargement of the ring, i.e. the increment of the clamping force.

The sun wheel derived in such a way has got a very simple design. It is able by itself to assure the initial tensioning force and then to assure the clamping force proportionally to the load, and furthermore to assure the smooth rolling on the planet wheels that were shown in our previous study [8]. The helical spring can be considered so as a split hollow cylinder with a highly increased split angle. The initial tensioning is assured so as the diameter of the unloaded spring is chosen to be greater than the diameter of the inner tangent circle determined by the planet wheels, and the adjacent coils of the spring during the installation, when the spring diameter is decreased, should not be in contact with each other. There could be other needs in relation with the drive. E.g. let the drive be able to work in both

directions or let the load of the drive be symmetric, or let the manufacturability of the sun wheel be easy.



Figure 8. The hollow cylinder having large split angle is a helical spring

4. BIDIRECTIONAL FUNCTIONALITY

The operating principle of the free-running clutches was used to assure the radial clamping force of the epicyclic traction drives, however the free-running function is usually not needed. Installing symmetrical locking bodies which are able to get stuck at any sense of rotation of the hub, causing the radial deflection of the split hollow cylinder, the problem can be solved simply without increasing the space requirement.

When, for example, the helical spring of the *Figure 8* having right hand side inclination, is driven through the middle point of its length, then the torque is transmitted towards the planet wheels through the part of spring between the driving point and the right free end, in case of reverse drive it is done by the left-hand side part of the spring. This solution causes the doubling of the width of the drive.

5. BALANCED HELICAL SPRING SUN WHEEL

When the lead of the symmetric design of helical spring is half left - half right, and it is driven through its middle point then a sun wheel with unidirectional functionality is obtained. The load distribution will be symmetric longitudinally, too as *Figure 9* shows. The situation is even more favorable if the spring is manufactured with double thread. It is easier to drive in the middle and is expected to have a better load distribution.

6. THE PRODUCTION OF HELICAL SPRINGS

Split rings should be developed from spring steel strip. The single thread helical spring of *Figure 9* should be manufactured from tube by cutting (turning, milling), that of the double thread by spark cutting. Recognising that the location of the obtained double, left-right-hand side threads are located on cylindrical surfaces, and knowing the unfoldability of the cylindrical surface, the pre-product of the spring winding can be made from sheet metal, practically without any waste by laser cutting. Prior to the windings of the two V shaped plates the minimum gap between the coils should be adjusted and the nose at the end should be bent.

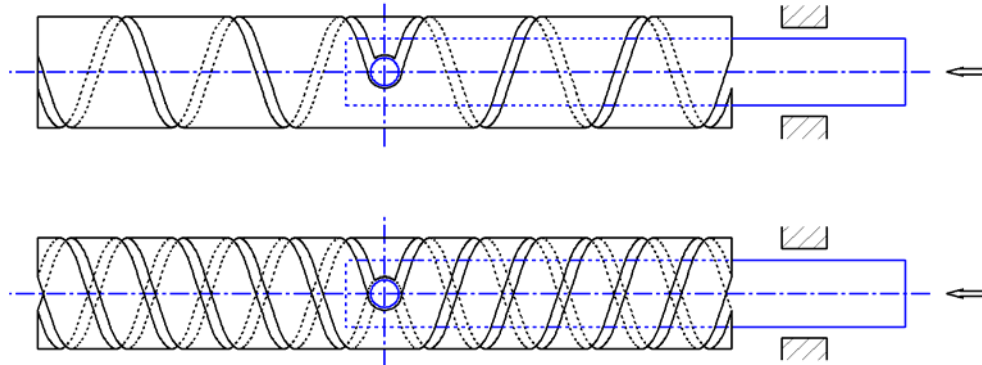


Figure 9. Symmetrical design helical springs (single and double threads)

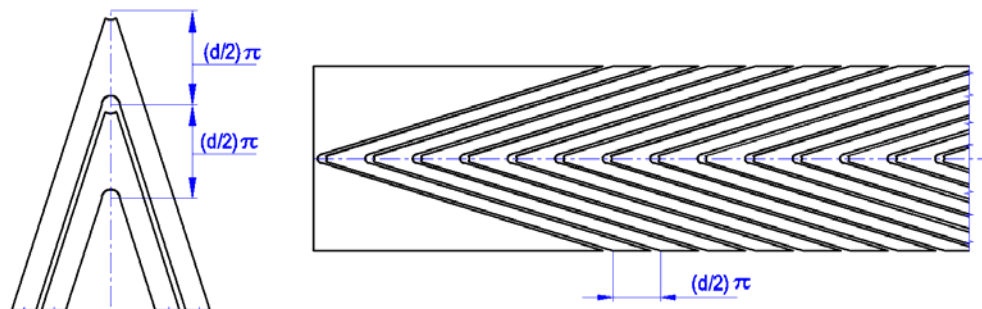


Figure 10. The plate pre-product of the balanced double thread helical spring

7. ASSEMBLY AND WINDING DIRECTION OF THE ELEMENTS IN THE EPI-CYCLIC TRACTION DRIVE

The principle and formation of flexible shafts is useable for the design of io type epicyclic traction drive. A flexible shaft consists of more layers of helical springs wound alternately and tightly on each other. Driving in the proper direction, the diameter of the outer layer is reduced. Let's consider an epicyclic drive, whose every rolling basic element is made of helical spring. The relationship between the winding direction and the sense of rotation of the springs is chosen to increase the diameter proportionally to the load in the outer connection (sun wheel – planet wheel) and to decrease the diameter at the ring gear. In such a way the generated clamping force between the elements will be proportional to the load. When all the rolling elements that is made of helical spring have symmetrical design, due to *Figure 9* and double thread, driven in at the middle of width, (or in case of ring wheel the middle point is fixed to the housing) then a flexibly operating, highly efficient drive is hoped of the described solution.

8. SUMMARY

One of the necessary constraints of the operation of epicyclic traction drives is the assurance of the proper clamping force. The well known solutions are based on mainly the self tensioning of a wedge roller, the relative axial displacement of the mating element in a drive containing conical element (*Figure 1*) or a mechanism transforming the axial displacement to radial one (*Figure 2*). Directly generated clamping force that proportional to the speed of the shaft is found only where the principle of the clamping device is on the centrifugal force. At the other group of the machine elements, namely at the free running clutches there are a lot of devices working on the principle of radial force closing. This paper investigates the usability of these principles at the area of epicyclic traction drives.

It was detected that the clamping device enveloped by flexible ring which has proper split angle may be suitable to ensure a clamping force proportionally to the load. It was also demonstrated that enlarging the split angle of the split hollow cylinder, a helical torsion spring is obtained. This spring is useable individually, too, and it is able to assure both the preliminary constraints of the high efficiency traction drives and the preliminary clamping force, and also the proportionality of the clamping force relatively to the load.

It was presented that the helical spring with symmetrical design, partly left- and right-hand wound, driven through the middle of its length and is favourable not only in terms of the loads but its material saving manufacturability also foresees the possibility of the economical design.

The join of the above described sun wheel and the driving shaft is easy through bending a nose part at the peak of the V-shaped plate strip (*Figure 10*). The ring wheel and possibly the planet wheels can be similarly formed. The design of bearings of the planet wheels to the planet carrier is not simple. The strength calculation of the helical torsion spring with sun wheel function was introduced in one of our previous papers [8], and the generation of uniformly stressed spring shape requires further analysis.

Acknowledgement

“This research was carried out as part of the TAMOP-4.2.1.B-10/2/KONV-2010-0001 project with support by the European Union, co-financed by the European Social Fund.”

References

- [1] B. A. Pronin–G.A. Revkov: *Fokozat nélküli hajtások*. Műszaki Könyvkiadó, Budapest, 1985, pp. 223–226, 367.
- [2] Z. Terplán– G. Nagy– I. Herczeg: *Különleges tengelykapcsolók*. Műszaki Könyvkiadó, Budapest, 1971. p. 680, 769.
- [3] N. I. Ceitlin–E. M. Cukerman: *Volnovie peredatsi*. Moscow, 1972. p. 95, 208.
- [4] A. Ettemeyer–O. Olbrich: *Feinwerktechnische Konstruktion*. Kapitel 13: Kupplungen; Fachhochschule München, Fachbereich 06 – Feinwerk- und Mikrotechnik, 2007, . www.fb06.fh-muenchen.de, p. 14, 24.
- [5] G. M. Roach–L. L. Howell: *Evaluation and comparison of alternative compliant overrunning clutch designs*. Journal of Mechanical Design, 124:485, 2002.
- [6] N. Bárány (Ed.): *Finommechanikai kézikönyv*. Műszaki Könyvkiadó, Budapest, 1974. p. 41, 588.
- [7] Y. Deyuan– G. Jingjing– Z. Xiaohong (1999): *New Symmetrically Loading Epicyclic Traction Drive Reducer (in Chinese)*. Journal of Beijing University of Astronautics, 1999. Vol. 25 Issue 2 pp.229–231.
- [8] G. Németh– J. Péter– Á. Döbröczöni: *Csavarrugó alkalmazásas dörzsbolygóműben*. OGÉT XX. Nemzetközi Gépészeti találkozó, EMT, Kolozsvár, 2012. pp. 327–330.

NATURAL ANALOGIES – CREATIVE PRINCIPLES OF THE NATURE AND THE PRODUCT DESIGNER

JÓZSEF PÉTER–GÉZA NÉMETH–CSABA DÖMÖTÖR

Department of Machine and Product Design, University of Miskolc

H-3515 Miskolc-Egyetemváros

machpj@uni-miskolc.hu; machng@uni-miskolc.hu; machdcs@uni-miskolc.hu

Abstract. Present paper analyses the creative principles of the nature and the product designer, and describes a possible way of research. The study is restricted to the analogical solutions of machine elements, machines and products. The paper detailed deals with principles, evocation, articulation, proportion, etc., available in the nature and the design process.

Keywords: natural analogy, linguistic analogy, articulation, evocation, proportion, proportionality, balance, symmetry, asymmetry, order, rhythm, direction, contrast

1. INTRODUCTION

Josiah Wedgwood who was born in 1730, was an English ceramist, founder of the power pottery making, in other words the creator of power arts. Wedgwood produced cheap, simply producible, well usable, durable, easily storable, transportable earthenware pots made of locally mined clay and not least available for many people. Wedgwood created flagship products **adapted to the needs and opportunities of his age** [4]. **The essence of creatures are the adaptive work, too**, e.g. the tree implements its genetic program and grows upwards in undisturbed conditions. In unfavourable circumstances, however, extends towards the sky asymmetrically and diagonally. **The plant responds the environmental influences, adapts and modifies its structure within a certain limits, taking advantages of inherent opportunities.** Charles Darwin (1809–1882, grandson of Josiah Wedgwood) summarized the design principles of ecosystem as the theory of coordination of opportunities and adaptation, in the work of “On the Origin of Species by Means of Natural Selection, or the Preservation of favoured races in the struggle for life” [1], published in 1959. In this paper the authors study the relations between the respond of the living and inanimate nature giving to the environmental challenges, and the possible technical works. The relations are illustrated by previously known or analysed examples.

2. ELEMENTS

The scope of elements and forming principles of the living and inanimate nature is extremely wide, therefore this study is restricted to the field of our competence, as the machine elements, the machine design, the product design and the solutions of nature can be associated with them (*Figure 1*).

The machines are structures composed of elements, to solve a special problem. Their repetitive elements, in accordance with the task and design, are the machine elements. Beyond their tasks the machine elements can be classified on the basis of shape, design, load, material, production, etc. Among the machine elements there are fasteners, shafts, cou-

plings and clutches, bearings, seals and the drives. The research of direct relation between the machine elements and the living and inanimate nature is a rough simplification so **the correlations should be located by the similarity or identity of the problem.**

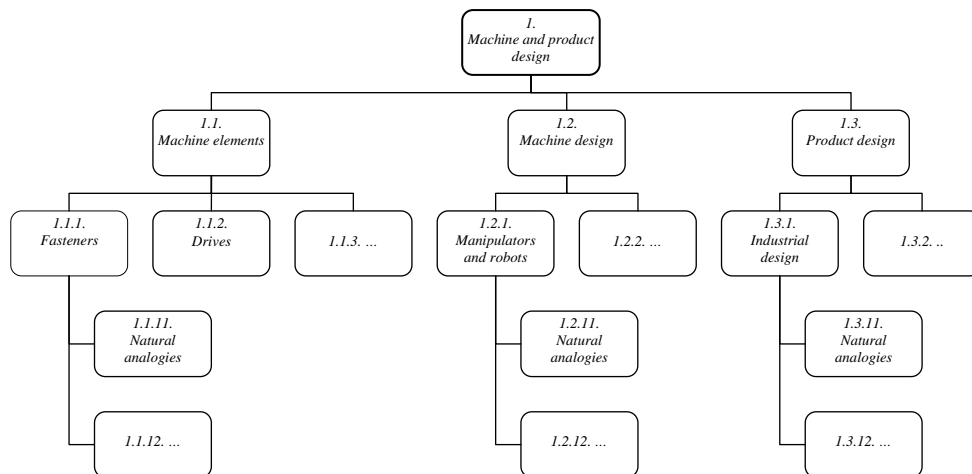


Figure 1. The studied areas of natural analogy

The frequently repeated elements of creatures and technical works are the fasteners assuring connection between the parts. The joints can be created by adding material, they can be force or shape closing, mixed shape and force closing, and elastic fasteners. The bonded joints are made by adding material, for example. Both nature and man use absorbing material, e.g. absorbing material covers the seeds of mistletoe (*Viscum album*), which sticking to birds and dropping of them assures the propagation of the plant. Shape closing joint is made e.g. between the cores of thistle (*Cardus nutans*) [(Figure 2.a)] and the fur of animal coming into contact with it.

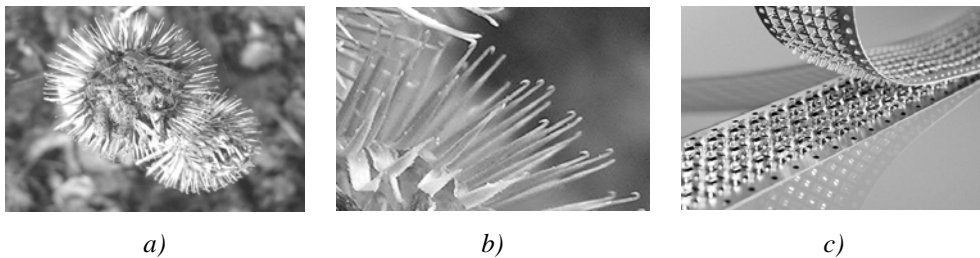


Figure 2. a) and b) Thistle and its hooked pins, c) Hook and loop fastener

The hook ended pins [(Figure 2. b)] assures the spreading of thistle as a free rider in large territory. 21–25 piece of reflexed hooks assure the break of sting of a honey bee (*Apis mellifera*) into the stabbed human being or animal, and to get the poison from the detaching gland to the stabbed body. Similar hooks are used to close clothes and shoes [2], or to fix machine parts [(Figure 2. c)]. The joint is shape closing between teeth of predator and the prey, or e.g. between the crocodile clip and the gripped electrical wiring. The joint is force

closing between the fingers of man and the gripped object [Figure 3. a)–f)] or e.g. between the sheet of paper and the fixing clip. The joint is both shape and force closing between the claws of predator and the prey. The joint is elastic between the skull bones of a newborn. Before the end of ossification the elastic parts assures the easier passage of the head through the birth canal, and the increment of volume of skull during the growing (the bones of skull, after the final formation are sutured and rigid joint is developed. By similar manner the elastic joint assures the relative displacement and rotation of rigid parts in the machines. **The examples illustrate the natural approach of machine element education and the possible attract of audience (captatio benevolentiae).**

3. COMPLEX STRUCTURES

The nature of machine parts are material, e.g. the machine elements and immaterial, e.g. the software used to control. For example, the robots belong to the complex machines. Their main parts are the frame, the arms, the drive system, the energy supply system and the controller. Tools and/or grippers belong to the arms, similarly to the creatures of nature having arms and legs. The ideal gripper would be the copy of the human hand [Figure 2. a)–f)], so it is not surprising that the human hand is the starting point of making the versatile robotic gripper structures. In Figure 3 there are characteristic types of gripping shown as a) with fingertip, b) cylindrical, c) with folded finger, d) spherical, e) rod end and f) gripping on side panel.

Since the shape, size and material of the object to grip is versatile, and similarly the operations and the environment have a wide range, too, the universal robotic gripper is usually large, heavy and expensive, relatively to the problem. To optimise the size, mass and costs, the robotic grippers are not universal, but task-qualified. Most frequently the relationship between the object and gripper is assured by shape closing or force closing. To the analogy of gripping with human hand, Figure 3. g), h) and j), show grippers with fingertip, cylindrical and on side panel, respectively.

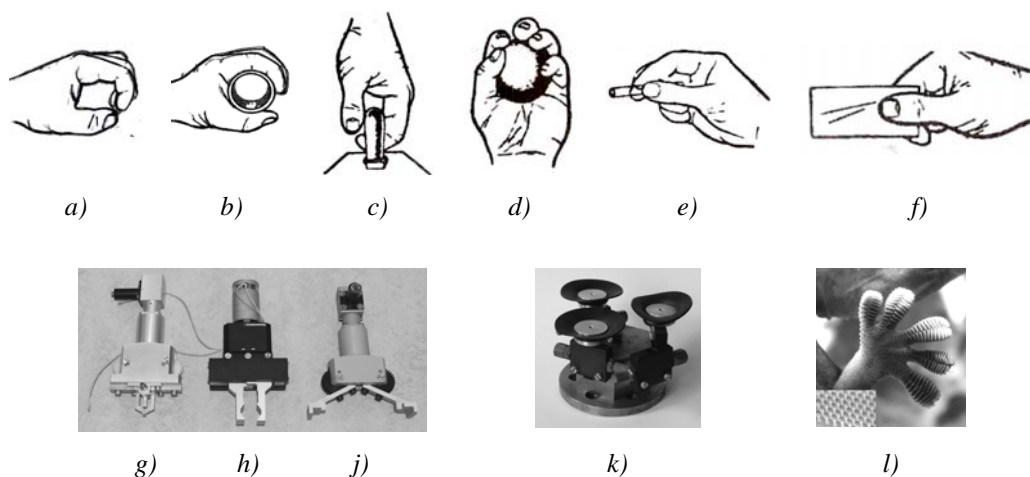


Figure 3. a)–f) Gripping with human hand, g)–k) robotic gripper, l) the sole of gecko

The *Figure 3. l)* shows the sole of a gecko, covered with millions of keratin hair having some micrometer. When the hairs get contact with some object, among the surface of object and each of hair fibre, a weak molecular attraction (van der Waals-type effect) occurs. These effects are tiny but the millions of fibres stick to the surface with a significant force. The *Figure 3. k)* shows a vacuum robotic gripper which joining effect is similar to the hair fibres but another one.

The product is, briefly and comprehensible saying, a work satisfying needs. Its content and interpretation are wider than that of the machine. Inherent parts of the product are, beyond the complex structure in which mechanical components interact, the effects on our visual, auditory, olfactory, or taste organs.

During the inquiry, to the analogy of machine elements, the part can be studied. Similarly, to the analogy of machine the complex creature and to the analogy of product the creature and its evoked effect can be studied.

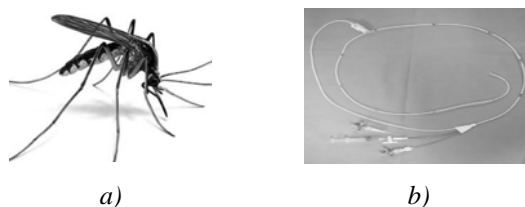


Figure 4. a) Blood-sucking female mosquito, b) medical catheter

For example, the piercing mouth organ of the mosquito can be inspected, the thin tube, which penetrates the skin causing no pain. Or that of the medical instrument similar to the sucker of mosquito can be studied, too, which is a catheter used to approach the inner parts of the body, to remove the undesirable parts, to widen any parts, etc. The parts of the mosquito as “a product” are the anticoagulant substance pressed into the pierced body, and also the “song” that evokes the presence and the sting of the mosquito.

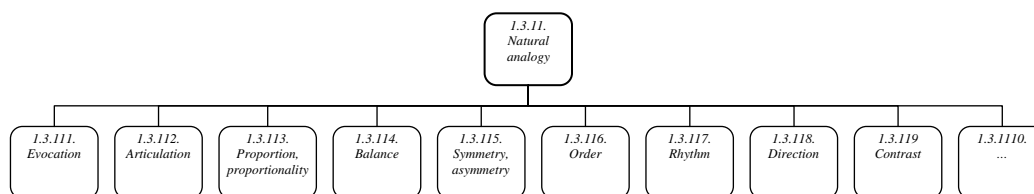


Figure 5. The components of the visual communication

4. LINGUISTIC ANALOGIES

When speaking one sounds the voices with the proper intensity to hear and to understand, creates words with **understandable length** from the voices and arranges the words into sentences with **comprehensible size**. The words obtain proper tone and emphasis in the sentences, according to their tasks, and **recall, tell something, following the rules of verbal communication**. The other creatures of the wildlife also communicate something with their sounds, they notify the demand over a territory, they search a partner of race or of op-

posite sex, they have their power felt, etc. **The animal sounds are also articulated, according to the essence of communication, those are emphasized and are diversified in accordance with the intention.**

The natural and artificial objects around us also let us know something, using the vision, the hearing, the touching, the taste and smell. The multitude of objects around us gives the most information about our environment. **The visual communication and understanding, based on the vision, have roles similar to the spoken language, which are learned by its users in cooperation with their environment during their development.** The visual perception is the active recording of things, which consist of a continuous consideration and comparison of the size, shape and colour of objects, and also the relationship among the parts, the whole product and the environment.

5. THE EVOCATION

The vision, hearing, touch, taste and smell of something produce the operation of their corresponding sensory organ. The sensory organ initiates a nerve process to the effect of stimulus, on the other hand it remains insensitive against the improper stimulus. If the intensity of the stimulus exceeds a certain threshold, it excites sensation. The notion is nothing more than the sum of sensations. **The evocation is interpreted as generating notions by seeing, hearing, tasting, touching, or smelling something.** The evocation is a valid category for both the human and the animal. **All carries a meaning, evokes something.** The man lives and socializes in a community and the decoding of sensations is based on the previously earned experiences, factual knowledge and the knowledge of the agreements within the community. For example the white cloth can be the sign of the purity or peace, but the evocation of death in other community. The evocation may be concrete and indirect. The sing of bird is concrete when it is recognised by the partners of species, and it is indirect when detecting the intensity of sound, the partners of species conclude on the physical condition of the singer. The meaning of a car logo in *Figure 6* is indirect; it evokes both the freedom of the wild horses galloping on the prairie and the sense of life of young people of the 1960's.



a)



b)

Figure 6. a) Galloping wild horses, b) Car logo of the Ford Mustang

6. ARTICULATION

The first step of the visual communication is the division into parts, the articulation. Similarly to the words, the parts should be noticeable, visible and tangible. The articulated parts differ from each other in form, size, volume, colour, surface quality, etc. **The essence of**

articulation is the separation of the parts, the function based distinction, the separation of parts corresponding to their essence.

Figure 7.a) shows a rhinoceros beetle (*Oryctes nasicornis*), its soft parts and inner organs is guarded by chitin shell. The shell is not a monolithic unit but the chain of the hard, considerable as rigid parts and the flexible hinge dominant parts. The articulated shell is not the gift of nature, **the articulation is determined by the function of parts**. In the *Figure 7.b*) the Ford KA brand car was given a simple, reduced to essentials, rain drop shape body to decrease the aerodynamic drag. **Distinct curves separate the functionally detached parts to evocate the relation between the function and the parts**. Contrary to the chassis of the Ford KA car, the body similar to a bar of soap which had lost its edges is easily forgettable, because the lack of the definitely distinct parts. **The inarticulate spatial formation, similarly to the inarticulate speech, do not maintain the interest and live no trace in our memory.**



a)



b)

Figure 7. a) Rhinoceros beetle and b) Ford KA brand car

There are creatures and man-made objects, which essence is the raising of no attention. The aim of the bird sitting on its eggs or the fawn crouching in the grass is the **hiding**. As a result of natural selection, they blend into their surroundings with then help of their feathers and fur, so **these animals constitute the inarticulate part of their surroundings**.



a)



b)

Figure 8. a) Nestling, crouching in the nest, b) soldiers in camouflage suits

One of the essential elements of the articulation is visualized by *Figure 8. a)*. There are three nestling blended into their surroundings, the fourth one however is stretching for feed, and is distinct from its surroundings by its bright red throat. The behaviour of the nestling is determined by the hiding or the attention-raising, as aim. Similarly to the nestling, the cam-

oufflage suits of the soldiers shown in *Figure 8. b*) are proper if they are inarticulate, undiscovered parts of the surrounding. If necessary, however, similarly to the nestling seeking feed, they sign their location to the friendly aircraft by a bright coloured sheathed. The examples illustrate that **the articulated or inarticulate being is determined by the aim and the task.**

7. PROPORTION AND PROPORTIONALITY

The scaling was developed from the counting, the appropriately chosen part of the numbered pattern, formation or mass, area are called unit mass, unit area, etc. For the sake of the visual communication the articulated parts are quantified, based on the unit, and the values can be compared to each other. **In a simple case the proportion is a comparison between two or among more values by the methods of the mathematics and the geometry.**

The designers have dealt with the proportion for a long time, e.g. the cause of beauty was searched by the scientists of antiquity, analysing the proportion of the human body [3], [5]. The cause of beauty was believed to be discovered, among others, in the golden section. Quantifying the lengths of the characteristic parts of the human body and comparing them, it was found that the ratio of the shorter and longer parts is equal to the ratio of the longer part and the whole.

The ratio of parts of the living and inanimate objects is independent of the observer, the relationship of the parts and its cause is searched by the man unintentionally. For example the crane bird lives in marshy, wooded countryside and eats sprouts of plants, rodents, fish and small mammals, standing on its tall legs it grabs the feed reaching far in advance and deeply by its neck, if necessary. Its long, slender legs and neck was adjusted to the way of life and the living environment by natural selection. The high, slender frame of a tower crane and the slender structure of the long extending jib are determined also by the problem. The load should be transmitted to a space domain, located far and occasionally deep from the tower. **In the case of creatures and the everyday objects the primary point of view is the expediency, the proportions are defined by the function.**

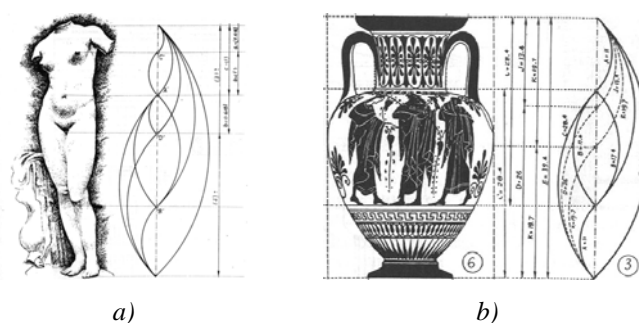


Figure 9. The golden section [3,5]

One of the simplest tools is the hammer, however, its dimensions and the proportions show diversity. The mass, the ratio of the handle and head are different in case of the hammer of the dentist, carpenter, the mason or the blacksmith who flatten thick steel plates. The func-

tion of tool determines its proportion. The thickness of the handle, however, varies in a relatively narrow range, regardless of the task, as the thickness and shape of the gripped part of the handle is determined by the dimensions and shape of the human hand. In other words, **the proportion of the parts of the tool is formed by the function of the tool and the man – tool relationship.**

8. BALANCE

The equilibrium or balance is a used term in both the everyday speech and the language of professions. The equilibrium is the status of a system when the resultant of the effects is zero. For example a mechanical system is in equilibrium when the resultants of forces and moments substituting the effect of the left parts are equal to zero. The parts may be in balance on the basis of their dimension, shape, surface quality, colour, sound, taste, etc., too. The balance is a natural part of the world of creatures and inanimate objects, one involuntarily looks for the cause when recognise the lack of balance.

9. SYMMETRY AND ASYMMETRY

A spatial formation is symmetric when its adequate parts are mirror images of each other, for the axis or the plane of symmetry. The parts of the planar symmetric formations are mirror images of each other, for the axis of symmetry or for a point. **The symmetry is an easily recognizable element of the living and inanimate, artificial and natural organs and formations.** The symmetric architecture has numerous messages. The *Figure 10. a)* shows a symmetric face part and healthy teeth. In case of a living organ **the symmetry evokes the physical integrity and health.** Let us think about its contrast, the physical deformations caused by injuries or certain diseases. Based on our experience, the symmetric bodies, completed by other constraints, are in equilibrium and they remain in rest, e.g. the builders of pyramids created stable structure that has announced the remembrance of their builders for thousands of years shown in *Figure 10.b)*. The dangerous machineries are formed symmetrical, e.g. the gas appliances shown in *Figure 10. c)*, too. **The symmetric form is the mediator of rest, timelessness and reliability.**

In our surroundings the most of the man-made objects are symmetric. The furnishings, equipment, books or the vehicles are usually symmetric, the symmetry is a generally used design principle. If you would like to focus attention onto something, it should be symmetrically prepared, e.g. the slot of a waste bin or the information desk is located in the middle to everyone can hit or find.

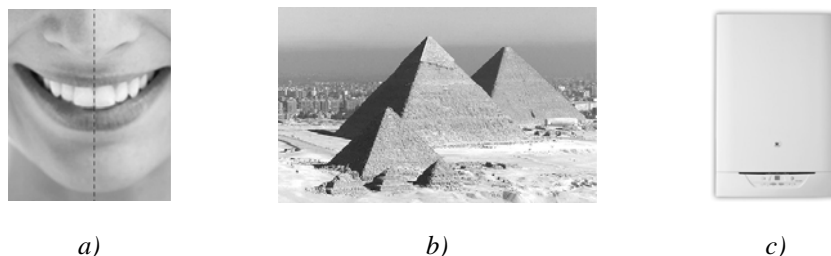


Figure 10. a) Symmetric face, b) symmetrically built pyramids and c) gas appliance

It is an everyday experience, that creation of a symmetric object or drawing of a perfect circle can be made only with some talent and adequate experience. The establishment of a regular spherical body gives satisfaction to both the creator and the viewer. The objects formed to symmetrical reveal about the talent of the creator. The ancient Pythagoreans considered the circle as a perfect planar object and the sphere as a perfect spatial body. Aristotle ascribed spherical forms to the celestial bodies as he considered them perfect creatures [5]. The balls, used in the advertising films, suggest the excellence of the institutions. The advertising graphic designers form the logo into a circle consciously, for this **evokes the perfection** in the observer [6]. **The symmetry symbolizes the order, the peace, the possession of knowledge necessary to control the processes, and the reliability in technical meaning.** The bodies of creatures are symmetric when looking superficially, however, having examined carefully, differences can be found on it. The phantom drawing is symmetric, but the picture taken of a living person is asymmetric a little, e.g. the eye, the nose, the ear differs from the symmetric formation which make the face come alive. **In the nature the symmetry and asymmetry exist together, the asymmetry is the embodiment of the living thing or phenomenon.** The asymmetry is usually the counterbalance of the symmetry, the tool for making the object come alive. The objects however can be asymmetric not only in their details but entirely, too, **when the destination intends so.** For example the hand tools, the small arms the cameras are usually one-handed and asymmetric, the handle assure a sure grip, following the form of the hollow of the right hand, and the control elements adjusted to the thumb and index finger of the right hand can be managed with natural motions. **In this case the asymmetric structure is the marker of the function.**



a)



b)

Figure 11. a) Asymmetric human hand, b) camera with asymmetrically arranged control elements

The asymmetric arrangement has a challenging effect, so the observer or user searches the cause asymmetry, e.g. at the control elements, **in the row of the same layout of buttons or keys, the asymmetrically located element calls the attention as visibly separated.** The balance of the asymmetrically arranged elements with each other has got the same effect as that of the symmetric design. **The destination decides between the symmetric and asymmetric design, the selection is always subject to the function.** The graphic designers can take advantage of the opportunity offered by the asymmetric arrangement of the shape; the asymmetrically located picture and text suggest vivid content. **The asymmetry is suggested by the content, and the varied content can be illustrated by asymmetric form.**



a)

b)

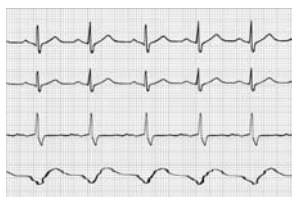
Figure 12. a) Order and b) disorder

10. ORDER

The message of the order is the same in both the nature and the man-made physical world, i.e. the conditions of existence, the growth and the enrichment are given, the things are going right and there are all the knowledge and skills available, which are necessary to the normal progress and control of the process. The disordered appearance speaks about the lack of conditions necessary to the normal being. In ordered condition, for the sake of good space utilisation the seeds are located along a logarithmic spiral in the plate of sunflower, as Figure 12. a) shows. In Figure 12. b) the disorder reveals the lack of order necessary to the cultured existence.

11. RHYTHM

The rhythm is a repeated articulation of any pattern. The rhythmical repetition is a basic human experience, such as the heartbeat, the healthy breathing and the return of the seasons. The modification or break in repetition may have a tragic consequence for both the individual and the community. **The rhythmic appearance of phenomena or patterns evokes that the process are going in order, as usual.**



a)



b)

Figure 13. a) Heart rhythm graph b) Greyhound coach
(Greyhound Corp., Pontiac, Michigan, 1954)

It is easy to recognise the rhythmic appearance, regardless of whether it is visual, auditory or touch based. **The rhythmic repetition amplifies the information.** The rhythmic articulation should be human scaled, i.e. the only repetition is understandable which is adapted to the sensitivity of our sense organ. The too high or too low frequency of appearance are felt no rhythmic repetition. The rhythmic appearance may have important role during the design

process. The side plates of coach shown in *Figure 13. b)* are corrugated, they evoke the orientation of progress of the vehicle. The corrugation of plates has got a point of view of strengthening, too. The flexural rigidity of the corrugated plate is higher by orders of magnitude than the flat plate having the same thickness. Further advantage of the corrugated plate is that the injuries and the repair do not cause as much as aesthetic error than that of on the flat plate. The operational temperature of prime movers, machines and electrical appliances are controllable by the help of radiator grilles, heat sinks and cooling fans. The rhythmic placement of the slots, the ribs or the blades of a fan is not a game with an end in itself, but the product function is converted into product design.

12. DIRECTION

Everyday experience is that the direction is in relation with the growth, enrichment or with the reduction, in other case with the displacement. The tree shown in *Figure 14. a)* well illustrates the spoken thoughts, its growth is not restricted by the surrounding and its shape points upwards. The essence of direction is illustrated by the logo of Lancaster University, shown in *Figure 14. b)*. **The university is universal but it does not unify and the limit of science is the starry sky. These are proclaimed by the four converging, similar but not identical bands which are pointing upwards** [6]. **The pyramid** shown in *Figure 10. b)* expands downwards, the resultant of the gravitational force acts inside the supporting surface, the structure is stable. **The form expanding downwards evokes the stability.** The *Figure 14. c)* shows the building of China Central Television in Peking. The visible part of the building **is not stable, the observer looks for the cause of the reason of staying standing up**, which lies in the design of the underground part of the building and the different distribution of mass of the standing and horizontal parts. **The purpose of amazing form is not the visualization of the stability but to attract the interest and the attention.**



Figure 14. a) Tree growing upwards, b) The logo of Lancaster University, c) The headquarter of China Central Television
(Rem Koolhaas and Ole Scheeren, *The Office for Metropolitan Architecture*)

The front panel or the windshield of the most vehicles is declined. The declined front panel is not a game with an end in itself, but there is less air resistance on it and it embodied a more favourable aerodynamic properties. **The declined front panel of the vehicles evokes**

the motion in both standing and moving conditions, the direction of progress and the advantageous design in the point of view of the losses of flow. Despite of this, a part of the chasses of the coaches are rectangular prism. **The standing front panel of these vehicles evokes not the direction of progress and speed but the intent of the designer that in a given volume the most number of passengers should be placed.**

13. CONTRAST

The terrestrial environment is created by natural a man-made object, which differ in dimension, mass, shape, proportion, colour, etc. The basis of contrast is the distinction, when the parts of the object and/or the environment are grouped on the basis of their evoking effect. The contrast is observable both in the worlds of creatures and man-made objects. In *Figure 15. a)* the bright feather dress of the male member of the pair of birds differs from its surroundings, contrarily to the simple feathers of the female blending into their surroundings. The contrast between the feather dresses is not an accidental phenomenon, the function is the raising awareness in the first case and that of the hiding on the other case.

The designer creates contrast with the shape, size, material and surface finish, pairing transparent and non-transparent materials, colours, patterns, etc., of the product. The baseline is not intention dependent, e.g. the tall is seen also tall and the small is seen also small when locating them next to each other. **In the contrast the difference makes the reception to be directed, e.g. the difference of two elements having the same form but differing sizes is recognized at once and the cause of difference is looked for, involuntarily.**



a)



b)

Figure 15. a) A pair of pheasants b) Wolf brand pruning shears

The contrast is not a game with an end in itself; it is created always on the basis of destination among the parts or between the object and its surroundings. The elements correlating with the usage can be highlighted or subordinated in such way, e.g. on the pruning shears shown in *Figure 15.b)* it is made visible that the cutting edges are strong and which part of the arms should be acted to, or what are the associated locations of the lock and the cutting edges. **During the design process the contrast is applied in correlation with the destination and also the usability of the product is highlighted with the contrast.**

14. SUMMARY

Our environment consists of living and inanimate creatures, natural and man-made objects. The proportional, symmetric and/or asymmetric body composition of the living creatures the rhythmic appearance of the parts, the direction of their formation, the relations among the parts or between the whole and its surroundings are the result of the natural selection,

the embodiment of the struggle for existence. The wildlife and the product designer use similar constructional principles to design functional, viable and competitive living creatures or products, respectively.

Acknowledgment

“This research was carried out as part of the TAMOP-4.2.1.B-10/2/KONV-2010-0001 project with support by the European Union, co-financed by the European Social Fund.”

References:

- [1] C. Darwin: *On the Origin of Species by Means of Natural Selection, or the Preservation of favored races in the struggle for life*. Fordítás: Charles Darwin: A fajok eredete. Természetes kiválasztódás útján. Neumann Kht., Budapest, 2004.
- [2] H. Debler: *Beitrag zur Rechnerunterstützten Verarbeitung von Werkstückinformationen in produktionsbezogenen Planungsprozessen*. Diss. TU Berlin, 1973.
- [3] Gy. Falusi: *Az aranykészítés legendája*. Magvető Kiadó, Budapest
- [4] H. Read: *Art and Industry*. Faber and Faber Ltd., London
- [5] S. Király: *Az arányosításról*. Magyar Iparművészeti Főiskola, Tölgyfa Kiadó, Budapest
- [6] Gy. Lissák: *A formáról*. Láng Kiadó és Holding Rt., Budapest
- [7] J. Péter–Cs. Dömötör: *Ipari design a fejlesztésben*. (Előadásjegyzet) Miskolc-Egyetemváros, 2012.

DYNAMICAL INVESTIGATION OF A SUPERFINISHING DEVICE

ATTILA SZILÁGYI–GYULA PATKÓ–TIBOR CSÁKI–BALÁZS BARNA
Machine Tools Department, University of Miskolc
H-3515 Miskolc-Egyetemváros
szilagyi.attila@uni-miskolc.hu; patko@uni-miskolc.hu;
csaki.tibor@uni-miskolc.hu; barna.balazs@uni-miskolc.hu

Abstract. This article concerns some dynamical aspects of the design process of a vibrational superfinishing device. As the first approximation, a linear dynamical model is applied, which is then replaced by an improved nonlinear one. The Coulomb-type damping, which is supposed to be the model of the superfinishing process, is considered to be the nonlinearity. The approximation solutions of the nonlinear governing equations are established by the method of linearization above the phase curve, thus the amplitude-frequency expressions and the expressions of the power characteristics in function of the system parameters can be set up. The optimal operation conditions have been established by revealing the extremums of these expressions. The results obtained analytically, have been proven and supported numerically.

Keywords: superfinishing, dynamical, nonlinear vibration, power characteristics

1. INTRODUCTION

Superfinishing is applied for fine manufacturing of cylindrical surfaces such as pistons, valves, raceways of rolling bearings etc. Such manufacturing process is generally performed by accessory devices adapted either by lathes or, in some cases, grinding machines as base machines. The smoothness of the manufactured surface is achieved as a superposition of a turning and an alternating motion produced by the basic machine and the superfinishing device. Since the superfinishing process requires vibration- and thermal-proof manufacturing environment, several dynamical problems, those are emerged during even the development process of the device, should be considered. Due to the capability of adaptation of such devices, their overall dimensions and weigh should also be considered carefully. These features are determined by the power characteristics of the device, which can be evaluated also by the means of dynamic analysis. The analysis can be performed on the basis of different types of models. Usually the linear model, which is the simplest, can already lead us to recognize some important phenomenon, whilst phenomenon of much wider range can be revealed by the application of nonlinear models.

2. INDUSTRIAL BACKGROUNDS

The Department of Machine Tools, University of Miskolc, as one of the members of a consortium established within an EU6 frame project, has participated in a project during the recent years to develop a superfinishing device which is capable of being mounted on a CNC turning machine of high precision for performing a combined superfinishing proce-

ture. To be able to perform such a combined superfinishing procedure (turning and finishing in one clamping), a device has been needed to construct, that can be integrated on a certain CNC turning machine. The task of the University of Miskolc was to develop the prototype device mentioned above, and its realization. Besides the University of Miskolc, the other members of the consortium were the Hembrug Machine Tool Company, Haarlem, The Netherlands, who was providing the CNC turning machine, the IPT, Fraunhofer Institute, Aachen, Germany, who was performing the manufacturing test series, the Cerobear and HWG bearing manufacturing companies from Germany, and the Diasfin Company from Romania providing the superfinishing stones. On the closing conference of the project, the industrial participants of the consortium raised the feasibility of a superfinishing device operated by a different principle, where the overall dimensions and weight of the new device is determined in such a way, that it could be adopted by a base machine without its reconstruction, and without blocking the displacement of the turret along the strokes. Due to some preconceptions, we think that if the power characteristics were to be increased and the revealed optimal superfinishing parameters were to be considered, a new device meeting the market requirements could be constructed, that works among significantly more efficient conditions, and thus it is much smaller and weighs less than the prototype device.

3. LITERATURE REVIEW

The power characteristics are revealed by the application of different mechanical models by the means of dynamic analysis, where the methods of the nonlinear vibrations and the mathematical methods concerning the approximation solutions of nonlinear motion-equations are applied [1, 3, 5, 6]. The approximation solutions of the nonlinear governing equations are achieved by the method of linearization above the phase-curve [7–8]. The results of the analytical solutions are compared to those of some numerical methods provided by the MAPLE12 and MATLAB/SIMULINK 6.5 softwares [2, 4].

4. THEORETICAL PRINCIPLES

Let the prototype superfinishing device, constructed and manufactured by the University of Miskolc, be assumed as a damped oscillating system, which is stimulated by a linear motor unit. The stimulation can be set up within a wide range of frequency and amplitude, so that the optimal superfinishing parameters could be established. The different combinations of superfinishing amplitude-frequency values will require different exciting force amplitudes and, of course, power. The higher the applied frequency and amplitude, the higher force amplitude and more power are required. However, if an appropriately tuned spring was connected to the oscillating parts of the device, thereby the device is tuned the appropriate manufacturing frequency, increased power characteristics could be obtained. The establishment of the optimum superfinishing parameters reduced the applied frequency and amplitude range to a significant extent, enabling the application of such a “well-tuned” spring mentioned above. Linear and non-linear models are assigned to the device, which enable us to explore the power characteristics of the device, and to establish the optimum superfinishing frequencies.

5. THE LINEAR DYNAMIC MODEL

The model of an electro-dynamical vibrator serves as the mechanical model of the devices under investigation *Figure 1*, where m , k and κ represent the mass of the oscillating parts, the spring stiffness and the coefficient of the linear damping which comes from the superfinishing process. As regards the electric parts, R_1 , R_2 and L_1 , L_2 represent the ohmic resistances and the self-inductances of the circuits 1 and 2, whilst M_{12} the flux-linkage. Symbols of U_1 and u_2 refer to the stimulating voltages of the circuits, and x_2 represents the displacement of the moving circuit 2.

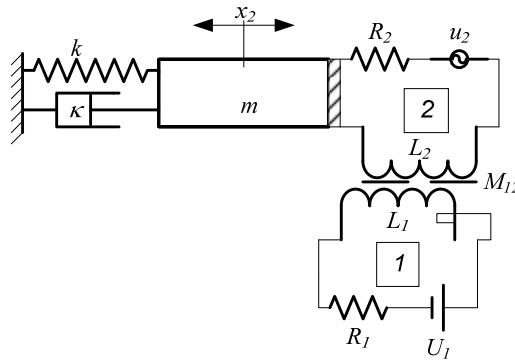


Figure 1. The linear electro-dynamical model

As usual in mechanical engineering practice, first the linear model with the linear governing equations evolved from the Lagrangian-equations of the second kind was established (1), where it was assumed that the maximum displacement of the moving body is considerably less than the longitudinal dimensions of the coils and the current state of the fixed coil as a separate exciter is not influenced by the moving part. The governing equation system takes the form of

$$\begin{aligned}
 m\ddot{x} + \kappa\dot{x} + kx - \alpha i &= 0 \\
 L \frac{di}{dt} + Ri + \Gamma\dot{x} &= U_0 \cos\Omega t \quad (1)
 \end{aligned}$$

where now U_0 and R refer only to the circuit 2. The expressions of the power characteristics, which come from the solutions of (1), and are established in function of the stimulating frequencies, display clearly that the optimum power characteristics are realized when the stimulating frequency is equal to the natural frequency of the device. The following diagrams display the extremums of some of the power characteristics ($\cos\psi_i$ the power-factor, and E_{be} the electric energy consumption), which refer to the optimum power condi-

tions (Figure 2), where f is the stimulating frequency, λ is the dimensionless frequency and, when $\lambda = 1$, the system is stimulated at its natural frequency.

It is pointed out numerically, that – whilst the same manufacturing conditions (A amplitude of the finishing motion, Ω angular frequency of finishing; Table 1) and system parameters are assumed, and then the power characteristics (i_0 current amplitude, F_0 amplitude of the pulling force, P_m , P_{eff} , P_s voltless, effective and apparent power etc) of both devices are compared to each other – the new device, which is stimulated at its natural frequency, operates among far more efficient power conditions than the prototype (Table 1).

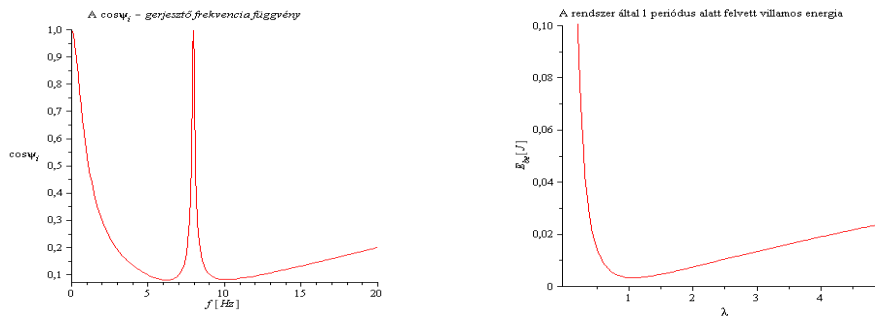


Figure 2. The extremums referring to the optimum power conditions

Table 1

The power characteristics of the prototype and the tuned device

Power characteristics		The values of the power characteristics	
		Prototype device ($k = 0$, $\Omega = \Omega_0 = 50 \frac{rad}{s}$)	New device ($k \neq 0$, tuned to its natural frequency: $\lambda = 1$)
$\sin \varphi_i$		0,994	0,000366
$\cos \varphi_i$		0,104	0,999999
A	[mm]	5	5
i_0	[A]	0,253	0,005
F_0	[N]	6,200	0,122
P_m	[VA]	0,755	0,000056
P_h	[W]	0,079	0,015
P_s	[VA]	0,759	0,015
Υ_R		0,806	0,001663
Υ_{Rh}		4,166	0,001665
E_R	[J]	0,008	0,000003254
E_{be}	[J]	0,010	0,001957

A similar dynamical analysis has been performed on the basis of a possible nonlinear model of the new, tuned superfinishing device, which is going to be discussed below.

6. THE NON-LINEAR DYNAMIC MODEL

A better model of the superfinishing process can be established with the application of a nonlinear damping characteristic such as, for example, the Coulomb-type dry friction, whose expression can be considered with the form of $S = -F_s \operatorname{sgn}(\dot{x})$, where F_s is the absolute value of the S kinetic friction force, and sgn is for the *signum* function. It is noted, that there is no difference distinguished between the static and kinetic friction forces during the analysis.

The nonlinear governing equations read

$$\begin{aligned} m\ddot{x} + F_s \operatorname{sgn}(\dot{x}) + kx - \alpha i &= 0 \\ L \frac{di}{dt} + Ri + \Gamma \dot{x} &= U_0 \cos \Omega t \end{aligned} \quad (2)$$

where the other symbols are already defined. In order to see the influence of the system parameters on the power conditions of the model, the solutions as the continuous functions of the parameters would be of interest. Thus the approximation solutions of the differential-equations (2) are established by the method of linearization above the phase curve [7][8]. Periodic solutions of (2) should be assumed, so that the linearization method could be applied. As a result of the linearization, the linear governing equation system reads

$$\begin{aligned} m\ddot{x} + \frac{4F_s}{\pi a_1 \Omega} \operatorname{sgn}(\dot{x}) + kx - \alpha i &= 0 \\ L \frac{di}{dt} + Ri + \Gamma \dot{x} &= U_0 \cos \Omega t \end{aligned} \quad (3)$$

where a_1 is the unknown displacement amplitude. When the method of linearization above the phase-curve is applied, the solutions are assumed to take the forms of $x(t) = a_1 \cos(\Omega t + \varphi_A)$ and $i(t) = i_0 \cos(\Omega t + \varphi_i)$, where $i(t)$ is the expression of the current-function along circuit 2 and i_0 is the unknown current-amplitude. φ_A and φ_i are the unknown angels of phases to the stimulating voltage. If $x(t)$ and $i(t)$ is replaced in (3) and the algebraic transformation of the expressions is carried out, then the analytical expressions of a_1 , i_0 , φ_A and φ_i as the functions of the stimulating angular frequency and the system parameters are obtained.

Introducing the $\frac{k}{m} = \nu^2$, $\frac{\Omega}{\nu} = \eta$, $\eta^2 = \xi$ new variables, the expression of

$$a_1^\pm(\eta) = -\frac{\frac{8F_s}{\pi} \alpha L R \nu \eta}{2\left\{[mR\nu^2(1-\eta^2)]^2 + \nu^2\eta^2[mLv^2(1-\eta^2) + \alpha L]^2\right\}^\pm}, \quad (4)$$

$$\pm \frac{\sqrt{\left(\frac{8F_s}{\pi} \alpha L R \nu \eta\right)^2 - 4\left\{[mR\nu^2(1-\eta^2)]^2 + \nu^2\eta^2[mLv^2(1-\eta^2) + \alpha L]^2\right\} \left\{\left(\frac{4F_s}{\pi}\right)^2 (R^2 + L^2\nu^2\eta^2) - (\alpha U_0)^2\right\}}}{2\left\{[mR\nu^2(1-\eta^2)]^2 + \nu^2\eta^2[mLv^2(1-\eta^2) + \alpha L]^2\right\}}$$

is obtained, where a_1^+ and a_1^- refer to the curves identified by the positive or negative sign in front of the expression of square root, and ν is the natural frequency of the system, and η is a dimensionless angular frequency. Since the exact solutions of (3) are obtained as the continuous functions of the system parameters, so their influence on the power conditions can be tracked down clearly and more or less exactly.

As the second result of the approximation method, two curves have been obtained for the displacement amplitude, so stability analysis had to be performed to decide whether which curve real numerical values belong to. When the real amplitude-curve is known, it is pointed out, that stimulating the nonlinear model at its natural frequency, whilst some combinations of parameters are fulfilled, it operates among optimum power conditions. The results obtained analytically, have been checked numerically.

7. THE POWER CONDITIONS

After the stable one of the curves (4) had been concluded, the expressions of the power characteristics can be established as the functions as the stimulating dimensionless frequencies. It was pointed out, that if the relations of

$$(\rho^2 - 2\gamma)^2 - 3(\gamma^2 - 2\rho^2) > 0, \quad \rho = \frac{R}{L\nu} \gg 1, \quad r = \frac{F_{S_H}}{F_S} \gg 1, \quad \rho = \frac{R}{L\nu} \gg 1$$

were fulfilled at one time and the system is stimulated at its natural frequency, then the device would operate among optimal power conditions. The analytical results have been checked by numerical investigations. The following diagram displays the extremums of some of the power characteristics (E_{be} the total electric energy consumption of the system, E_R the electric energy consumption of the ohmic resistance, E_h the electric energy consumption of the Coulomb-damping, which is considered to be equivalent to the finishing process), which refer to the optimum power conditions (Figure 3). η is the dimensionless frequency.

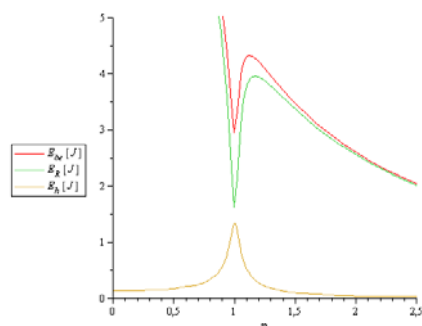


Figure 3. The extremums of some power characteristics at resonance frequency

The following table contains the numerical values of each power characteristic by which the power conditions of the nonlinear models of the prototype and the new devices are compared to each other, whilst the manufacturing parameters are assumed to be the same for both models (Table 2). It can be seen clearly, that adding an appropriate flexible element to the prototype device, the optimum manufacturing parameters can be achieved by less pulling force (F_0) and non-significant wattles power (P_m), whilst the electric energy (E_{be}) and the current consumption (i_0) is significantly reduced comparing to those of the prototype device.

Table 2

The power conditions of the prototype and the properly tuned devices based on nonlinear models

Power characteristics	Prototype device ($k = 0$)	New device ($k \neq 0$, tuned to its natural frequency: $\eta = 1$)
$\sin \varphi_i$	0,63	0,083
$\cos \varphi_i$	0,77	0,996
A [mm]	1	1
i_0 [A]	23,19	3,74
F_0 [N]	728,16	76,40
P_m [VAR]	605,04	4,62
P_h [W]	733,93	54,95
P [VA]	951,17	55,15
Y_R	0,99	0,86
Y_{Rh}	98,98	6,57
E_R [J]	24,21	1,59
E_{be} [J]	24,46	1,83

These optimum power conditions make it possible for us to construct such a linear motor driven device, whose overall dimensions and weigh is much more favourable than those of

the prototype device, and thus can be adopted on a certain ultraprecise hard-turning machine without significant reconstructions and producing thermal and vibrational disturbances which would have some effects on the work-room of the base-machine.

8. SUMMARY

This article is a brief summary of the results of some dynamic and power calculations emerging in the development process of a superfinishing prototype-device. The subject of the investigation is a 1-phase electromechanical superfinishing device operated by electricity and performing an oscillating movement of short-stroke. Linear and non-linear models are assigned to the device, which enables us to explore the power characteristics of the device and to establish the optimum superfinishing frequencies. The positive effect of the appropriate flexible element was demonstrated, i.e. considering constant manufacturing parameters, and exciting the non-linear system at its natural frequency, it becomes possible to construct an improved device of a significantly smaller size and of increased power consumption efficiency than the prototype.

Acknowledgement

“This research was carried out as part of the TAMOP-4.2.1.B-10/2/KONV-2010-0001 project with support by the European Union, co-financed by the European Social Fund.”

References

- [1] Harris–Crede: *Shock and vibration handbook*. McGraw-Hill Co. Inc., 1956.
- [2] A. Heck: *Bevezetés a Maple használatába*. Juhász Gyula Felsőoktatási Kiadó, Zenon Kft., Szeged, 1999.
- [3] J. D. W.ordan–P. Smith: *Nonlinear ordinary differential equations*. Oxford University Press, 1999.
- [4] J. L. Meriam–L. G. Kraige– B. D. Harper: *Dynamics – Solving dynamics problems in Maple*. John Wiley & Sons, Inc., 2007.
- [5] A. H. Nayfeh–D.T. Mook: *Nonlinear oscillations*. John Wiley & Sons, Inc. 1995.
- [6] J. M. T Thompson–H. B. Stewart: *Nonlinear dynamics and chaos*. John Wiley & Sons, 2001.
- [7] Gy. Patkó: *Dinamikai eredmények és alkalmazások a gépészetben*. A Miskolci Egyetem Habilitációs Füzetek, Miskolc, 1998.
- [8] Gy. Patkó: *Közelítő módszer nemlineáris rezgések vizsgálatára*. Kandidátusi értekezés, Miskolc, 1984.

ANALYTICAL MODEL TO DETERMINE MESHING STIFFNESS OF SPUR GEARS

RENÁTA SZÚCS–LÁSZLÓ KAMONDI

Department of Machine and Product Design, University of Miskolc

H-3515 Miskolc-Egyetemváros

szucs.renata@citromail.hu; machkl@uni-miskolc.hu

Abstract. During dynamic analysis of gears correct determination of the meshing stiffness bears great importance. In order to determine meshing stiffness first of all the contact points have to be located. In this work a general method is presented for determining the contact points i.e. the contact curve, and a special method for involute profiles. An analytical method for deflection analysis of spur gears is formulated. During deflection analysis elastic deformation of the teeth is taken into account and as a consequence of the model and the calculation method failure in the base pitch and the profile can be treated.

Keywords: gear mesh, meshing stiffness, elastic deflection, non-linear dynamics

1. INTRODUCTION

Due to the increasing demands analysis of reasons of noise sources and dynamic effects is important, it is also indicated by the numbers of works published even nowadays in this area. On one hand installation inaccuracies and on the other hand elastic deformation of the teeth and base pitch and profile errors are the most common reasons of the undesired dynamic effects.

Endeavour to increase volume performance and service life of drive gears results in installation of gears of smaller accuracy grade. In case of these accuracy grades scale of elastic deformations and teeth errors can be the same. In order to decrease the disturbing effect of elastic deformation trimming of the tooth tip is a common procedure, but from the point of analysis of stress conditions, knowing deflections of the tooth at the whole contact region is essential.

Before wide-spreading of computers only analytical methods were available for deflection analysis. In that time authors [Karas, Weber] modelled the tooth as a cantilever. Between these models the main difference was the description of the tooth profile i.e. some models only approximate the involute curve, while others deal with the real curve. Of course these models vary on approximation of other conditions too. Nowadays papers dealing with tooth deflection of external spur gears can be divided into two main groups. Studies belonged to the first groups [2–5] model the tooth as a cantilever beam even nowadays, but owing to development of calculation and modelling methods approximations are more accurate and on the other hand in most cases authors supplement their results with FEA analysis. Studies of the second group [6–9] use FEM analysis for determine tooth deflection of gears. Regarding the considered and neglected stresses (e.g. pressing, bending, shearing) causing deflection studies also differ from each other.

By the help of Finite Element Method analysis of gears is realizable in 3Ds, but it bears more importance in case of helical gears. From this point of view authors study tooth deflection by analytical methods in which the tooth is modelled by a cantilever, in this work

this method is presented in case of involute profiles. In this paper the model established by the authors neglects installation inaccuracies and friction, only takes into account the effects of elastic deformation. In later studies our aim is to verify results of this paper by FEM.

2. DYNAMIC MODELL

For dynamic analysis of gear drives a model shown in *Figure 1* has been developed [10, 11, 12]. The driver and the driven gear are modelled by masses rotating around the central points of the gears, while meshing is modelled by an equivalent spring and a damping proportional with the velocity in the direction of line of action. This model contains backlash which is neglected from the point of contact analysis at this stage. The model neglects friction and installation inaccuracies.

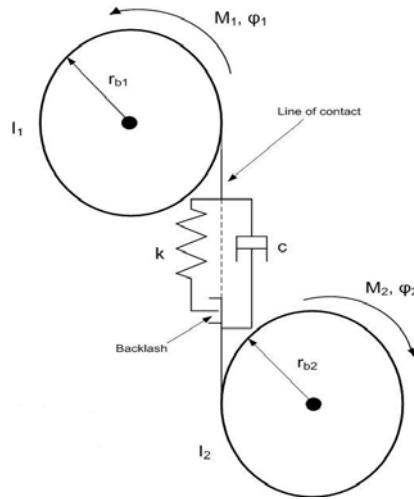


Figure 1. Dynamic model

Apart from development for the equation of motion the following relation can be written:

$$m \cdot \ddot{x} + c \cdot \dot{x} + k(t) \cdot h(x) = f_T(t) + f_M(t), \quad (1)$$

where:

$$m = \frac{I_1 \cdot I_2}{I_1 \cdot r_{b2}^2 + I_2 \cdot r_{b1}^2}, \quad (2)$$

$$f_T(t) = \frac{r_{b1} \cdot I_2 \cdot M_1 - r_{b2} \cdot I_1 \cdot M_2}{I_1 \cdot r_{b2}^2 + I_2 \cdot r_{b1}^2}, \quad (3)$$

$$f_M(t) = -m \cdot \ddot{\epsilon}(t), \quad (4)$$

$$h(x) = \begin{cases} x - b, & x \geq b \\ 0, & |x| > b \\ x + b, & x \leq -b \end{cases} \quad (5)$$

Table 1

List of symbols and parameters

I_1, I_2	moments of inertia
φ_1, φ_2	rotational angles
$x = r_{b1}\varphi_1 - r_{b2}\varphi_2$	relative displacement
r_{b1}, r_{b2}	radii of base circles
M_1, M_2	external torques
$2b$	whole backlash
c	damping
$k(t)$	meshing stiffness
$e(t)$	static transmission error

Aim of this study is to determine meshing stiffness $[k(t)]$, in order to introduce it into equation (1) for further works.

3. MESHING CONDITIONS

Determining of contact points is essential in order to calculate meshing stiffness during the course of meshing. In this section a general method and a special procedure adaptable to involute profiles can be found for contact analysis.

3.1. General tooth profile

Supposing that that curves of the mating gear profiles are known for determining the law of motion well-elaborated methods are available [1]. During the solution of this problem three coordinate systems should be employed, two of them are moving coordinate systems (S_1, S_2) rigidly connected to gear 1 and gear 2 respectively (centre of gear 1 and 2 are O_1 and O_2). The third coordinate system is a fixed coordinate system, which is in rigid connection with the frame. Then equations of the individual tooth profiles and their normal vectors are prescribed in their own moving coordinate systems:

$$\boldsymbol{\rho}_i = \boldsymbol{\rho}_i(u_i) \quad i = 1, 2, \quad (6)$$

$$\mathbf{e}_i = \mathbf{e}_i(u_i) \quad i = 1, 2 \quad (7)$$

Let us transform eq. (5) and eq. (6) into the fix coordinate system S. In the function of individual rotational angles φ_1, φ_2 equations of the tooth profiles and the normal vectors are given:

$$\boldsymbol{\rho}^{(i)} = \boldsymbol{\rho}^{(i)}(u_i, \varphi_i) \quad i = 1, 2, \quad (8)$$

$$\mathbf{e}^{(i)} = \mathbf{e}^{(i)}(u_i, \varphi_i) \quad i = 1, 2 \quad (9)$$

If the two gears are in contact, both the radius vectors of these two profiles and both the basic vectors of the normal profiles should be the same, supposing the same orientation:

$$\boldsymbol{\rho}^{(1)}(u_1, \varphi_1) = \boldsymbol{\rho}^{(2)}(u_2, \varphi_2) \quad (10)$$

$$\mathbf{e}^{(1)}(u_1, \varphi_1) = \mathbf{e}^{(2)}(u_2, \varphi_2) \quad (11)$$

Solving equation (7) and (8) three independent scalar equations can be obtained. Knowing rotational angle φ_1 , as the function of this angle, displacement function can be determined.

As a consequence of the fore-mentioned in case of general, prescribed profile curves determination of contact points is possible and so based on deflection analysis (See in Section 4) calculation of meshing stiffness.

3.2. Involute profile

Still nowadays one of the most widely used gear profile is involute. So analysis of the involute profile as a special case is reasonable. Compared to the general case for involute tooth profile several simplifications can be applied. The biggest advantage is that the contact curve is a line with direction angle of working pressure angle α_w and, which passes through point C (pitch point). Theoretically meshing can take place on this line between point A and E. The tooth contact begins at point A and terminates at point E during the course of tooth contact. Points A and E are intersected by the addendum circles of the respecting gears. In a given moment of the mesh by producing the mating involute profiles their pedal points can be obtained in the base circle (e.g. E – B_{E2}) (See Figure 2). Selecting the mating at point C as a base, any of the mating positions can be described by these pedal angles (α_{E2}).

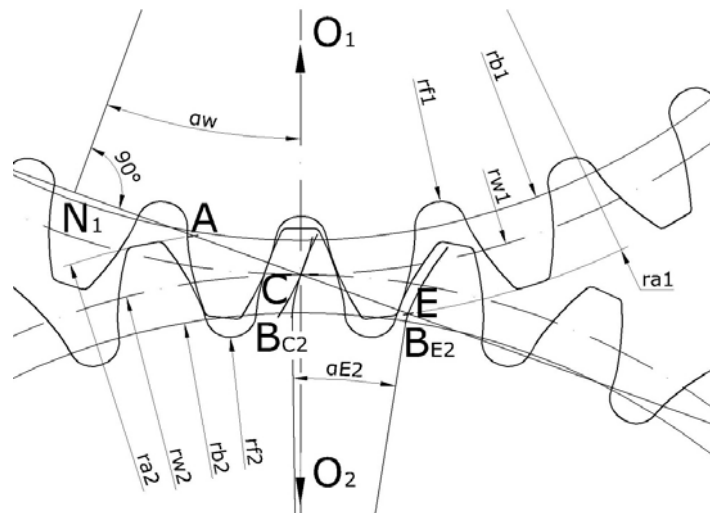


Figure 2. Contact line in case of error-free, involute profile

Since we assumed that the geometrical dimensions of the gears are known the tooth thickness measured at the working circle (s_w) is also known. Coordinates of the profile are established from profile point P, located at the working circle.

An arbitrary point of the tooth profile is J, and j presents its motion during the contact. Position of J^j related to point P can be described by α_j^j (See Figure 3). Variation of α_j^j also describes meshing.

Coordinates x_j^j, y_j^j of an arbitrary point J^j can be determined by angles ψ_j^j, α_j^j and by the radius of the base circle (r_b):

$$x_j^j = \frac{r_b}{\cos \alpha_j^j} \sin \psi_j^j, \quad (12)$$

$$y_j^j = \frac{r_b}{\cos \alpha_j^j} \cos \psi_j^j. \quad (13)$$

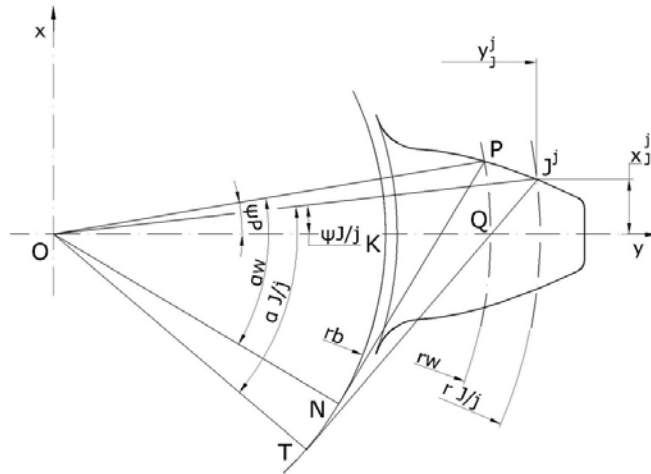


Figure 3. Explanation of point J^j

Angle α_j^j belonged to point J^j can be determined by distance $\overline{J^jT}$ and by the radius of the base circle (r_b):

$$\alpha_j^j = \frac{\overline{J^jT}}{r_b} = \frac{\overline{PN} + \widehat{NT}}{r_b}. \quad (14)$$

Angle Ψ_j^j determining location of point J^j can be calculated by the help of tooth thickness of the working circle. While angle ψ_p (POx) can be determined as

$$\Psi_p = \frac{s_w}{2r_w}, \quad (15)$$

where: $\overline{PQ} = 0,5 \cdot s_w$.

According to the fore-mentioned we can establish the following relation for angle Ψ_j^j :

$$\Psi_j^j = \Psi_p + \text{inv}\Psi_p - \text{inv}\alpha_j^j. \quad (16)$$

By continuous change of angle α_j^j coordinates of the involute profile can be determined from the addendum circle to the limit circle. It is important because in fact meshing not only in the AE region can intervene but before point A and after point E. By the help of this method the whole gear profile can be described while mesh at the root curve does not intervene.

4. DETERMINATION OF DEFLECTIONS

The tooth is considered to be elastic and modelled as a non-uniform cantilever embedded through its width b . Cross section of the cantilever is changing in the function of the tooth width at the relevant point. The mating tooth pair is loaded by nominal load F_N . Due to this load the tooth deflects and flattens at the point of contact. This deformation results that the angular rotation determined by the gear ratio differ from the real gear ratio since the axis of the driven gear differ from the axis of the driver gear.

4.1. Model of the tooth and introduction of parameters

Deformation arising from different deflections is determined as the resultant of the “individual” tooth sections, because deflection depends on location of fulcrum of the load, i.e. instantaneous contact point. Deformation arising from interpenetration is determined aggregately to the whole tooth as it roughly constant along the contact path.

Deformation of the mating teeth is determined by the resultant of displacements in direction of the line of action.

As a result of the normal force the following displacements projected to direction of the line of action can be determined:

- δ_{fa}^j : from bending,
- δ_{fb}^j : from shearing,
- δ_{fp}^j : from pressing,
- δ_{fc}^j : fillet-foundation,
- $\delta_{fd1,2}^j$: contact deflection.

In this study we neglect deflection due to pressing, in the following we only take into account the remaining four elements.

For calculation of these deformation we divided cross section of the tooth into n segments which height is $y_k - y_{k-1}$, and length is x_k as shown in *Figure 4*. For the segment s_k we get

$$\bar{I}_k = \frac{I_k + I_{k-1}}{2}, \quad (17)$$

$$I_k = \frac{1}{12} b(2x_k)^3, \quad (18)$$

Height of cross section of the tooth can be obtained as:

$$s_k = y_k - y_{k-1}. \quad (24)$$

Supposing plain stress condition, i.e. along face stress is zero, principal strain directions and principal stress direction are coincided, we can introduce elasticity module depending on Poisson ratio (ν):

$$E_\nu = \frac{E}{1 - \nu^2}. \quad (25)$$

4.2. Bending deflection

Component $F_{NJ}^j \cdot \cos\gamma_j^j$ of load F_{NJ}^j acting at point J^j bends and shears the tooth, while concentrated moment $F_{NJ}^j \cdot \sin\gamma_j^j \cdot x_j^j$ at point D_j^j bends the tooth in opposite direction. We note that load component $F_{NJ}^j \cdot \sin\gamma_j^j$ subjects the tooth to compression load, but it is ignored as it was mentioned in Section 1.

Deformation can be calculated from balance of the external and internal forces.

Let us treat the tooth rigid from fulcrum of the load to section k and segment while segment s_k is considered to be elastic. According to [14] strain in direction x of point D_j and rotation of the neutral plane can be calculated.

For stain $\delta_{xa1}^{j,k}$ arising from the bending caused by component $F_{NJ}^j \cdot \cos\gamma_j^j$ we get:

$$\delta_{xa1}^{j,k} = \frac{F_{NJ}^j \cdot \cos\gamma_j^j \cdot s_k}{6E_\nu \bar{I}_K} (2s_k^2 + 5F_K s_K + 3F_K^2), \quad (26)$$

for rotation of the neutral plain:

$$\theta_{j1}^{j,k} = \frac{F_{NJ}^j \cdot \cos\gamma_j^j \cdot s_k}{2E_\nu \bar{I}_K} (s_k + 2F_K). \quad (27)$$

For stain of D_j ($\delta_{xa2}^{j,k}$) arising from the concentrated moment we have:

$$\delta_{xa2}^{j,k} = -\frac{F_{NJ}^j \cdot \sin\gamma_j^j \cdot x_j^j \cdot s_k}{2E_\nu \bar{I}_K} (s_k + 2F_K), \quad (28)$$

while angular rotation $\theta_{j2}^{j,k}$ is

$$\theta_{a2}^{j,k} = -\frac{F_{NJ}^j \cdot \sin\gamma_j^j \cdot x_j^j \cdot s_k}{E_\nu \bar{I}_K}. \quad (29)$$

Accomplishing calculations, resultant strain and angular rotation can be expressed according to the following equations:

$$\delta_{xa1}^j = \frac{F_{NJ}^j \cdot \cos\gamma_j^j}{6E_\nu} \sum_{k=1}^N \frac{s_k}{\bar{I}_k} (2s_k^2 + 5F_K s_K + 3F_K^2), \quad (30)$$

$$\theta_{J1}^j = \frac{F_{NJ}^j \cdot \cos\gamma_J^j}{2E_v} \sum_{k=1}^N \frac{S_k}{I_k} (s_k + 2F_k), \quad (31)$$

$$\delta_{xa,2}^j = -\frac{F_{NJ}^j \cdot \sin\gamma_J^j \cdot x_J^j}{2E_v} \sum_{k=1}^N \frac{S_k}{I_k} (s_k + 2F_k), \quad (32)$$

$$\theta_{a2}^j = -\frac{F_{NJ}^j \cdot \sin\gamma_J^j \cdot x_J^j}{E_v} \sum_{k=1}^N \frac{S_k}{I_k}. \quad (33)$$

Strain in direction of the line of contact is given by

$$\delta^j = \delta_x^j \cdot \cos\gamma_J^j, \quad (34)$$

where $\delta_x^j = \overline{J'A^j} - \overline{C^jA^j}$.

Resulting from triangle $A_jA^jD^j$: $\overline{C^jA^j} = x_J^j \cdot \theta_J^j \cdot \tan\gamma_J^j$.

Recalling eq. (34) we can write:

$$\delta^j = \delta_{xi}^j \cdot \cos\gamma_J^j - x_J^j \cdot \theta_J^j \cdot \sin\gamma_J^j, \quad (35)$$

where $i=a, b, c$.

Substituting equations (30-33) into eq. (35) strain is then:

$$\begin{aligned} \delta_{Ja}^j = \frac{F_{NJ}^j}{E_v} & \left[\frac{\cos^2\gamma_J^j}{6} \sum_{k=1}^N \frac{S_k}{I_k} (2s_k^2 + 5F_k s_k + 3F_k^2) - \cos\gamma_J^j \sin\gamma_J^j \right. \\ & \left. \cdot x_J^j \sum_{k=1}^N \frac{S_k}{I_k} (s_k + 2F_k) + \sin^2\gamma_J^j \cdot (x_J^j)^2 \sum_{k=1}^N \frac{S_k}{I_k} \right], \end{aligned} \quad (36)$$

where

$$\delta_{xa}^j = \delta_{xa1}^j + \delta_{xa2}^j \text{ and } \theta_J^j = \theta_{J1}^j + \theta_{J2}^j. \quad (37)$$

4.3. Shearing deflection

Component $F_{NJ}^j \cdot \cos\gamma_J^j$ of the load F_{NJ}^j acts as a shearing force which produces deformation of the tooth in direction x . As a consequence of nature of the deformation segment of the tooth between Y_k and Y_{k-1} behaves as a rigid element so it displaces in the direction of axis x , but it is not subjected to angular rotation.

According to [14] displacement for the k^{th} segments can be written as

$$\delta_{xb}^{j,k} = \frac{1,2F_{NJ}^j \cdot \cos\gamma_J^j \cdot S_k}{G \cdot A_k}, \quad (38)$$

by substituting it for every k segments, for distance $\overline{D^j D^j}$ the following can be obtained:

$$\delta_{xb}^j = \frac{1,2F_{NJ}^j \cdot \cos\gamma_j^j}{G} \sum_{k=1}^N \frac{s_k}{\overline{A_k}}, \quad (39)$$

and for angular rotation:

$$\theta_{j1}^j = 0. \quad (40)$$

Displacement arising from shearing in the direction of the line of contact is:

$$\delta_{jb}^j = \delta_{xb}^j \cdot \cos\gamma_j^j = \frac{1,2F_{NJ}^j \cdot \cos^2\gamma_j^j}{G} \sum_{k=1}^N \frac{s_k}{\overline{A_k}}. \quad (41)$$

4.4. Fillet-foundation deflection

The relative slender tooth connects to a bulky gear body. Connection of the gear body and the tooth has certain flexibility. If the tooth is considered to be rigid then displacement of work point J^j also arises from fillet-foundation deflection as a consequence of angular rotation of the tooth. Deformation is generated by the effect of moment $F_{NJ}^j [\cos\gamma_j^j \cdot (y_j^j - y_F) - \sin\gamma_j^j \cdot x_j^j]$.

For displacement as a result of the moment we get [14]:

$$\delta_{xc}^j = \frac{1,327F_{NJ}^j \cdot [\cos\gamma_j^j \cdot (y_j^j - y_F) - \sin\gamma_j^j \cdot x_j^j] \cdot (y_j^j - y_F)}{E_v \cdot x_F^2 \cdot b}, \quad (42)$$

for angular rotation:

$$\theta_{j1}^j = \frac{1,327F_{NJ}^j \cdot [\cos\gamma_j^j \cdot (y_j^j - y_F) - \sin\gamma_j^j \cdot x_j^j]}{E_v \cdot x_F^2 \cdot b}. \quad (43)$$

Displacement in the direction of the line of contact:

$$\delta_{jc}^j = \frac{1,327F_{NJ}^j \cdot [\cos\gamma_j^j \cdot (y_j^j - y_F) - \sin\gamma_j^j \cdot x_j^j]^2}{E_v \cdot x_F^2 \cdot b}. \quad (44)$$

4.5. Contact deflection

Conjunct deformation arising from flattening of the mating tooth pair can be determined according to [15] assuming that tooth are replace by cylinders with radii corresponding to them circles of curvature. Approach of the two cylinders is:

$$\delta_{jd1,2}^j = \frac{3 \cdot 10^{-4} \cdot \varepsilon_{EV}^{2,7} \cdot F_{NJ}^{0,9}}{b_{1,2}^{0,8}}, \quad (45)$$

where $b_{1,2}$ is the common tooth width of the contacting teeth,

$$\varepsilon_{Ev} = \sqrt[3]{\frac{11,5(E_{v1} + E_{v2})}{E_{v1} \cdot E_{v2}}}, \quad (46)$$

where

$$E_{v1,2} = \frac{2 \cdot E_{v1} \cdot E_{v2}}{E_{v1} + E_{v2}}. \quad (47)$$

So for eq. (45) we get:

$$\delta_{Jd1,2}^j = \frac{2,55 \cdot F_{NJ}^{j \cdot 0,9}}{E_{v1,2}^{0,9} \cdot b_{1,2}^{0,8}}, \quad (48)$$

where $F_{NJ}^j = 0,5F_{NJ}$ supposing contact of two teeth.

5. DETERMINATION OF THE MESHING STIFFNESS

According to the deflections specified in Section 4 meshing stiffness can be determined.

Meshing stiffness arising from bending deflection is given by:

$$k_{Ja}^j = \frac{F_{NJ}^j}{\delta_{Ja}^j}. \quad (49)$$

Meshing stiffness arising from shearing deflection is given by:

$$k_{Jb}^j = \frac{F_{NJ}^j}{\delta_{Jb}^j}. \quad (50)$$

Meshing stiffness arising from fillet-foundation deflection is given by:

$$k_{Jc}^j = \frac{F_{NJ}^j}{\delta_{Jc}^j}. \quad (51)$$

Meshing stiffness arising from contact deflection is given by:

$$k_{Jd1,2}^j = \frac{F_{NJ}^j}{\delta_{Jd1,2}^j}. \quad (52)$$

For one pair of teeth in contact the summarized meshing stiffness can be calculated from the sum of the individual meshing stiffness (15-18):

$$k_{1,2}^j = k_{J1,abc}^j + k_{J2,abc}^j + k_{J1,2}^j. \quad (53)$$

As deflections are continuously changing during the meshing cycle, so meshing stiffness changes too.

5.1. More than one tooth pair in contact

Of course there are cases when more than one tooth pair is in contact. The mating tooth pairs are individually modelled by springs connected in parallel (See *Figure 5*), so for the entire contact can be treated as a spring system [12]. In this case the components of the load should be divided between the tooth pairs. Determination of this division is subject to an individual study. After specifying this division the fore-presented method can be employed for the individual springs (k_1, k_2, \dots, k_n) and the resultant mesh stiffness can be calculated according to the following equation:

$$k_{\Sigma} = k_1 + k_2 + \dots + k_n . \quad (54)$$

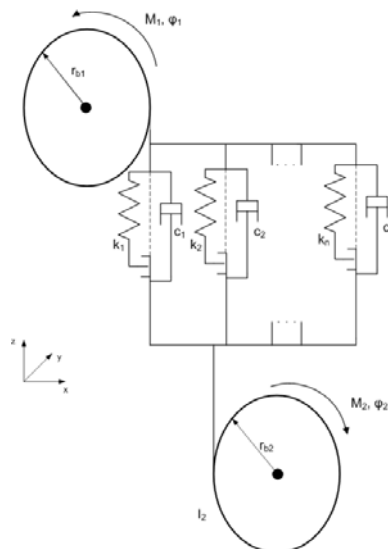


Figure 5. Modified model

6. CONCLUSION

For calculation of meshing stiffness of involute spur gears an analytical method is presented in this work. Based on the proposed method a computer program computing deflections is possible. The goal of this work is to integrate results of Section 4 into dynamic analysis and thus connect gear kinematics with gear dynamics. Of course verification of these results should be done by measurements and by FEM analysis. Aim of the authors to accomplish these confirmation steps in further studies.

Our calculation method for determining the contact points of gears with involute profile is a special one and have not adopted in studies [2-9].

Comparing our analytical methods with papers [2-9], calculation of the individual deflection components differs. Considering the method itself, the most similar method can be found in works [2-3], but there are differences in the obtained formulas of the individual deflection components. In works [2, 3] bending and shearing deflection is calculated jointly, and the applied model of the Hertzian contact also disagrees.

Acknowledgement

“This research was carried out as part of the TAMOP-4.2.1.B-10/2/KONV-2010-0001 project with support by the European Union, co-financed by the European Social Fund.”

References

- [1] F. L. Litvin: *A fogaskerek kapcsolódás elmélete*. Műszaki Könyvkiadó, Budapest, 1972.
- [2] F. Chaari–W. Baccar–M. S. Abbes–M. Haddar: *Effect of spalling or tooth breakage on gear-mesh stiffness and dynamic response of a one-stage spur gear transmission*. *European Journal of Mechanics A/Solids* 27 (2008), pp. 691–705.
- [3] F. Chaari–T. Fakhfakh–M. Haddar: *Analytical modelling of spur gear tooth crack and influence on gearmesh stiffness*. *European Journal of Mechanics A/Solids* (2009), pp. 461–468.
- [4] K. Markovic–M. Franulovic: *Contact stresses in gear teeth due to tip relief profile modification*. *Eng. Rev.* 31–1. 2011. pp. 19–26.
- [5] J.J. Zhang–I.I. Esat–Y.H. Shi: *Load analysis with varying mesh stiffness*. *Computers and structures* 70 (1999), pp. 273–280.
- [6] J. Hedlund–A. Lehtovaara: *Modeling of helical gear contact with tooth deflection*. *Tribology International* 40, 2007. pp. 613–619.
- [7] J. I. Pedrero–M. Pleguetuelos–M. Artés–J. A. Antona: *Load distribution model along the line of contact for involute external gears*. *Mechanism and Machine Theory* 45, 2010. pp. 780–794.
- [8] L. Walha–T. Fakhfakh–M. Haddar: *Nonlinear dynamics of a two-stage gear system with mesh stiffness fluctuation, bearing flexibility and backlash*. *Mechanism and Machine Theory* 44, 2009. pp. 1058–1069.
- [9] A. Andersson–L. Vedmar: *A dynamic model to determine vibrations in involute helical gears*. *Journal of Sound and Vibration* 260, 2003. pp. 195–212.
- [10] G. Litak–M. I. Friswell: *Vibration in gear systems*. *Chaos, Solitons and Fractals* (2003), p.p. 795–800.
- [11] R. Szűcs–L. Kamondi: *Fogaskerekek dinamikai vizsgálatának egy lehetősége*. Kolozsvár: Erdélyi Magyar Műszaki Tudományos Társaság, Műszaki Szemle, 2010. pp. 416–419.
- [12] R. Szűcs–L. Kamondi: *Bevezetés a geometria dinamikai vizsgálatokra gyakorolt hatásába*. *GÉP LXI.* (2010/9–10.), Gépipari Tudományos Egyesület Műszaki Folyóirata, pp. 102–104.
- [13] R. Szűcs–L. Kamondi: *Bevezetés a fogaskerek kapcsolódás végeelem módszerrel történő vizsgálati lehetőségeibe*. *GÉP LXII.* (2011/11), Gépipari Tudományos Egyesület Műszaki Folyóirata, pp. 37–39.
- [14] James M. Gere–Barry J. Goodno: *Mechanics of Materials, Eighth Edition*. 2009 Cengage Learning
- [15] M. J. Puttock–E. G. Thwaite: *Elastic Compression of Spheres and Cylinders at Point and Line Contact*. National Standards Laboratory Technical Paper, No. 25, Commonwealth Scientific and Industrial Research Organization, Australia, Melbourne 1969.

DETERMINATION OF BACKLASH FOR GEAR DYNAMIC ANALYSIS

RENÁTA SZÚCS–LÁSZLÓ KAMONDI

Department of Machine and Product Design, University of Miskolc

H-3515, Miskolc-Egyetemváros

szucs.renata@citromail.hu; machkl@uni-miskolc.hu

Abstract. In this paper our aim is to determine the backlash introduced to the mechanical model of gears. On one hand an overview of the relevant standards is presented and on the other hand definition of backlash in the motion of equation is also demonstrated as well as its relationship with other important gear characteristics namely with meshing stiffness and tooth thickness. Backlash is a very significant parameter with great influence on the dynamic behaviour of gears.

1. INTRODUCTION

Gears are one of the most frequently used power transmission machine elements. As a consequence of combination of the increased demands claimed against gears and economical production nonlinear dynamic analysis has a great importance still nowadays. During this dynamic analysis the correct chose of backlash is pivotal.

On one hand backlash is necessary because of wear, thermal expansion, manufacturing errors, lubrication etc. but on the other hand due to backlash dynamic behaviour of gears are worse than backlash-free gears. Practically, backlash-free gears exist only theoretically on account of the fore-mentioned reasons. We can say that backlash is the necessary evil. Since manufacturing costs are greatly increased by reduction of backlash designers have great responsibility for choosing the right value of backlash. In case of gears of lower accuracy wider tolerances can be allowed but for precise machines backlash should be minimized. From the point of the application the maximum allowable backlash should be determined, this backlash is that by which the required performance can be achieved by the minimum manufacturing costs i.e. between the maximum allowable tolerances. In case of gears smaller in size determination of backlash are also very important. The aim is to use tolerances not tighter than necessary to obtain the required performance.

In this study we would like to show the correlation between meshing stiffness and backlash as well as the recommendations for backlash according to ISO standards.

2. EQUATION OF MOTION

For dynamic analysis of gear drives a model shown on *Figure 1* has been developed [4–6]. The driver and the driven gear are modeled by masses rotating around the central points of the gears, while meshing is modeled by an equivalent spring and a damping proportional with the velocity in the direction of line of action. This model contains backlash but neglects friction and installation inaccuracies.

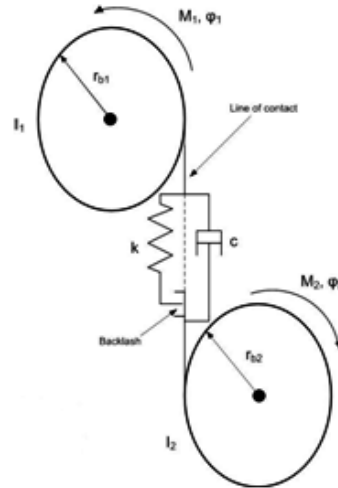


Figure 1. Dynamic model

Apart from development for the equation of motion the following relation can be written:

$$m \cdot \ddot{x} + c \cdot \dot{x} + k(t) \cdot h(x) = f_T(t) + f_M(t) \quad (1)$$

where:

$$m = \frac{I_1 \cdot I_2}{I_1 \cdot r_{b2}^2 + I_2 \cdot r_{b1}^2} \quad (2)$$

$$f_T(t) = \frac{r_{b1} \cdot I_2 \cdot M_1 - r_{b2} \cdot I_1 \cdot M_2}{I_1 \cdot r_{b2}^2 + I_2 \cdot r_{b1}^2} \quad (3)$$

$$f_M(t) = -m \cdot \ddot{e}(t) \quad (4)$$

$$h(x) = \begin{cases} x - b, & x \geq b \\ 0, & |x| < b \\ x + b, & x \leq -b \end{cases} \quad (5)$$

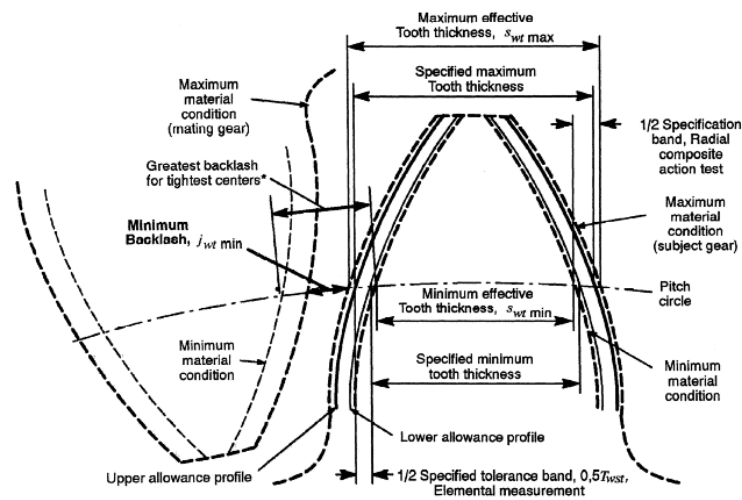
Table 1

List of symbols and parameters

I_1, I_2	moments of inertia
φ_1, φ_2	rotational angles
$x = r_{b1}\varphi_1 - r_{b2}\varphi_2 - e(t)$	relative displacement
r_{b1}, r_{b2}	base circles
M_1, M_2	external torques
$2b$	whole backlash
c	damping
$k(t)$	meshing stiffness
$e(t)$	static transmission error

3. DEFINITION OF BACKLASH

Backlash is the amount by which a tooth space exceeds the thickness of a gear tooth engaged in mesh. The general purpose of backlash is to prevent gears from jamming by making contact on both sides of their teeth simultaneously [3]. Usually the backlash under stabilized working conditions (working backlash) is different from (smaller than) the backlash which is measured when the gears are mounted in the housing under static conditions (assembly backlash) [2].



* THIS FIGURE IS DRAWN AT THE POSITION OF TIGHTEST CENTER DISTANCE; if center distance is increased backlash will increase.

Figure 2. Tooth thickness, transverse plane [2]

According to ISO 1122-1 and ISO TR 10064-2 the following backlashes are determined [1, 2]:

- Circumferential backlash (j_{wt}): length of arc of the pitch circle through which a gear can be turned when the mating gear is fixed.

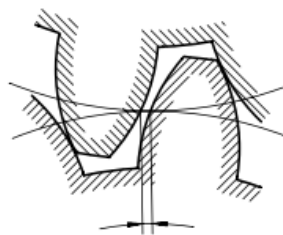


Figure 3. Circumferential backlash [1]

- Normal backlash (j_{bn}): is the shortest distance between non-operating flanks when the operating flanks are in contact.

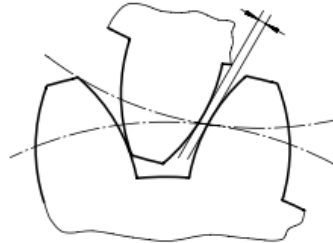


Figure 4. Normal backlash [1]

- *Reference backlash*: length of arc of the reference circle, equal to the product of the reference diameter and the circumferential backlash, divided by the pitch diameter.
- *Angular backlash* (j_θ): maximum value of the angle through which a gear can be turned when the mating gear is fixed and the centre distance has the specified value.
- *Radial backlash* (j_r): is the amount by which the center distance has to be diminished till the position in which left and right flanks of mating gears are in contact.
- *Minimum backlash* ($j_{t,min}$): is the minimum circumferential backlash on the pitch circle when the gear tooth with the greatest allowable effective tooth thickness is in mesh with the mating gear tooth having its greatest allowable effective tooth thickness, at the tightest allowable center distance, under static conditions. The tightest center distance is the minimum working center distance for external gears.
- *Maximum backlash* ($j_{t,max}$): is the maximum circumferential backlash on the pitch circle when the gear tooth with the smallest allowable effective tooth thickness is in mesh with the mating gear tooth having its smallest allowable effective tooth thickness, at the largest allowable center distance, under static conditions.

In case of spur gears the following relationships can be written between the different types of backlashes [3]:

$$j_{bn} = j_{wt} \cdot \cos\alpha_{wt} \quad (6)$$

$$j_r = \frac{j_{wt}}{2 \cdot \tan\alpha_{wt}} \quad (7)$$

$$j_\theta = j_{wt} \cdot \frac{360}{\pi d} \quad (8)$$

4. BACKLASH ACCORDING TO ISO STANDARDS

For selecting and measuring of backlash recommendations can be found in ISO TR 10064-2.

Backlash, j , in an assembled gear set is the clearance between the teeth of the meshing gears. Backlash may be measured in the normal plane or along the line of action, but it is calculated and specified in the transverse plane or in the plane of action (base tangent plane) [2].

An individual gear does not have backlash, it has only a tooth thickness. Backlash in a mesh is governed by the center distance at which a pair of gears is operated and the effective tooth thickness of each of the gears [2].

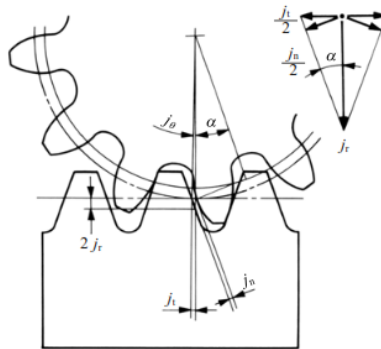


Figure 5. Kinds of backlash and their direction [3]

Backlash in a given mesh varies during operation as a result of changes in speed, temperature, load, etc. Adequate backlash should be present during static conditions, when it can be measured, to assure sufficient backlash under load at the most adverse working condition [2].

4.1. Maximum Tooth Thickness [2]

Maximum tooth thickness of a gear is determined as if the gear were in mesh with a perfect mating gear at the minimum center distance, allowing for the desired minimum backlash. Tooth thickness deviations reduce the maximum tooth thickness from the maximum value, and increase backlash.

For $x = 0$ gears, the theoretical or nominal tooth thickness is customarily equal to one half the circular pitch on the reference circle. Unless otherwise specified, the actual maximum tooth thickness on an unassembled gear will usually be less than the theoretical value, since the manufacturer usually makes a reduction in tooth thickness to allow for backlash.

4.2. Minimum Backlash [2]

Minimum backlash $j_{bn,min}$, is the minimum backlash allowable when the gear tooth with the greatest allowable effective tooth thickness is in mesh with a mating tooth having its greatest allowable effective tooth thickness at the tightest allowable center distance, under static conditions. This is the traditional “backlash allowance” provided by the designer to provide for:

- deflections of housings, shafts and bearings
- misalignments of gear axes due to housing deviations and bearing clearances
- skew of gear axes due to housing deviations and bearing clearances
- mounting errors such as shaft eccentricity
- bearing runouts

- f) temperature effects (a function of temperature differences between housing and gear elements, center distance and material difference)
- g) centrifugal growth of rotating elements
- h) other factors, such as allowance for contamination of lubricant and swelling of non-metallic gear materials

The value of minimum backlash can be small if the factors listed above are controlled. Each factor can be evaluated by analyzing the tolerances, and then a minimum requirement can be calculated. Judgment and experience are required to assess the minimum expected requirement, since the worst case tolerances are not likely to coincide.

Figure 6 shows values of minimum backlash recommended for industrial drives with ferrous gears in ferrous housings, working at pitchline speeds less than 15 m/s, with typical commercial manufacturing tolerances for housings, shafts and bearings.

The values found in Figure 6 may be calculated from $j_{bn\ min} = \left(\frac{2}{3}\right) [0,06 + 0,0005a_i + 0,03m_n]$.

m_n in mm	Minimum center distance a_i in mm					
	50	100	200	400	800	1600
1,5	0,09	0,11	---	---	---	---
2	0,10	0,12	0,15	---	---	---
3	0,12	0,14	0,17	0,24	---	---
5	---	0,18	0,21	0,28	---	---
8	---	0,24	0,27	0,34	0,47	---
12	---	---	0,35	0,42	0,55	---
18	---	---	---	0,54	0,67	0,94

Figure 6. Recommended values minimum backlash $j_{bn\ min}$ for coarse pitch gears [2]

4.3. Maximum Backlash [2]

The maximum backlash in a gear set, $j_{bn,max}$, is the sum of tooth thickness tolerance, the effect of center distance variation, and the effects of gear tooth geometry variation. The theoretical maximum backlash occurs when two perfect gears, made to the minimum tooth thickness specification, are meshed at the loosest allowable center distance. The loosest center distance is the maximum for external gears or the minimum for internals.

The maximum theoretical backlash will also occur when two teeth, made to the minimum effective tooth thickness, $s_{wt\ min}$, coincide while operating at the loosest center distance. Neither occurrence is likely in practice.

The maximum expected backlash is a function of $j_{bn,max}$ and the statistical distribution of the individual elements of tooth and center distance variation. Any tooth deviations due to manufacturing will decrease the maximum expected backlash. Experience and judgment are required to estimate reasonable values.

If maximum backlash must be controlled, a careful study of each element of maximum backlash must be made and an accuracy grade selected which will limit tooth deviations as necessary.

When maximum backlash of an assembled gear drive, particularly a gear drive with multiple stages, is used as an acceptance criterion, the maximum acceptable value must be

carefully chosen to allow reasonable manufacturing tolerances for each part in the assembly.

4.4. Limits [2]

The (actual) sizes of the tooth thicknesses of pinion and gear and of the shaft center distance, together with the respective gear element deviations, determine the backlash j of the gear teeth; i.e. the clearance between the non-working flanks at the working diameter.

Usually, maximum backlash does not affect the function or smoothness of transmission motion, and effective tooth thickness deviation is not the main consideration in the selection of gear accuracy. In many applications, allowing a larger range of tooth thickness tolerance or working backlash will not affect the performance or load capacity of gears and may allow more economical manufacturing. A tight tooth thickness tolerance should not be used unless absolutely necessary, since it has a strong influence on manufacturing cost. In those cases where maximum backlash must be closely controlled, a careful study of the influence factors must be made and the gear accuracy grade, center distance tolerance and measurement methods must be carefully specified.

It may be necessary to specify a more precise accuracy grade to hold maximum backlash within the desired limits.

Minimum working backlash may not be allowed to become zero or negative. Because working backlash is determined by the assembled backlash and the working conditions; i.e., by the influences of deflections, misalignment, bearing runouts, temperature effects, and any unknowns, one has to distinguish: assembled backlash and working backlash.

Backlash does not have a fixed value, but may vary at different tooth positions due to manufacturing tolerances and working conditions.

The values given for tooth thickness and backlash are to be selected by the designer to suit the application.

4.5. Backlash from our point of view

Several kind of backlash are determined by standards but as it can be seen from section 4.1–4.4 standards does not give strict values for backlash only recommendations and for coarse pitch gears some minimum values can be found. Backlash is influenced by several parameters which have to be taken into account during design. Our aim is to determine the minimum and maximum backlash by which the desired working conditions can be achieved. It includes the optimization of the tooth profile and of the tolerances. Solution of Eq. 1 should be done for the working backlash, but dynamic behavior, i.e. determination of vibration, of the gear transmission should also be determined in the case of the minimum and maximum backlashes in order to provide the desired dynamic parameters under these conditions. While a few parameters such as lubrication, housing etc. are not included in our dynamic model we have to take them into account at the stage of determination of the minimum and maximum backlashes.

In our studies we deal with not commonly used gears but with gears for special applications where parameters such as tooth deflection can't be neglected. For these kind of gears factual values can't be found even in standards. Recommendation included in standard mostly relates to gears not for special application. The goal of our research is to give not

$$\delta_{fb}^j = \delta_{xb}^j \cdot \cos\gamma_j^j = \frac{1,2F_{NJ}^j \cdot \cos^2\gamma_j^j}{G} \sum_{k=1}^N \frac{s_k}{A_k}, k_{fb}^j = \frac{F_{NJ}^j}{\delta_{fb}^j} \quad (10)$$

Fillet-foundation deflection and meshing stiffness arising from it:

$$\delta_{Jc}^j = \frac{1,327F_{NJ}^j \cdot [\cos\gamma_j^j \cdot (y_j^j - y_F) - \sin\gamma_j^j \cdot x_j^j]^2}{E_v \cdot x_F^2 \cdot b}, k_{Jc}^j = \frac{F_{NJ}^j}{\delta_{Jc}^j} \quad (11)$$

Contact deflection and meshing stiffness arising from it:

$$\delta_{Jd1,2}^j = \frac{5 \cdot 10^{-3} \cdot F_{NJ}^{j,0,9}}{E_{v1,2}^{0,9} \cdot b_{1,2}^{0,8}}, k_{Jd1,2}^j = \frac{F_{NJ}^j}{\delta_{Jd1,2}^j} \quad (12)$$

For $k(t)$, when one pair of teeth in contact the following relationship has been obtained:

$$k_{1,2}^j = k_{J1,abc}^j + k_{J2,abc}^j + k_{Jd1,2}^j.$$

As it can be seen from (2–5), actual tooth thickness (tolerance of the nominal tooth thickness) has a significant influence on meshing stiffness while directly relates backlash. So tolerances on the thickness are very important factors.

5.1. Backlash in the motion of equation

According to Eq. 5 backlash can be illustrated by *Figure 8* considering teeth configuration in pursuance of *Figure 9*.

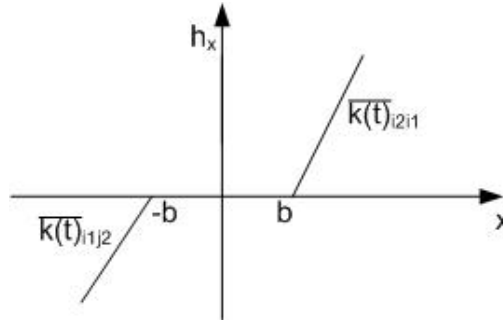


Figure 8. Backlash

Key for *Figure 8*:

$\overline{k(t)}_{i1j2}$: linearized meshing stiffness between tooth i of gear 1 and tooth j of gear 2;

$\overline{k(t)}_{i2i1}$: linearized meshing stiffness between tooth i of gear 2 and tooth i of gear 1;

Figure 9 shows the teeth configuration.

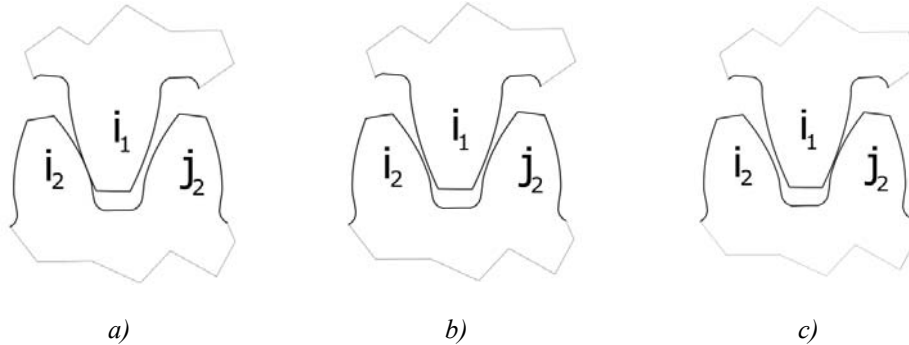


Figure 9. Teeth configuration: a) – first case, $x \geq b$
 b) – second case, $|x| > b$; c) – third case, $x \leq -b$

In the second case backlash causes contact loss which results bad dynamic behaviour (noise, vibration) mainly in case of low loaded gears.

According to the above-mentioned Eq. 1 can be divided into three sub-equation:

a) if $x \geq b$:

$$m \cdot \ddot{x} + c \cdot \dot{x} + k(t) \cdot (x - b) = f_T(t) + f_M(t)$$

so $k(t)$ and c should be determined between tooth i of gear 2 and tooth i of gear 1;

b) if $|x| > b$:

$$m \cdot \ddot{x} = f_T(t) + f_M(t)$$

so there is no contact;

c) if $x \leq b$:

$$m \cdot \ddot{x} + c \cdot \dot{x} + k(t) \cdot (x - b) = f_T(t) + f_M(t)$$

so $k(t)$ and c should be determined between tooth j of gear 2 and tooth i of gear 1.

5.2. Methods of Controlling Backlash

For reducing backlash two methods are available: a static and a dynamic method. The static method concerns means of assembling gears and the making proper adjustments to achieve the desired low backlash. The dynamic method introduces an external force which continually eliminated all backlash regardless of rotational position. [3]

6. SUMMARY

Since backlash has great influence on the dynamic behaviour of gears determination of its value a very important task. The minimum and maximum value also should be determine in such a way that provides the desired performance. As backlash is in close relation with tooth thickness and meshing stiffness it can't be investigated as an individual parameter it should be determined as part of the optimizing process in which parameters influencing Eq. 1 are handled together. Our aim is to give factual data for the optimum gear profile under

the specified load that contains the tolerance of the tooth profile determining the minimum and maximum value of backlash.

Acknowledgement

“This research was carried out as part of the TAMOP-4.2.1.B-10/2/KONV-2010-0001 project with support by the European Union, co-financed by the European Social Fund.”

References

- [1] ISO 1122-1:1998(E/F): Vocabulary of gear terms – Part 1: Definitions related to geometry, Second edition, 1998-08-01
- [2] ISO TR 10064-2: *Cylindrical gears – Code of inspection practice*. Part 2: Inspection related to radial composite deviations, runout, tooth thickness and backlash, First edition, 1996.
- [3] *Practical Information on Gears*. Kohara Gear Industry Co., Ltd.: http://www.khkgears.co.jp/de/gear_technology/pdf/gear_guide2.pdf
- [4] R. Szűcs–L. Kamondi: *Fogaskerekek dinamikai vizsgálatának egy lehetősége*. Kolozsvár: Erdélyi Magyar Műszaki Tudományos Társaság, *Műszaki Szemle* (2010), pp. 416–419.
- [5] R. Szűcs–L. Kamondi: *Bevezetés a geometria dinamikai vizsgálatokra gyakorolt hatásába*. GÉP LXI. (2010/9-10.), Gépipari Tudományos Egyesület Műszaki Folyóirata, pp. 102–104.
- [6] R. Szűcs–L. Kamondi: *Analytical model for determine meshing stiffness of spur gears*. *Advanced Engineering* 6 (2012)

ENVIRONMENTALLY FRIENDLY DESIGN TOOLS – POSSIBILITIES OF THE APPLICATION

ÁGNES TAKÁCS

Department of Machine and Product Design, University of Miskolc
H-3515 Miskolc-Egyetemváros
takacs.agnes@uni-miskolc.hu

Abstract: The paper introduces where and how DfE or Design for Environment is located among Dfx techniques. Those steps of the design process also need to be defined, where the tools of the DfE are suggested to keep in front of the engineer's eyes.

Keywords: design theory, methodology, Design for Environment

1. INTRODUCTION

The importance of this special field of engineering sciences is also confirmed by the energy backup of the World that is lower and lower day-by-day. Solar panels are more often seen on the roofs of houses and the range of other green energy sources is wider and wider. These energy sources make it possible that the energy consumption of the Planet is slower and less amount of pollutants get into the air. It is a task for nowadays engineers during the whole design process to pay attention to producing products for the shelves of the shops in the same quality as earlier, despite the less harmful production. This is not an easy mission and without engineering creativity it is not possible.

2. BASIC PHILOSOPHIES

2.1. 3R theory

3R theory means nothing else but recycling used materials into the product market instead of throwing them away. Reduce means decreasing the quantity of the garbage; reuse is the method when we select the parts that can be reused from the garbage during the new-product manufacturing process. Recycling of the garbage occurs when, for example, we gather PET bottles and according to chemical reactions we produce new PET bottles. This cycle is shown in *Figure 1*.

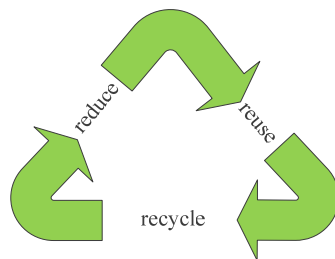


Figure 1. The 3R philosophy

2.2. Product-material lifecycle

Figure 2 shows the stages of the product lifecycle in the point of view of the material. The process starts with the extraction of the raw material, with that the production of the stock can be started. From the stock products are prepared. These products become wastage after using them. Waste can be reused in several ways. By reusing those elements of products that have longer life, than other parts, products can be fixed (*for instance scrap yards*). In case of remanufacturing elements of the product are in the production line again (*Remy Automotive*). During the recycling process new materials are produced from the used ones (*gathering PET bottles*).

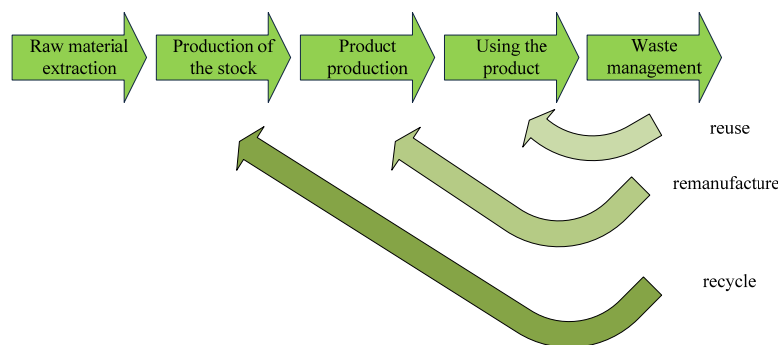


Figure 2. Product-material-lifecycle [1]

2.3. Dfx techniques

Systemizing Dfx techniques is quite a complicated task. Figure 3 shows the approach how design activities or Dfx techniques can be gathered together into an enormous set, into a 3D space that is determined by costs (C), quality (Qlt) and quantity (Qnt). In this space there are Dfx techniques that are working as an umbrella term, so collecting other techniques in that special field of engineering. The DfE, so the Design for the Environment is a very good example, as it will be introduced later. Although in the space of design activities there are also Dfx techniques that can be defined as separate activities. These ones are denoted by the points.

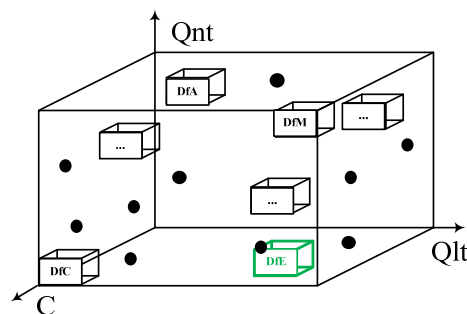


Figure 3. 3D space of Design for-activities

3. DESIGN FOR THE ENVIRONMENT

Dfx, or design according to a given viewpoint [2] can be any formal period of the design process, or any important aspect that can be followed during the whole design activity as the main principle. Dfx is an enormous set of design principles that is really hard to describe, because this set is increasing day-by-day. Scientists define more and more principles, and for those principles methods are also created. These methods denote or can denote the adaption of Dfx techniques to computer. DfE, that is Design for the Environment is collecting the aspects of environmentally friendly design. As it is shown in *Figure 4* it consists of seven essential areas. According to different aspects these can be divided into other different principles. This figure also confirms why it is so complicated to collect all the Dfx techniques and to group them.

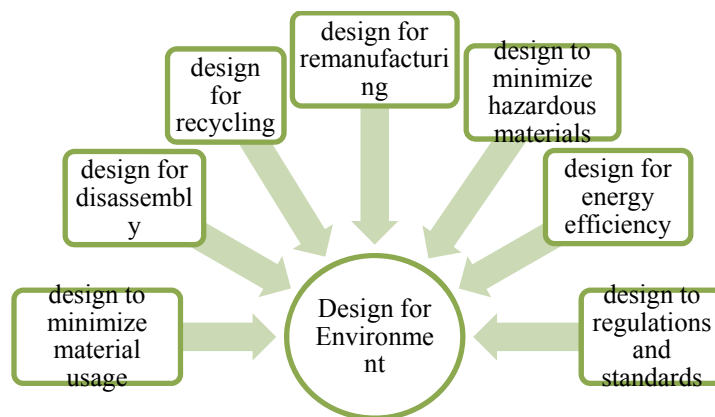


Figure 4. Design for the Environment [1]

3.1. DfE in the design process

Figure 5 introduces the whole design process on the basis of VDI 2221. The original flow-chart suggested by the VDI (*Verein Deutscher Ingenieure*) on the right-hand side contains the results of the different steps. The figure modified here shows, which tools demonstrated in *Figure 4* can be ad verted on the different design stages determined by VDI. It can be seen that there are DfE tools th at can be considered in several steps. According to my present researches the first four steps (*Clarification and definition of the design task, Determining functions and their structures, Searching for solution principles and their combinations, Determining subassemblies*) of the design process can be important. As the basis of my present researches is the conceptual design process defined in my thesis [4] (*Figure 6*) the above mentioned four steps can be narrowed for the next three steps:

- Clarification and definition of the design task,
- Determining functions and their structures,
- Determining subassemblies.

Figure 6 [3], [4], [5] focuses on the main scope of my researches; it summarises the phase of the conceptual design. Design process according to the VDI involves the whole design process as it can be seen in *Figure 5*. The above mentioned four steps of this process

mean the conceptual design. The suggested method introduced by *Figure 6* implies a relatively simple algorithm, so the process is adaptable for computer. In the modern World of our days it significantly facilitates the task of the engineering designer.

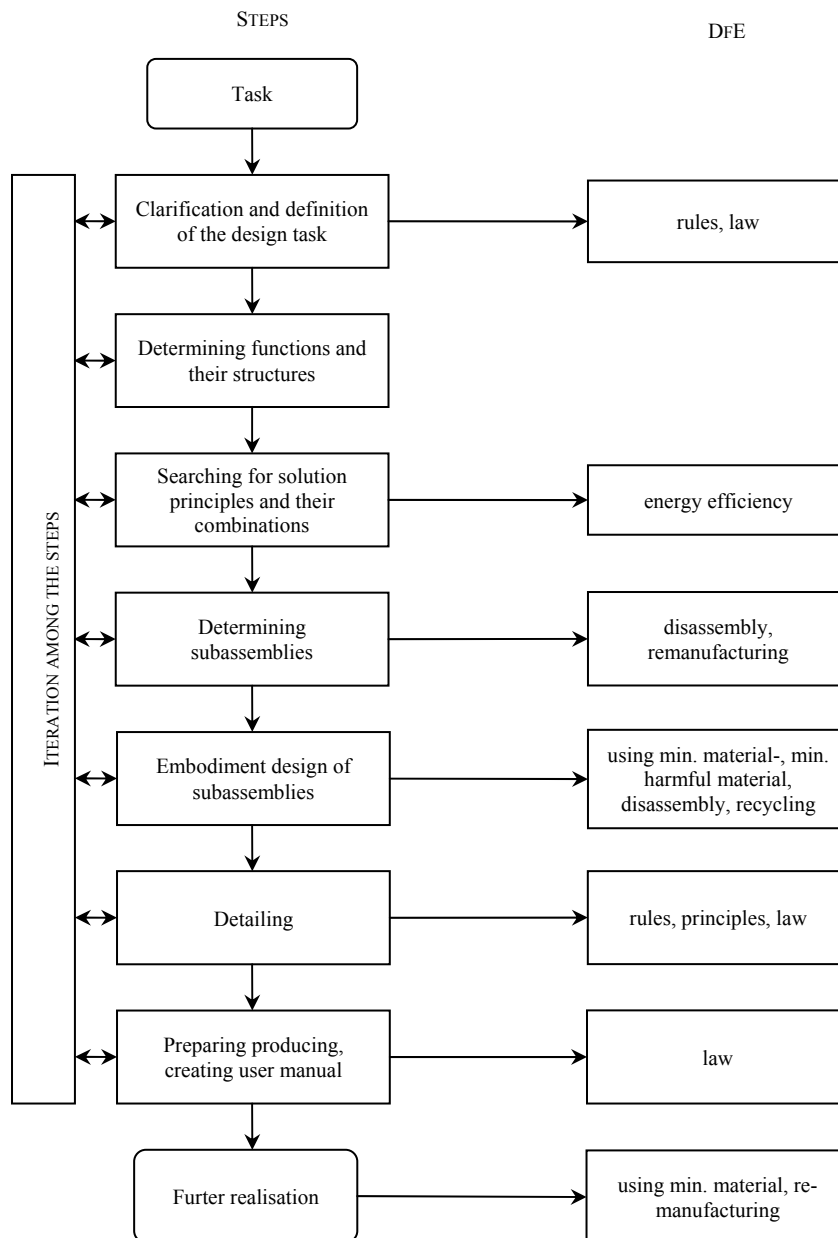


Figure 5. Design process on the basis of VDI2221 [6]

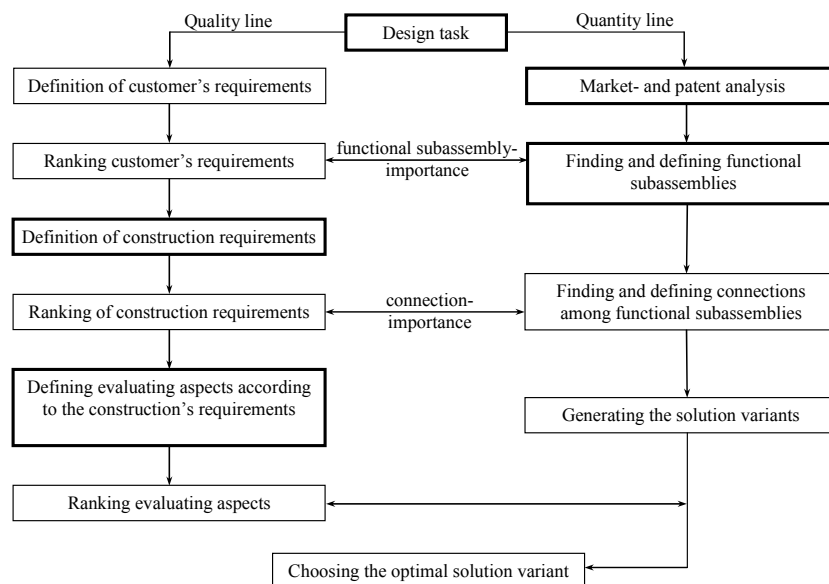


Figure 6. Conceptual design process – a suggestion

3.2. Environmentally friendly design thinking

As it is shown in Figure 6 [3], [4], [5] certain steps of the conceptual design process are indicated by thick line. These are the steps where the creativity of the designer appears and the designer has to pay attention to the given circumstances, rules, laws and in these steps the tools of the DfE can also be taken into consideration. Let us analyse whether DfE tools indicated in Figure 5 suggested by VDI in case of steps signed in the process suggested by Figure 6 can also be applied or more other tools can be used!

Design task in the suggested system and Clarification and definition of the design task according to the VDI are the same. This is the step, where the prescription of rules and regulations must be analysed.

During the market and patent analysis there are two things the designer has to pay attention to. The first one is that analysing earlier solutions functional subassemblies can be determined; the other benefit is that this way concrete embodiment can be examined for the further embodiment design. So this step has an effect on the embodiment design that is the reason that all the tools of DfE can occur. But if it is only the conceptual design process we should keep in mind, a concrete DfE tool cannot be mentioned, except for rules and laws.

There is a significant difference between the two methods: VDI separates the function, the solution principle and the subassembly. In this case function means a task that is solved by different parts, assemblies of the designed product but it is not defined according to what principles what kind of assemblies. Solution principle means physical principles that make it possible for the given function to be realised. Although it is still not known what kind of assembly the given task will solve. According to VDI determining subassemblies is the part of the whole embodiment design. This is the step, where concrete subassemblies are de-

fined. In case of *Figure 6* instead of functions, solution principles and subassemblies there are only functional subassemblies. These are a little bit more specific than functions that are very abstract in most of the cases. Neither concrete subassembly is a functional subassembly. In the step of conceptual design even solution principles (*physical laws*) for functional subassemblies are not necessary to be determined.

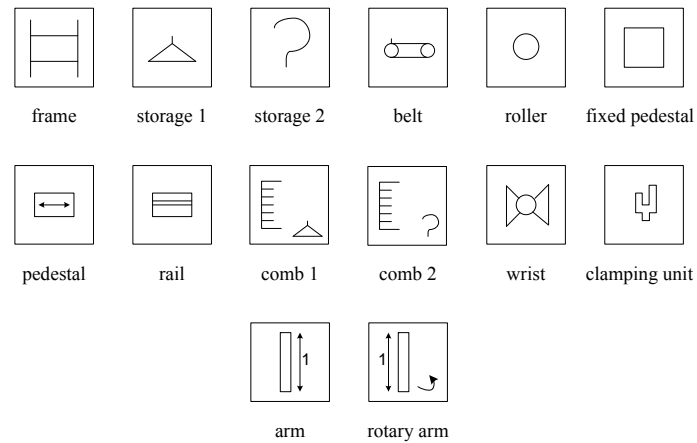


Figure 7. Functional subassemblies of assembling equipment

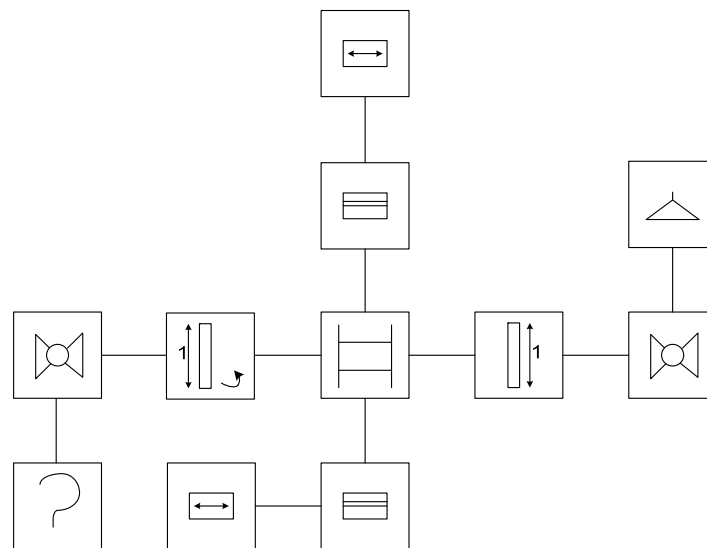


Figure 8. A possible function-structure of assembling equipment

A possible concept for hanger assembling equipment is quite an easy example for that. In *Figure 7* used functional subassemblies are introduced. A possible function-structure built

up of them is shown in *Figure 8*; a possible concept on the basis of *Figure 8* can be seen in *Figure 9*. It is foreseeable according to the figures that the functional subassembly called pedestal moves on a rail, but finding out how this movement will be realised is a further task. This kind of linear movement can be achieved by different principles; in case of this example during embodiment design it was pneumatics as an obvious solution.

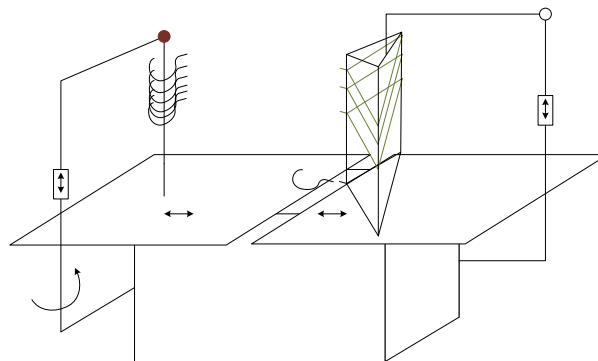


Figure 9. A possible concept for assembling equipment

According to the process introduced by VDI functions are such abstract notions as: dis-unite, mix, connect, etc. So these cannot be compared with the tools of DfE. And determining subassemblies is the part of the embodiment design, according to VDI.

In case of the method according to *Figure 6* defining functional subassemblies design to minimize material usage and design for energy efficiency can be used. At this point of the design process concerning a lying surface of bed functional subassemblies can be a mattress, water-mattress, spring-mattress, etc. It is evident among these options mattress filled with air seems to be the most material-saving solution, because the consumer can pump it even at home. This way only a shell needs to be designed and produced. The other possibilities are more complicated in terms of production, so this way not only the material, but even energy is saved. So summing up functions a simple structure can be reached that is a key for using less material.

Defining construction requirements and the evaluation of them all DfE tools can be taken into consideration. During the design process this is the first step when expectations for the product defined in the requirements list should be examined. Construction requirements should be highlighted here that are possible to be taken into account even in the early phase of the design process like this. These requirements can be the ones rules and laws make necessary, for example protective screen at dangerous points. Using two buttons for starting the equipment pushed at the same time can be also a solution for saving the user. This solution needs two hands, the user cannot reach the moving elements during the operation. These need to be counted as separate functional subassemblies when finding and defining the functional subassemblies and as evaluating aspects when defining construction requirements. Here the designer can, and he/she has to pay attention to environmentally friendly aspects as well. So different environmental laws and orders should be studied in this phase of the conceptual design. The case when the regulation orders using cleaning equipment can be a construction requirement as well: it can be examined whether the con-

cept contains a unit like this, or not. So this means the regulations and laws in connection with the environment can be taken into consideration here in this step of the process.

4. SUMMARY OF THE NEW SCIENTIFIC RESULTS

For the suggested method in *Figure 6* according to my thesis and other earlier publications [3], [4], [5] it is easy to make an algorithm and adapting it to the computer is the main advantage. Besides that the algorithm is not eliminating the creativity and individual ideas of the designer even it appears on more points than in other earlier works. As the method ensures several possibilities for the designer-engineer for his/her experiences, ideas, results of market-analysis as parameters put into the algorithm and the software based on it, it provides an opportunity for the systematisation of the design process-results that was impossible earlier. It is also a significant result that the suggested method seems to be more effective than for instance the method suggested by VDI in the viewpoint of the environmentally friendly design as well, as the tools of the DfE are also possible to be taken into consideration in more steps of the process.

5. DIRECTIONS AND POSSIBILITIES OF DEVELOPMENT

In the case of the suggested method further analysis of DfE tools determined here has to be carried out. It must be examined how, in what ways these tools appear in the different steps of the conceptual design process. Practical examples must be collected that confirm the realisation of DfE tools suggested in certain steps of the mentioned process.

Acknowledgement

“This research was carried out as part of the TAMOP-4.2.1.B-10/2/KONV-2010-0001 project with support by the European Union, co-financed by the European Social Fund.”

References

- [1] K. Otto–K. Wood: *Product Design – Techniques in Reverse Engineering and New Product Development*. Prentice Hall, 2008.
- [2] G. Pahl–W. Beitz: *Engineering Design – A Systematic Approach*. Springer Verlag, London, 2005.
- [3] Á. Takács–L. Kamondi: *On Design Theories Fundamentals of a Neuvel Approach*. Advanced Engineering, Vol. 5, No. 1, 2011.
- [4] Á. Takács: *Számítógéppel segített koncepcionális tervezési módszer*. Doktori (PhD.) disszertáció, Miskolc, 2010.
- [5] Á. Takács–L. Kamondi: *Design Science – A neuvel approach for the product design*. Advanced Engineering, Vol. 2, No. 1, 2008.
- [6] VDI 2221: *Methodik zum Entwickeln und Konstruieren technischer Systeme und Produkte*. VDI-Verlag GmbH, Düsseldorf, 1993.

REVIEWING COMMITTEE

- K. BÁRCZY Department of English Linguistics and Literature
University of Miskolc
H-3515 Miskolc-Egyetemváros, Hungary
bolklara@uni-miskolc.hu
- Á. DÖBRÖCZÖNI Department of Machine- and Product Design
University of Miskolc
H-3515 Miskolc-Egyetemváros, Hungary
machda@uni-miskolc.hu
- M. GERGELY Acceleration Bt.
mihaly_gergely@freemail.hu
- K. JÁRMAI Department of Materials Handling and Logistics
University of Miskolc
H-3515 Miskolc-Egyetemváros, Hungary
altjar@uni-miskolc.hu
- I. KERÉKES Department of Mechanics
University of Miskolc,
H-3515 Miskolc-Egyetemváros, Hungary
mechker@uni-miskolc.hu
- T. KOLLÁNYI Rábaparti Kft.
kollanyi.t@gmail.com
- F. J. SZABÓ Department of Machine- and Product Design
University of Miskolc
H-3515 Miskolc-Egyetemváros, Hungary
machszf@uni-miskolc.hu
- A. SZILÁGYI Department of Machine Tools
University of Miskolc
H-3515 Miskolc-Egyetemváros, Hungary
szilagyi.attila@uni-miskolc.hu

University of Miskolc, Department of Research Management and International Relations
Responsible for publication: Prof. Dr. Mihály Dobróka prorector
Miskolc-Egyetemváros
Editor: Dr. Ágnes Takács
Published by the Miskolc University Press under leadership of Erzsébet Burmeister
Responsible for duplication: Erzsébet Pásztor, works manager
Number of copies printed: 49
Put to the Press on November, 2012
Number of permission: 479

HU ISSN 1785-6892